

**Deanship of Graduate Studies  
Al-Quds University**



**Geoelectrical Investigation for Possible Artificial  
Groundwater Recharge Site in Al-Jiftlik / Wadi Al-Faria**

**Osama Khaled Abdul-Majid Bahar**

**M.S.c Thesis**

**Jerusalem-Palestine**

**September 2008**

**Geoelectrical Investigation for Possible Artificial  
Groundwater Recharge Site in Al-Jiftlik / Wadi Al-Faria**

**By  
Osama Khaled Bahar  
(20411628)**

**Supervision: Dr. Amer Marei**

**A Thesis Submitted in Partial Fulfillment of the Requirement  
for the Degree of Master Science in Environmental Studies  
Department of Applied Earth and Environmental Studies  
Faculty of Science and Technology- Al-Quds University.**

**2008/1429**

**Al-Quds University  
Deanship of Graduate Studies  
Environmental Science**

**Thesis Approval**

**Geoelectrical Investigation for Possible Artificial  
Groundwater Recharge Site in Al-Jiftlik / Wadi Al-Faria**

**Prepared By: Osama Khaled Abdul-Majid Bahar  
Registration No.: 20411628**

**Supervisor: Dr. Amer Marei**

**Master thesis submitted and accepted, date**

**The names and signatures of the examining committee  
members are the follows:**

- 1- Head of Committee:.....Signature.....**
- 2- Internal Examiner:.....Signature.....**
- 3- External Examiner:.....Signature.....**

**Jerusalem-Palestine**

**To my family my love**

**Declaration:**

I certify that this thesis submitted for the degree of Master is the result of my own research, except where otherwise acknowledged, and that this thesis (or any part of the same) has not been submitted for a higher degree to any other university or institution.

Signed.....

**Osama Khaled Bahar)**

Date: ...13/9/2008.....

**Bahar\_planet@Yahoo.Com**

## **Acknowledgments**

I would like to thank Dr. Amer Marei for his support, advice and knowledge while serving as my major advisor during the course of this study.

Much appreciation is offered to: the German Central Ministry of Education Science Research & Technology (BMPF) for partial funding through the research project " Sustainable Management of Available Water Resources with Innovative Technologies", (SMART)

Special thanks go to Dr. S. Kayat and Dr. A. Tamimi my examiners

Special thanks go for Mr. M. Sbeih, Mr. A. Amer, Mr. M. Amarna, A. Kahleh, Miss M.Khatib and Mrs Y. Abdel Al for the technical support in the field and laboratory.

Special thanks goes for my family Nesreen, Nour Ed-din, Anwar, Aseel, Hadeel, and Sajeda, for bearing with me all difficulties.

Finally, my parents, and brothers, and all my friends deserve special thanks for their continuous encouragements and support, without their constant faith in me, this study would have never been finished.

## **ABSTRACT**

Al-Faria watershed is located in the northeastern region of the West Bank. The watershed extends for 30 km from Nablus in the west to the Jordan River in the east, with area of 331 km<sup>2</sup>. Wadi Al-Faria area is considered an important agricultural resource in Palestine.

Fresh water is scarce in Palestine, and especially in Al-Faria area. Since more than three million cubic meters of fresh water flow in the Wadi during winter months, the idea of this research is to store this good quality fresh water in underground with minimum negative quality impact and to make it possible for extraction during summer time when demand reach the highest peak.

Through Vertical Resistivity Sounding, the underground lithological profile with a depth up to 150 m is constructed. The investigated site locates in the lower part of Al-Jiftlik area, and cover an area of 1.5 km<sup>2</sup>. A gravel layer with 20 m thick, and located by 20 m depth, with total volume of 30X10<sup>6</sup> m<sup>3</sup> could be to store 8-10 mcm.

Deep infiltration ponds or injection wells are recommended to be used in ground water artificial recharge because of low hydraulic conductivity ( 38.9 x10<sup>-6</sup> m/s) that dominate the soil cover and remnants of Lisan formation, which locate in some locations very close to the surface which could influence the quality of infiltrated water through this method.

The hydrochemistry of the groundwater of the area shoes its un suitability for domestic purposes, since it's EC is very high ( $\approx 4.0$  mS/cm), and the chloride concentration is range between 700 and 1000mg/L

## ملخص

تعتبر منطقة وادي الفارعة من أهم المناطق الزراعية في فلسطين، فترتبتها الخصبة واعتدال مناخها يؤهلها لإنتاج المزروعات الصيفية والشتوية . وفي فصل الشتاء يزود الوادي السكان القاطنين حوله بكمية معقولة من المياه العذبة والتي يستخدمونها في الزراعة وفي الاستعمال البيتي.

ونظرا لقلّة المياه العذبة في فلسطين عموما، وامكانية الاستفادة من مياه الفيضانات في وادي الفارعة ، تبلورت فكرة البحث عن استغلال مياه الوادي المتدفقة في فصل الشتاء والتي تقدر بحوالي ثلاثة ملايين مترا مكعبا من المياه في السنة. ان مشكلة البحث هي ايجاد أنسب مكان لتخزين المياه السطحية حتى يتسنى لها ان تنساب داخل الارض، مما يزيد كمية المياه الجوفية المخزنة ويحسن نوعيتها، لتصبح أكثر ملائمة للاستخدامات الزراعية.

لقد استخدمت طريقة قياس المقاومة الجيوفيزيائية في التعرف على البناء الطبقي لمنطقة الجفتلك السفلى وذلك لعدة اسباب منها توفر التجهيزات الفنية لعمل القياس ولسهولة تطبيقها وبذلك تم تنفيذ ثلاثة مقاطع عرضية (شمال - جنوب) ومقطعين طوليين (غرب - شرق)، وقد تم التعرف على طبقات الطمي السطحي الحصوية بالاضافة الى طبقات الكونغلوميرات التابعة لعصر النيوجين.

لقد تم التعرف على طبقة من الحصى تصلح لتخزين مياه الفيضانات تقع على عمق 20 مترا تحت مستوى سطح الارض وقد تم تقدير مساميتها بحوالي 30% وقد تم تقدير حجمها بحوالي 30 مليون مترا مكعبا، وبذلك يمكن ان يتم تخزين 8-10 مليون مترا مكعبا من مياه الفيضانات في هذه المنطقة في حالة توفر الية لتخزين المياه في داخل الارض خلال فترة الفيضانات القصيرة.

ولكننا ومن خلال الدراسة لا ننصح بالطمر السطحي للماء وذلك لقلّة النفاذية والمسامية للتربة ، وعوضا عن ذلك ننصح بتجميع مياه الوادي في أحواض اصطناعية وبعد فترة بسيطة من الشوائب، تضخ مباشرة إلى الآبار المجاورة للوادي؟

في المنطقة السفلى من الجفتلك توجد بقية من طبقة اللسان والتي رفعت قيمة الموصلية الكهربائية للمياه الجوفية إلى 4.62 ملي سيمنز/سم . كما ان ذوبان الكالسايت والهيمايت رفع قيم الكلور والكبريت في المياه الجوفية.

<b>Table of Content</b>	<b>Page</b>
<b>Dedication</b>	i
<b>Declaration</b>	ii
<b>Acknowledgments</b>	Iii
<b>Abstract</b>	iv
<b>Table of content</b>	Viii
<b>List of figures</b>	Xi
<b>List of tables</b>	Xiii
<b>1. Chapter one: INTRODUCTION</b>	1
1.1 Topography and Terrain	1
1.2 Problem statement	2
1.3 Objectives of the study	2
1.4 Hypothesis of the study	3
1.5 Importance of the study	3
<b>2. Chapter Two: Literature Review</b>	4
<b>3. Chapter Three: Hydrogeology</b>	6
3.1 Geography of Faria Basin	6
3.2 Hydrology of Faria Basin	8
3.3 Aquifer System	16
<b>4. Chapter Four: Theoretical Framework</b>	17
4.1 Resistivity work	18
4.1.1: Vertical Electrical sounding	18
4.1.2: Lateral Pro filing or Mapping	19
<b>5. Chapter Five: Methodology</b>	22
5.1 Geophysical profiling results and analyzing	25
5.1.1: First profile	25
5.1.2: Second profile	29
5.1.3: Third profile	32
5.1.4: Fourth profile	35
5.1.5: Fifth profile	39
5.2 Sieve Analysis	42
5.3 Hydrochemistry of the ground water wells	55
<b>6. Chapter six: Results, Conclusions, and Recommendations</b>	65
6.1 Results	65
6.2 Conclusion	67
6.3 Recommendations	67
<b>7. References</b>	68
<b>8. Appendices</b>	71

## List of Figures

Fig. No.	Figure Title	Page
3.1:	Location of the study area	6
3.2:	Geologic map of Wadi Al-Faria	7
3.3:	The average monthly precipitation rates at Nablus and Al-Jiftlik stations	9
3.4:	Mean annual rain fall in Wadi Al-Faria	11
4.1:	Wenner- Shlumberger Array	18
4.2	The resistivity of rocks, soils, minerals and chemicals	20
5.1:	Location of the wells in the study area	23
5.2:	Location of the profiles	25
5.3:	Pseudo cross section for the first profile	26
5.4:	Expected lithology for the first profile	27
5.5:	Pseudo cross -section for the second profile	29
5.6:	Expected lithology of the second profile	30
5.7:	Pseudo cross -section of the third profile	33
5.8:	Expected lithology of third profile	33
5.9:	Pseudo cross- section for the fourth profile	36
5.10	Expected lithology for the fourth profile	36
5.11:	Pseudo cross- section for the fifth profile	39
5.12:	Expected lithology for the fifth profile	40
5.13:	Soil sampling sites	42
5.14:	Grain size distribution curves for the three samples A1,A2,A3	45
5.15:	Grain size distribution curves for the three samples B1,B 2,B3	50
5.16:	Grain size distribution curves for the two samplesC1,C2	53
5.17:	Texture triangle for Faria soil	54
5.18:	The electrical conductivity of the wells in the study area	56
5.19:	The temperature of the wells in the study area	56
5.20:	Concentration of TDS	57
5.21:	Concentration of Ca <sup>2+</sup> , Mg <sup>2+</sup>	58
5.22:	Concentration of Na <sup>+</sup> , K <sup>+</sup>	58
5.23:	Concentration of sulfate	59
5.24:	Contour map of sulfate	60
5.25:	Concentration of chloride	60
5.26:	Contour map of chloride	61
5.27:	Gypsum saturated index of the studied wells	63
5.28:	Aragonite saturated index of the wells	63
5.29:	Calcite saturation index of the wells	64
5.30:	Dolomite saturation index of the wells	64
B.1:	Dourove Diagrane	79
<b>B.2:</b>	Piper diagram to the studied groundwater	80
B3:	Shoeller Diagrane	81
C1:	Hydrochemical analysis to the existed wells in the study area	83
C2:	The allowed volume for artificial recharge in the whole Al-Jiftlik area	84
C3:	Possible site for artificial recharge at the study area / Al-Jiftlik	85

## List of tables

<b>Table No.</b>	<b>Table Title</b>	<b>Page</b>
3.1:	The annual precipitation for the different climatic zones of al-Faria watershed	10
3.2:	Monthly Rainfall for Faria Station 1966-1997	12
3.3:	Monthly average values for climatic variables in Al-Jiftlik	15
5.1:	Groundwater table to the existing wells in the study area	22
5.2:	Coordination of the location of soil sampling	23
5.3:	Lithology with the corresponding resistivity according to Loke, 2001	26
5.4:	Results of laboratory sieve tests for sample A1	43
5.5:	Results of laboratory sieve tests for sample A2	43
5.6:	Results of laboratory sieve tests for sample <b>A3</b>	44
5.7:	Results of laboratory sieve tests for sample B1	47
5.8:	Results of laboratory sieve tests for sample <b>B2</b>	48
5.9:	Results of laboratory sieve tests for sample <b>B3</b>	49
5.10:	Results of laboratory sieve tests for sample C1	51
5.11:	Results of laboratory sieve tests for sample C2	52
5.12:	Class name for the above samples, depending on the textural triangle	55
5.13:	Concentration of Dolomite, Calcite, Aragonite, and Gypsum	63

# CHAPTER 1

## INTRODUCTION

Palestine is located on the East coast of the Mediterranean Sea, West of Jordan and to the south of Lebanon. It lies on the north western part of the Arabian shield. During its geologic history, this shield separated from the great Afro-Arabian shield along the Red Sea line. Branch of this breakage extended along the line of Aqaba, Wadi Araba, the Dead Sea, and the Jordan Valley, and continued northwards to Lebanon, Syria and Turkey. The West Bank occupies the western part of this branch, known as the Jordan Rift Valley.

### 1.1 Topography and Terrain

**Coastal and Inner Plains:** these are among the best fertile land in Palestine and elsewhere, with adequate resources of irrigation. They are where most of the Palestinian citrus groves used to stand. The coastal stretch is divided by Jabal al-Karmel into the plain of Akka and the plain of Palestine. The inner part consists, largely, of Marj Bin A'amir. This one is triangular in shape, with Jenin and Nazareth as its base and the SE edge of the Akka plain as its sharp corner.

**The Mountains and Hills:** this part is largely rocky but has terraces which make it suitable for a number of trees. Olives is one of the most planted trees, (almonds, apples and others) in these regions. Also, there are patches of plains scattered in this region, and these are fully utilized.

They are planted with wheat, barely, lentils in winter and vegetables during the summer (mostly tomatoes, melons, maize and other vegetation that stands the hot weather).

**The Jordan Valley:** This is well below sea level, hence the name Ghor, with very good soil but very little water resources. Agriculture depends on irrigation either from local streams or the Jordan River before 1967. Due to the unique climate, that region used to produce summer vegetables in late winter stretching the availability of fresh products during winter months.

**The Southern Desert:** This region comprises almost half of Palestine. It is also triangular in shape. The base is fertile and the rest, with its apex near the town of Aqaba, is poor with scattered patches of regions suitable for cultivation. Bi'r as-sab' is the main town in that region.

## **1.2 Problem Statements**

Faria area is one of the fertile areas in the West Bank. The extended of the rain fed farming is reducing in the Wadi; farmers transferred their agricultural lands from rain fed to irrigation depending on the wells water (Environmental Quality Authority, 2006).

The Faria basin lies within the Eastern drainage basins of the West Bank. In the study area, there is a lack of hydrological knowledge and there is no reliable recharge estimation of the area. In winter, the western slopes of Al-Faria basin receive an annual rainfall of 500-700 mm and in the eastern part of these slopes receive about 350 mm (Ghanem, 1999). Approximately three million cubic meters flow in the Wadi during winter months (Forward,1998). The total recharge volume of the groundwater was estimated to be 60 million cubic meters, with infiltration rate of about 26%. (Ghanem, 1999).

The runoff cause flash floods in Wadi Al-Faria between January and March, so the question is how to use the runoff in the Wadi and which method could be used to store this water.

A shortage in fresh water recourses, inefficient use of resources, deterioration in the quality of both surface and ground water, overuse of agrochemicals, disturbed cropping patterns, and discharges of raw wastewater into natural streams and typical environmental problems in this watershed (Environmental Quality Authority ,2006)

The inefficient use of resources causes problems in the area. Also the use of open ditches as a conveyance system is still used in the Wadi. These practices lead to considerable losses in water quantities through seepage evaporation (Environmental Quality Authority.2006). In this study we will try to investigate this problem through the following objectives

## **1.3 Objectives**

The overall objective is to improve water resource in Al-Jiftlik area by using floodwater for artificial recharge, while the specific objectives are:

- 1-To investigate the areal distribution of the gravel aquifer in Al- (Jiftlik)
- 2- To investigate the thickness and physical properties of the aquifer strata.
- 3- To determine the physical properties of the soil cover.
- 4- To analyze the quality of groundwater and to compare it with the lithology.

## **1.4 Hypothesis**

1. The thickness of the unsaturated gravel aquifer in the lower part of the Wadi could be used to store flood water.
2. The physical properties of the aquifer and the overlying soil is suitable for plane artificial recharge
3. Soil type and soil thickness are responsible for reducing infiltration.

## **1.5 Importance of the Study**

The study aims to make a geoelectrical survey of the lower part of Al-Jiftlik area and to investigate if this place is suitable to store flood water in the underground water. Identify the thickness of the soil; the structural features are essential for artificial recharge. The study also aims to make a lithological map for the aquifer in the study area, by using geoelectrical methods. The importance of the study is to determine the recharge volume that can be stored in the underground depending on hydrogeological and lithological results that could be extracted from the geoelectrical investigation. Also the socio-economic revenue will increase by improving the quality of groundwater in Al-Jiftlik area.

This study is divided to six chapters, in the first chapter general idea and present about the problem statements, the hypothesis, and the objectives of the study. The second chapter covers the literature about the area. The third chapter covers the hydrology of the study, by explaining the geography of the study area, geology, hydrology of Farea basin, and aquifer system of the study area. The fourth chapter covers the theoretical frame work of vertical electrical sounding, and lateral profiling.

Chapter five covers the methodology, field and lab work, geophysical profiling, analyzing data, drawing and interpretation to the geophysical profiles, and sieve analysis to the areas soil, also hydrochemistry analysis for some groundwater wells. Results, conclusions, and recommendations are presented in the sixth chapter.

## **CHAPTER2**

### **LITRATURE REVIW**

Groundwater is considered to be the main fresh water resource in the West Bank. Water resources in the Jordan Rift valley are scarce in nature. Rapid population growth associated with rapid development in the Faria basin has put more pressure on the existing limited resources. The steep gradient of the Jordan Valley produces a shadow effect, which reduces the quantity of the rainfall in the Jordan Rift valley. There is however a considerable amount of rainfall on the West Banks (Schwartz, 1980). The Faria basin lies within the Eastern drainage basins of the West Bank. In the study area, there is a lack of hydrological knowledge and there is no reliable recharge estimation of the area

Barakat ( 2000 ) in his study for utilizing rates of rainfall and rates of runoff in the mountainous sub-catchments of Soreq stream near Jerusalem used the Unit Hydrograph and the Soil Conservation Service ( SCS ) methods .Using data obtained from (1957- 1994 ) for frequency analysis and Intensity – Duration Frequency (IDF) curves , the models were applied to simulate a unit hydrograph of the mountains of Soreq.

Ben Zvi (1996) described a model which relates the magnitude and frequency of runoff events in the arid Negev to measurable properties of the contributing watershed. A linear regression model was found to the daily volume of the direct surface runoff in Hazor River in the northern Israel with the daily depth of the causative rainfall. He resulted that the cloud seeding causes a change in the rainfall - runoff relationships and enhances the generation of the runoff.

A quantitative assessment of the surface inflows into the arid alluvial basin of the Arva valley in the southern Israel is studied by using the environmental tracers and mixing cell model.

A hydrogeological as well as hydrochemical study in the Faria drainage basin indicates that the groundwater balance is estimated to be + 16.6 mcm in the area and could be exploited without any negative affect to the aquifer system in Faria area (Ghanem, 1999). A new study by Palestine Water Authority ( PWA) shows that around 20 mcm could be exploited (PWA,2008).

An analytical study of the Rainfall / Runoff using the synthetic unit hydrograph for Wadi Faria catchments was done by Bashir (2003). In this study rainfall data are considered the major

parameter in the analysis of the rainfall- runoff relation for surface water management. The study also provides a comprehensive overview and analysis of the available rainfall data for stations in the Faria catchments, depending on data from (PWA).

Al –Nubani N.I. (2000) in his study Rainfall / Runoff Process, and Rain Fall Analysis for Nablus Basin developed an Intensity Duration Frequency curves for Nablus district by using the developed rainfall-runoff relation and obtained a Synthetic Unit Hydrograph for Rujeeb catchments.

A hydrochemical study is conducted in Al-Jiftlik area to define water types and to determine hydrochemical parameters of the aquifer system was done by Marei A, Ghanem 2007. More than 150 water samples were analyzed during the period 1995 to 1999, which covered all springs and wells. The physical and chemical properties were determined. The major cations  $\text{Ca}^{2+}$ ,  $\text{Mg}^{2+}$ ,  $\text{Na}^+$  and  $\text{K}^+$  and the major anions  $\text{HCO}_3^-$ ,  $\text{Cl}^-$ ,  $\text{SO}_4^{2-}$  and  $\text{NO}_3^-$  were analyzed. The minor constituents of  $\text{SiO}_2$ ,  $\text{F}^-$ ,  $\text{Br}^-$  and  $\text{PO}_4^{3-}$  and the trace elements Cu, Cd, Fe, Mn, Cr, Zn and Pb were determined. The main aim of this study is to determine the source of water (which layer or aquifer) (Marei. A, Ghanem 2007)

Through out this study our hydrochemical results confirm with (Marei. A, Ghanem 2007) since both studies reaches the same results which can be summarized as an increasing trend of  $\text{Ca}^{2+} > \text{Mg}^{2+} > \text{Na}^+ + \text{K}^+$  from west to east. Also  $\text{Cl}^- > \text{HCO}_3^- > \text{SO}_4^{2-} > \text{NO}_3^-$  in the phreatic eastern sub-aquifers.

Agriculture is the future sustainability to Faria's area, so water degradation and scarcity are very important for any future development of Faria area. The major idea of this study is to investigate the underground in al-Jiftlik area in order to find out the suitable site/s for artificial recharge, and as a result to identify artificial ponds, or wells for groundwater feedings (Awadallah W.and Owaiwi M, 2005).

## CHAPTER 3 HYDROGEOLOGY

### 3.1 Geography of the area

The Faria drainage basin lies in the northeastern part of the West Bank Fig.( 3.1). The basin of Faria is shaped like a fan with a length of 36 km and an area of 320 km<sup>2</sup>. From the geological and structural point of view Fig.(3.2), the Faria area is considered to be a complex with major structural features, faults and folds (Rofe and Raffetey,1965)

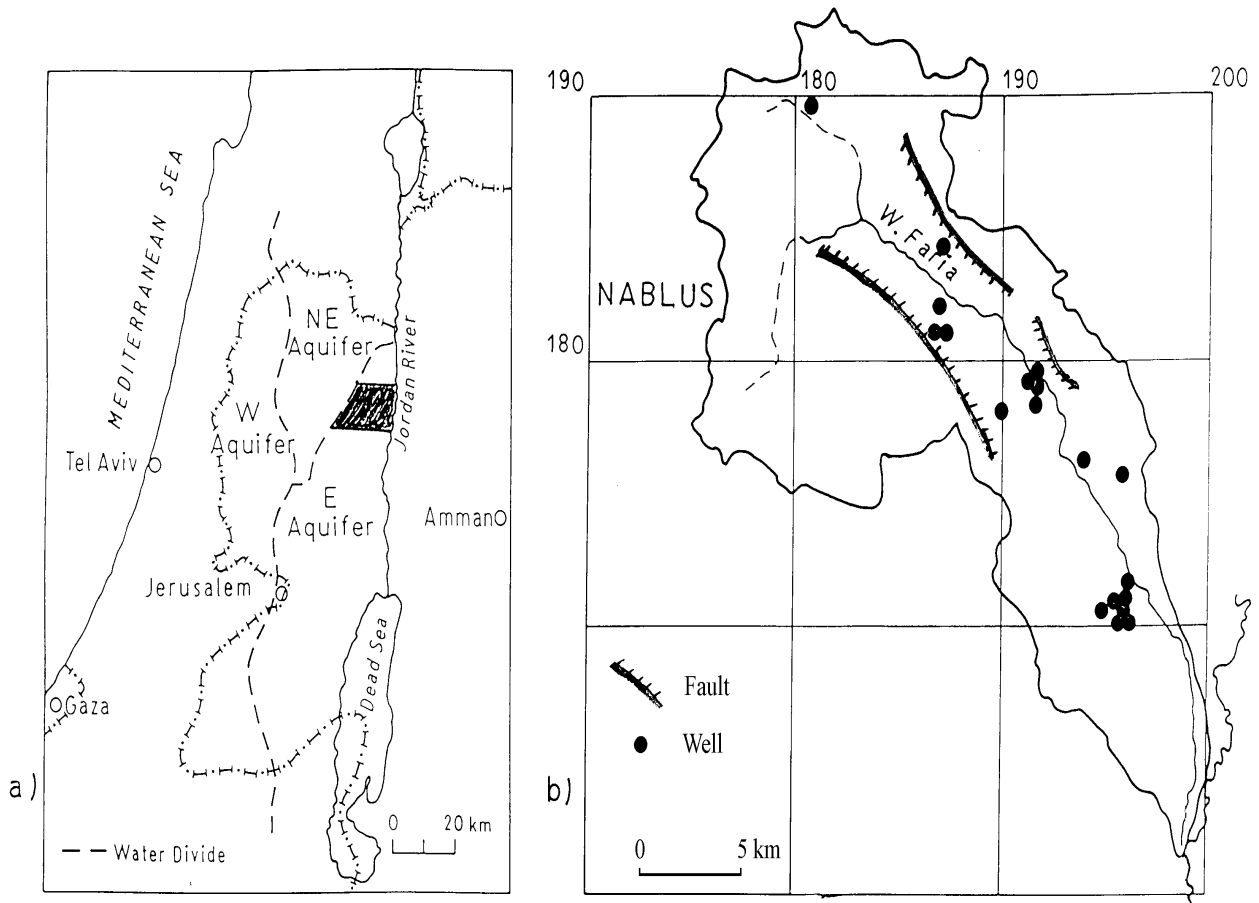


Figure 3.1: The location of the study area, a: The major groundwater basins of the West Bank  
b: The Faria Basin with the wells location



The area of study lies within the following coordinates:

Latitude: national 160000 - 195000m N (international 32° 2' - 32° 12' N),

Longitude: national 175000 - 200000 m E (international 35° 12' - 35° 35' E)

The elevation varies from 704 m above sea level in the western parts to 302 m below sea level in the Jordan Rift valley. This means in about 30 kilometers of length there is a 1.3 kilometer drop in elevation which indicates an average slope of more than 4%. A general water divide bounds the area from the west and the Jordan River from the east. The eastern part of the catchments lies within the Jordan Rift valley, which are the major structural events in the area. The western boundary of the study area is the main watershed between the Mediterranean coastal area and the Jordan Rift valley. (Ghanem M, 1999, 2007)

Based on the geomorphologic and topographical aspects, Wadi Al-Faria can be divided into four parts: (Environmental Quality Authority., 2006)

- a) post upper zone ( East of Nablus, Masaken Sha'biyya, Askar, Azmout, Beit Foreek, Beit Dajan, Tamomoun and Tubas )
- b) upper zone ( Ras Al-Faria, Wadi Al-Faria village, Khirbat Qashda and Al-Bathan )
- c) middle zone (Al-Aqrabaniyya, Al-Nassariyya, Khirbat Tall El-Ghar, Beit hassan, Ein Shebli )
- d) lower zone ( Frush Beit Dajan and Al-Jeftlik) ( Environmental Quality Authority,2006 ).

### **3.2 Hydrology of Faria Basin**

Faria basin as an agricultural area depends on rain fall in winter which vibrates from year to year. Precipitation occurs during the winter (November until May) followed by a completely dry summer. It decreases dramatically from north to south and from west to east. The number of days per year with precipitation events varies from 25 to 55 days at different stations (Rofe and Raffety, 1965). In the western part, the average rainfall is around 500-600 mm/y, towards the east and southeast, there is a sharp decrease reading.

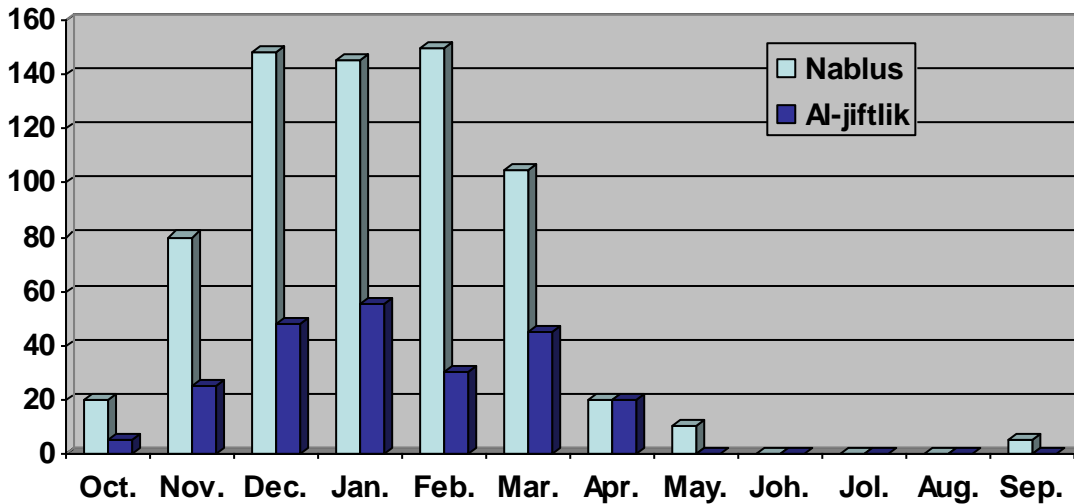


Figure3.3: The average monthly precipitation rates at Nablus and Al-Jiftlik stations (Environmental Quality Authority. The Faria and Jerash Integrated Watershed Management Project FJIWMP, 2006)

Fig.( 3.3) shows that the rainy months are from October to April, the maximum rainfall rate happens during December to March. Published data by the Metrological office of the department of Transportation (MoT, 1998) showed that for the period of 1969 to 1981, the average precipitation in Al-Jitlik was 225 mm. While based on PWA database for the period 1953 to 1989, the average annual precipitation in Al-Jiftlik was 198.6mm. And it was 182 mm per year according to Palestinian Hydrology group for the period 1965 to 2007. This fresh rain water could be collected in the area and stored as ground water, and the main obstacle her is to identify the geology and the structural features of the proposed site in the area, and determine the best place to inject the water to ground water.

Rainfall data for the Faria Basin is accessible from seven stations (Table 3-1); daily data for Beit Dajan, Toubas and Talluza; monthly data for the Faria agricultural station, Nablus, Meithlun and annual data for the Faria Police station, Faria agricultural station and Beit Dajan Station. The number of days per year with precipitation events varies from 25 to 55 days at different stations (Rofe and Raffety, 1965)

Table3.1: The annual precipitation for the different climatic zones of al-Faria watershed (Environmental Quality Authority. 2006)

Station Name	Climatic Zone	Average annual precipitation ( mm )	Year Record
Talluza	Post upper zone	630.5	1964-2002
Nablus	Post upper zone	642.6	1947-2002
Tubas	Upper zone	415.2	1968-2002
Beit Dajan	Upper zone	379.1	1953-2002
Tammoun	Central zone	322.3	1967-2002
Al-Jiftlik	Lower zone	198.6	1953-1989

Table(3.1) shows the annual precipitation for the different climatic zones of Al-Faria watershed, the average annual precipitation in Al-Jiftlik is 198.6 mm during the years ( 1953 – 1989 ) while it is 642.6 mm in Nablus , (Environmental Quality Authority. ,2006)

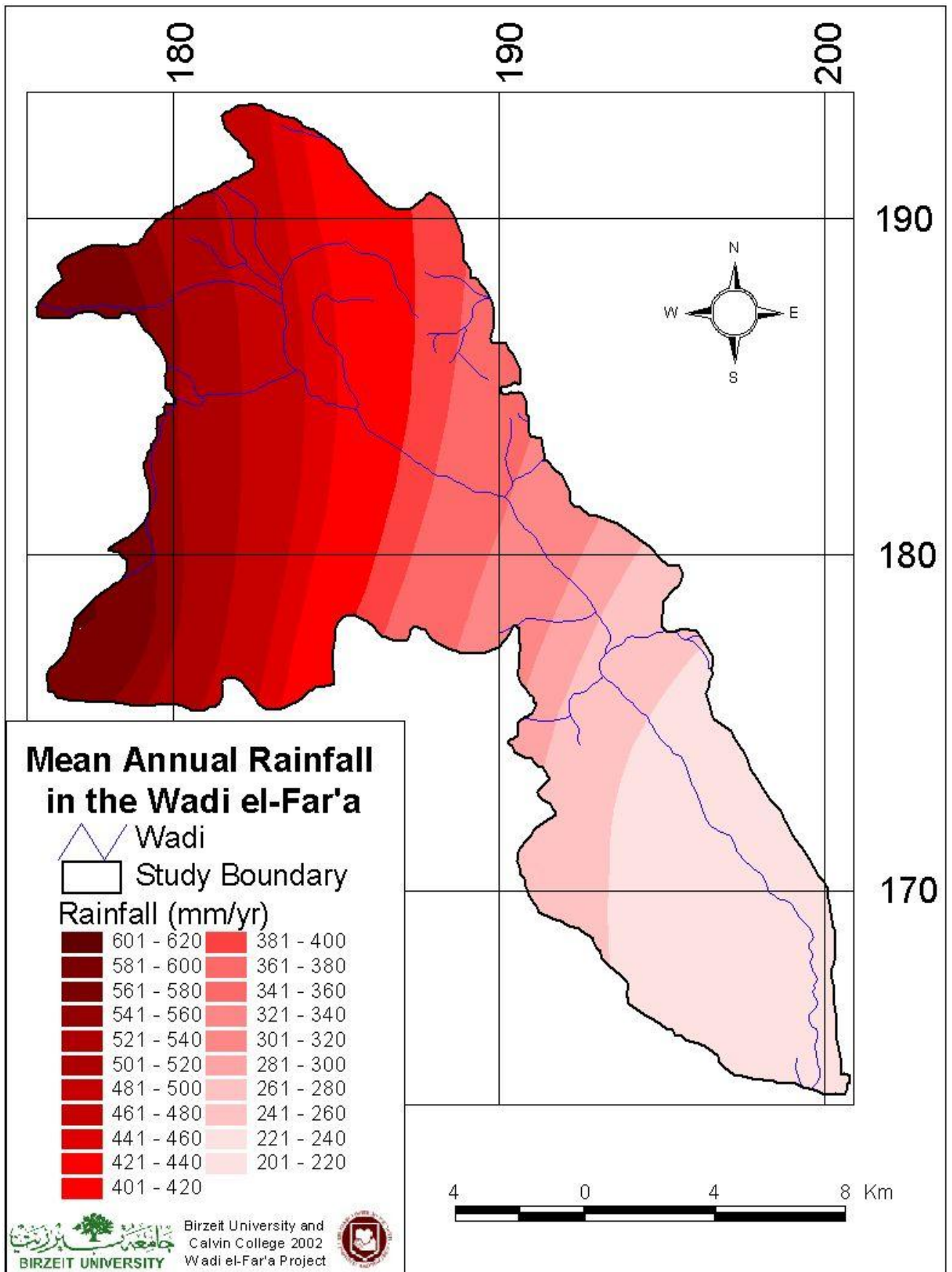


Figure 3.4: Mean annual rain fall in Wadi Al- Faria source Birzet University and Callvin College 2002

Fig.(3.4) shows that in the western part, the average rainfall is around 500-600 mm/y, towards the east and southeast, there is a sharp decrease reading ( 200- 220 ) mm/y . (Bashir, 2003)

Table 3.2: Monthly Rainfall for Faria Station 1966-1997, (Bashir 2003)

Year	Hydrological year	Oct	Nov	Dec	Jan	Feb	Mar	Apr	Ma y	Jun	Jul	Aug	Sep	Yearly rainfall
1966	1965/1966			45	22	48	61							176
1967	1966/1967				83	31	103	0	29					245
1968	1967/1968			22	78	14	27	10	6					158
1969	1968/1969	2	4	55	51	10	50							172
1970	1969/1970	17	23	130										170
1972	1971/1972		51	68	49	52	67	14						301
1973	1972/1973	7	23	28	60	2	52							173
1974	1973/1974		48	11	209	60	57	27						411
1975	1974/1975		25	35	13	79	22	7						180
1976	1975/1976		26	37	15	57	41	10						186
1977	1976/1977	7	50	6	73	17	62	29						243
1978	1977/1978			74	19	12	15							119
1980	1979/1980	28	38											65
1982	1981/1982	6	27	2										34
1983	1982/1983					78								78
1986	1985/1986							8	22					30
1987	1986/1987	9	114	40	26	15	26	1						230
1988	1987/1988	26	3	61	55	107	24	6						280
1989	1988/1989	5	20	78	44	39	216							401
1995	1994/1995	34	127											161
1997	1996/1997		10											10
	Average	14	39	46	57	41	59	11	19					182
	Standard Diviation	11	36	33	50	31	51	10	12					109
	Min	2	3	2	13	2	15	0	6					10
	Max	34	127	130	209	107	216	29	29					411
	P20	4	8	18	15	15	16	3	9					90
	P80	23	70	74	99	67	101	19	29					274

Table (3.2) shows that the rainy months in Faria Station located at Al-Jiftlik area occur during November to April, the maximum rainfall in January with an average of 57 mm / year. ( Bashir 2003 )

$P_{20}$  is probability of non-exceedence with 20%, where  $P_{20} = \text{Average} - 0.84 * \text{Standard deviation}$ .

$P_{80}$  is probability of non-exceedence with 80%, where  $P_{80} = \text{Average} + 0.84 * \text{Standard deviation}$ . (De Laat, P.J.M., 1999, Workshop on Hydrology, Lecture Notes, Delft University, The Netherlands)

**Evapotranspiration:** Potential evapotranspiration is defined as the water loss from continuous surface of turf which fully shades the ground, exerts little or no resistance to the flow of water into the atmosphere, and always has an adequate supply of soil water (California Irrigation Management System. Potential evapotranspiration is important in predicting the water requirements of turf grown under irrigation (California Irrigation Management System, 2005)

Potential evapotranspiration can be calculated by: Penman, Priestley-Taylor and Makkink methods.1998. The choice for either of the three is governed by: user preference, and availability of weather data. The Penman method is preferred and applied for the case of water requirement to the date palm (Hasan R. Shabana, 1996) and requires the availability (in the weather data file) of five weather variables which are: radiation, maximum and minimum temperature, wind speed and vapor pressure. The Priestley-Taylor and Makkink methods only require radiation and minimum and maximum temperature (California Irrigation Management System, 2005).

Penman equation predicts the daily Potential evapotranspiration based on net radiation, vapor pressure, and wind speed, it is given by the formula

$$\lambda ET = \frac{(\Delta(Rn - G) + \rho_a c_p)(e_s - e_a)}{\Delta + \gamma(1 + r_s/r_a)} \quad \text{eq. 3.1}$$

where  $R_n$  is the net radiation,  $G$  is the soil heat flux,  $(e_s - e_a)$  represents the vapor pressure deficit of the air,  $\rho_a$  is the mean air density at constant pressure,  $c_p$  is the specific heat of the air,  $\Delta$  is the slope of the saturation vapor pressure – temperature relationship,  $\gamma$  is the psychrometric constant,  $r_s$  and  $r_a$  are the ( bulk ) surface and aerodynamic resistance which is given by the formula

$$r_a = \frac{\ln \left( \frac{Z_m - d}{Z_{om}} \right) \ln \left( \frac{Z_h - d}{Z_{oh}} \right)}{k^2 U_z} \quad \text{eq. 3.2}$$

$$r_s = r_l / LA_{\text{active}} \quad \text{eq. 3.3}$$

Where

$r_a$  aerodynamic resistance (  $\text{sm}^{-1}$  )

$r_s$  bulk surface resistance (  $\text{sm}^{-1}$  )

$Z_m$  height of wind measurements (m)

$Z_h$  height of humidity measurements (m)

$d$  zero plane displacement height ( m )

$Z_{om}$  roughness length governing momentum transfer ( m )

$Z_{oh}$  roughness length governing momentum transfer of heat and vapor ( m )

$K$  von Karaman's constant, - 0.41

$U_z$  wind speed at height  $z$  ( $\text{ms}^{-1}$ )

$r_l$  bulk stomatal resistance of the well-illuminated leaf (  $\text{s m}^{-1}$  )

$LA_{\text{active}}$  active sunlight leaf area index ( $\text{m}^2$  leaf area  $\text{m}^{-2}$  soil surface. (California Irrigation Management system, 2005)

Potential evapotranspiration reaches a total of 300 mm per month in summer, and 120 mm during winter in the lower Faria. In other months of the transitional period, it ranges between 180 to 240 mm (Meteorological service, 1997, Ghanem.M 2007).

The yearly average of potential evapotranspiration in the Upper Faria ranges between 1560 and 1750 mm/year .The average actual evapotranspiration is calculated to be 345.4 mm per year for the whole basin, (Ghanem .M, Marei A. 2007).

Thus monthly average values for climatic variables in Al-Jiftlik were measured from a US Class. A pan at Al-Jiftlik station for the period 1970-1992 as shown in the table 3.3.(Ministry of Transport,1998 , Environmental Quality Authority ,2006 )

Table3.3: Monthly average values for climatic variables in Al-Jiftlik (Ministry of Transport, 1998, Environmental Quality Authority, 2006)

Month	Max. Tem. ( ° C )	Min. Tem. ( ° C )	Mean Temp. ( ° C )	Wind Speed(at 2m high in km/day )	Relative Humidity ( % )
September	36.6	22.9	29.8	5.1	43
October	33.5	20.2	26.9	5.8	54
November	27.9	16.8	22.4	5.8	55
December	21.5	11.9	16.7	7.9	67
January	19.5	9.3	14.4	4.6	73
February	20.2	9.2	14.7	6.5	73
March	24.3	12.1	18.2	10.8	63
April	29.1	14.4	21.7	9.7	63
May	34.6	19.0	26.8	6.5	52
June	37.1	21.1	29.1	5.1	51
July	39.4	22.7	31.1	5.1	51
August	38.5	24.2	31.4	5.4	52
Annual	30.2	17.0	23.6	6.5	58

**Temperature:** In the western higher elevated parts of the study area, the daily maximum temperature in the winter months ranges between 13°C and 14.8 °C; while in summer the records are between 17.2 and 19.7 °C. The average daily maximum in the eastern lower elevated parts of the area range from 16°C ( in January) and 35.7°C (in July).

**Humidity:** The source of humidity in the region is the Mediterranean Sea and only western winds bring humidity to the area. Eastern winds coming from the desert are usually dry.

In the period 1970 to 1979, the average daily maximum relative humidity in the western part of the area is 77% in winter and 83% in summer (meteorological service, 1997). For the same period in the eastern parts, the annual maximum is about 60% and the yearly minimum range between 5 to 10% during hot days and 80 to 90 % on rainy days. (Environmental Quality Authority. 2006)

**Wind:** The main wind direction is from west, southwest and northwest at a speed of 10 - 13 knots and 10 - 12 knots, respectively. Variations during winter are associated with the pattern of atmospheric depressions passing from west to east over the Mediterranean. During the khamaseen, the temperature increases, the humidity decreases and the atmosphere becomes hazy with dust of desert orison. Wind velocities decrease with elevation, the annual average wind speed in Al-Jiftlik was estimated at 106 km/day at highest of 2 meters.(Environmental Quality Authority ,2006 )

**Runoff and Surface Water:** Surface runoff in the eastern slopes of West Bank is mostly intermediate and occurs when rainfall exceeds 50 mm in one day or 70 mm in two consecutive days ( Bestire , 2002, Marei A, Ghanem 2007 ).

Surface runoff of Wadi Al-Faria is high compared to other Wadis in the West Bank because of the steep slopes of the area. Runoff decreases from west to east as the slope becomes more gentile eastwards down the Wadi and rainfall rates reduce.

### **3.3 Aquifer System**

The Eocene aquifer consists mainly of limestone with chalk, chert bands and marl; while the Pleistocene aquifer consists of unconsolidated beds of sands, gravel, cobbles, and boulders. The Neogene Aquifer consists of well cemented conglomerates. Limestone and dolomite build up the cenomanian Turonian. (Marei A, Ghanem, 2007).

The various local aquifers may be grouped into two major aquifer systems:

The alluvial aquifer is present at the floor of the Jordan Valley and the fans of the incoming wadis, where the alluvium is in contact with the aquifers of Upper Cretaceous age. The thickness of the alluvium in the Jordan Valley varies from zero along the eastern boundary to about 750 m in the deepest part of the basin near the Jordan River. On the western side of the Jordan Valley, the term Shallow Aquifer Hydraulic complex is used. It comprises Pleistocene sedimentary and alluvial deposits of the Quaternary age which receive localized annual recharge from wadi flows. The extent to which this aquifer is recharged from lower aquifers has not been determined and may be a function of faulting and fracturing (Marei A, Ghanem 2007)

**Upper Cretaceous Limestone Aquifer System:** The aquifer system is subdivided in at least an upper and a lower aquifer system. In terms of extracted volumes, this is the most important aquifer system in the region. It receives the major part of the groundwater recharge in the area, occurring mainly in the high mountain regions. (Marei A, Ghanem 2007)

## CHAPTER 4

### Theoretical Framework

Geoelectrical investigation of ground water in Faria Basin was done by the electrical resistivity method which is widely used for soil or rock lithology identification, groundwater investigation. The depth of investigation of ground resistivity is related to the spacing of the electrodes and electrode configurations.

The choice of the best type for a field survey depends on the type of structure to be mapped. Practically the arrays that are most commonly used are: (M .H. Loke, 2001)

- a) Wenner array
- b) Wenner –Schlumberger array
- c) Dipole-dipole array
- d) Pole-pole
- e) Pole dipole (M .H. Loke , 2001 )

Among the characteristics of any array that should be considered are: (M .H. Loke , 2001 )

- 1) The depth of the investigation
- 2) The sensitivity of the array to vertical and horizontal changes in the subsurface resistivity
- 3) The horizontal data coverage, and
- 4) The signal strength.

Schlumberger method was used to conduct geoelectrical investigation by using Earth Resistivity Meter (ERM) to draw geophysical profiles to Al-Jiftlik site.

The Wenner array is an attractive choice for a survey carried out in a noisy area (because of its high signal strength), and also if good vertical resolution is required. The dipole-dipole array might be a more suitable choice if horizontal resolution and data coverage is important assuming the resistivity meter is sufficiently sensitive and there is good ground contact .The Wenner-Schlumberger array is a reasonable all-round alternative if both good lateral and vertical resolutions are needed, particularly if good signal strength is also required. The pole-dipole array with measurements in both the forward and reverse direction might be a viable

choice if the electrical system with a limited number of electrodes. For surveys that required electrodes spacing and good horizontal coverage the pole-pole array might be a suitable choice (Loke M.H,2001).

#### 4.1: Resistivity work

##### 4.1.1: Vertical Electrical Sounding VES:

The fraction of total current that flows at depth varies with the current – electrode separation, the field procedure use a fixed center with an expanding spread. Although the pole-dipole array is not suited to this technique, the presence of horizontal or gently dipping beds of different resistivities is best detected by the expanding spread. Hence the method is useful in determining depth of overburden, depth, structure, and resistivity of flat – lying sedimentary beds and possibly of basement also if it is not too deep.

It is frequently necessary to carry out this expansion procedure at several locations in an area, even when the main interest may be in lateral exploration, to establish proper electrode spacing for the lateral search. (Telford W.M, Geldart L.P., and Sheriff R.E.,1990).

Wenner – Shlumberger use VES method in field surveys to measure the resistivity by injecting current into the ground through the two current electrodes (A and B in Figure 4.1), and measuring the resulting voltage difference at two potential electrodes (M and N). From the current (I) and potential (V) values, an apparent resistivity ( $\rho_a$ ) value is calculated.

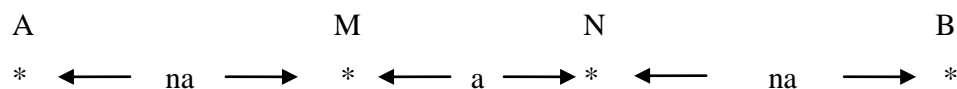


Fig.4.1: Wenner – Shlumberger Array

$$\rho_a = k \Delta V / I \quad \text{eq. (4.1)}$$

Where k is a geometric factor given by:

$$k = \pi n (n+1) a \quad \text{eq. (4.2)}$$

"n" is an integer value, non integer values can also be used.

(M.H. Loke, 2001)

#### 4.1.2: Lateral Profiling or Mapping:

This method is particularly useful in mineral exploration, where the detection of isolated bodies of anomalous resistivity is required. Any of the electrode arrangements may be used, the selection depending mainly on the field situation. In Wenner, Schlumberger, and Pole-Dipole surveys the apparent resistivity is plotted at the midpoint of the potential electrodes, except where one of these is effectively at infinity, as in the modified three-probe system, when the station is reckoned at the near potential electrode. (Telford W.M ,Geldart L. P ., and Sheriff R.E .1990 )

For the double – dipole, the station is at the barray midpoint. When the potential electrodes are closely spaced with respect to the current spread, as in the Schumberger and possibly of the three-point system, the measurement is effectively of potential gradient at the midpoint, this can be seen from equation (4.3), ( Telford W.M ,Geldart L. P ., and Sheriff R.E .1990 )

$$\rho_a = \frac{\pi L^2 (\Delta V)}{I (\Delta r)} \quad \text{eq. (4-3)}$$

Where

$\rho_a$  The apparent resistivity ohm meter

$I$  the current m. ampere

$\Delta V$  the voltage m. volt

$\Delta r$  the distance between current electrodes pair m

$L$  the distance between voltage electrodes pair m (Telford W.M ,Geldart L. P ., and Sheriff R.E .1990 )

The ground resistivity is related to various geological parameters such as the mineral and fluid content, porosity, and degree of water saturation in the rock. Electrical resistivity surveys have been used for many decades in hydrogeological, mining, and geotechnical investigations. ( M. Loke 2001 ). Resistivity of natural water and sediments without clay vary from 1 to 100  $\Omega\text{m}$  while the resistivity of wet clays alone may vary from 1 to 120  $\Omega\text{m}$  ( Parasnis 1986 , Fouad, Shaaban 2001 )

The resistivity of common rocks, soil materials, minerals and chemicals (Telford et al. 1990) is shown in Fig.(4.2).

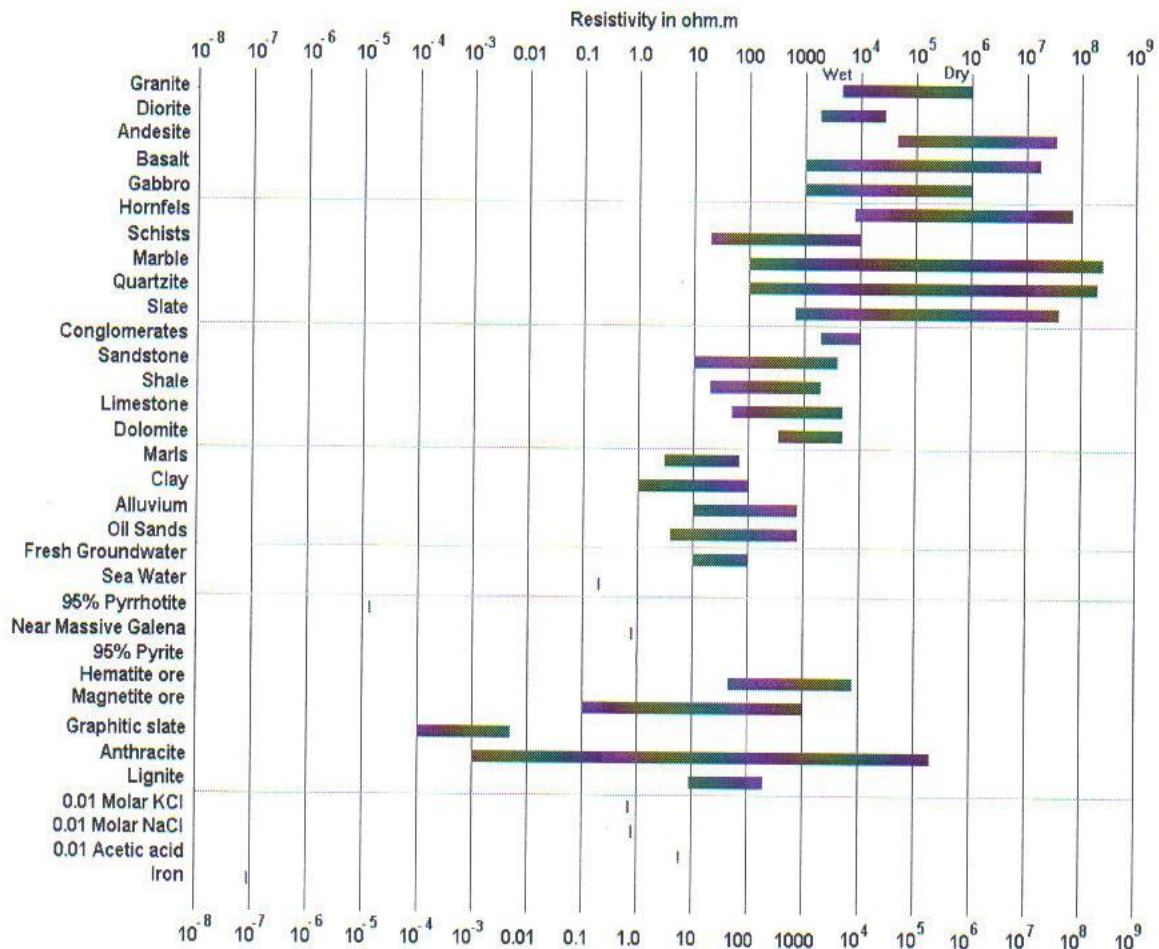


Figure4.2: The resistivity of rocks, soils and minerals (Telford et al. 1990)

Resistivity of natural water and sediments without clay may vary from 1 to 100  $\Omega$ m while the resistivity of wet clays alone may vary from 1 to 120  $\Omega$ .m ( Parasnis 1986 , Found , Shaaban 2001 ) .

The resistivity of a layer saturate by saline water and some dissolved solids are in the range of 8- 50 $\Omega$  ( De Beuk and De Moor 1969 ,Sohdy 1969 , Claudia Sainato et al 2003 ) .

Layer resistivity obtained by the inversion process is controlled by the resistivity of the pore water and resistivity of the host rock ( Telford 1990 , Burger 1992 ). Two dimensional (2 D) electrical surveys are the most practical economic compromise between obtaining very accurate results and keeping the survey costs down ( Dahlin 1996 ) .

Two dimensional electrical imaging / tomography surveys are usually carried out using a large number of electrodes 25 or more connected to a multi –core cable (Griffiths & Barker 1993). Geographic Information System (GIS ) provides powerful tool for geoelectrical data analysis and interpretation ( Jafar Ghayoumian et al 2005 ) .

All resistivity methods employ an artificial source of current , which is introduced into the ground through point electrodes or long line contacts , the latter arrangement is rarely used nowadays ( Telford 1990 ). Another classical survey technique is the profiling method. In this case, the spacing between the electrodes remains fixed, but the entire array is moved along a straight line .This gives some information about lateral changes in the subsurface resistivity, but it cannot detect vertical changes in the resistivity. Interpretation of data from profiling survey is mainly qualitative (M.H.Loke 2001).

## CHAPTER 5

### Methodology

Field work and field survey were basic modules in every aspect of this study , especially to confirm the data collected from site visit, identifying and mapping the existing target water resources, identifying and mapping possible drainage pathways, in addition to water level measurements and water flow rate to and out of Faria Basin. The soil type is determined and the soil thickness is investigated in addition to the textural features exist in the place.

The following procedures and activities are done in order to achieve the study objectives:

1. Ground water table is measured to eight wells in Al-Jiftlik area; the results are shown in table (5.1), The locations of these wells are shown in Fig.( 5.1)

Table (5.1): Ground water table to the existing wells in the study area

Well ID	Owner	X coordinate	Y coordinate	Z coordinate	Water Table m
19-17/055	Jawad Al Masri	196150	173400	-230	53
19-17/007	Fathalla Al Masri	196640	172290	-244	45
19-17/027	Issa Smadi	196250	171470	-249	41
19-17/002	'Inad Al Masri	196520	171240	-253	37
19-17/031	Solayman Abo - Awage	197680	171060	-256	25
19-17/021	Hazza' Majed	196520	171560	-249	41
19-17/001	'Inad Al Masri	196900	170740	-255	35.5
19-17/028	Ali Dahdur	198150	170500	-268	33

2. Due to the fact that the whole area were plugged at depth of 50 cm, eight soil samples were collected from the study area at depth 5-10 cm table (5.2) present the coordination of the samples sites. Fig.(5.13) represent the location of soil sampling.
3. Sieve analysis to the soil is done, and grain size distribution curves are drawn, and hydraulic conductivity is estimated to eight soil samples, the procedure and results of sieve analysis are shown in section 5.2 pages 42-55.
4. The soil type was described, and its thickness, porosity, permeability

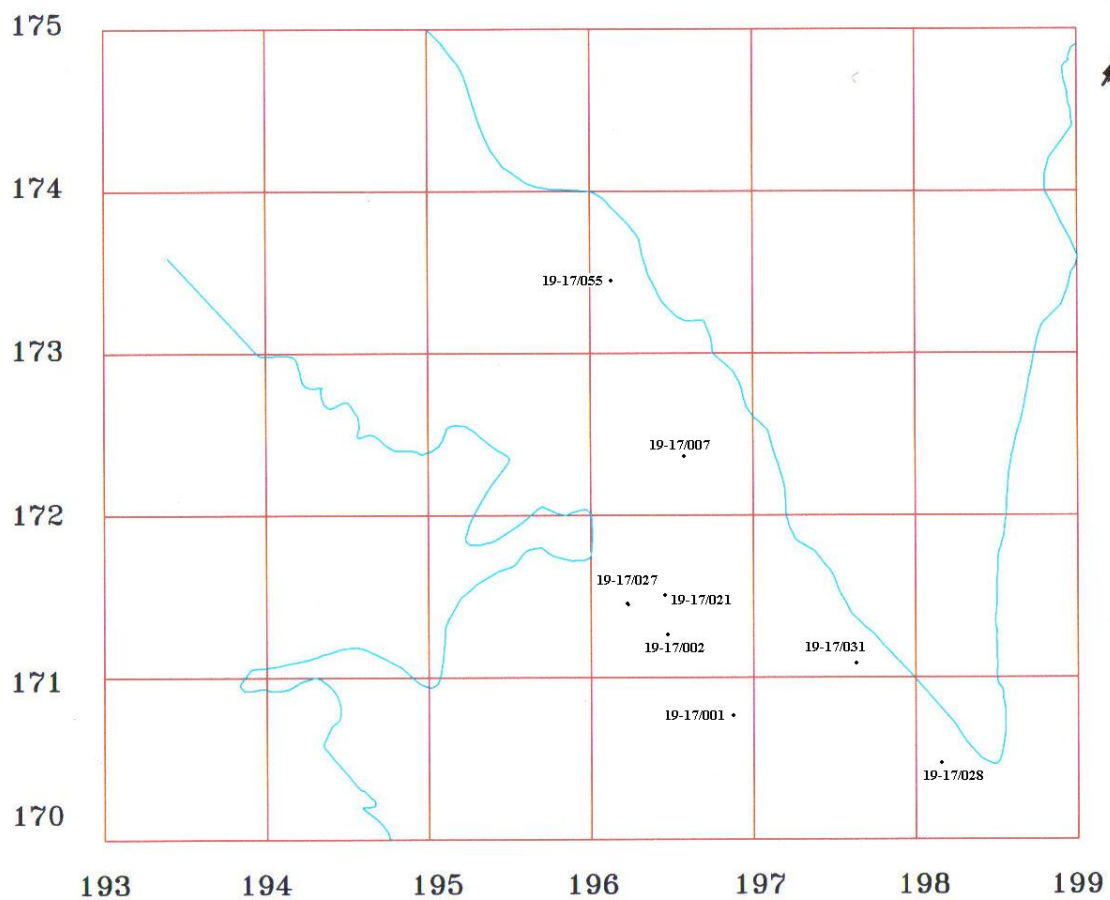


Fig.(5.1): Location of groundwater wells

Table (5.2): Coordination of the location of soil sampling

Sample ID	X coordinate	Y coordinate
A1	198080	170428
A2	198107	170470
A3	198083	170428
B1	197356	171137
B2	197379	171183
B3	197332	171090
C1	196941	171550
C2	196950	171595

See Fig.(5.13) for soil sampling site.

5. The resistivity of five sections was determined across the Wadi, see Fig (5.2).

Resistivity sounding method provide information about the geophysical properties of the layers of an area, by measuring the phase shift of current injected into the ground and the voltage seen at the potential electrodes with resolution. The resistivity technique is superior at least theoretically, because quantitative results are obtained by using a controlled source of special dimensions.( Telford et al, 1990).

Schlumberger method was used to conduct geoelectrical investigation by using Earth Resistivity Meter (ERM) to draw geophysical profiles in Al-Jiftlik area. The aim of this investigation is to determine the thickness and distribution of different strata and to determine possible artificial groundwater recharge in some sites along the Wadi.

The collected data was then introduced to the computer via IPI2WIN( MT) v.2.0 free software program from Moscow State University Geological Faculty Department of Geophysics.

## 5.1: Geophysical Profiling, Results and Discussion

### 5.1.1: First Profile

This profile covers a distance of a bout 1000 m long and reaches a depth of 200 m in the southern part, 100 m in the middle and 80 m in the northern part of the profile, it locates within the Palestinian coordinates X = 197933 – 198107m, Y = 170304 – 170470m, and with an elevation 251m bsl, as shown in Fig 5.2

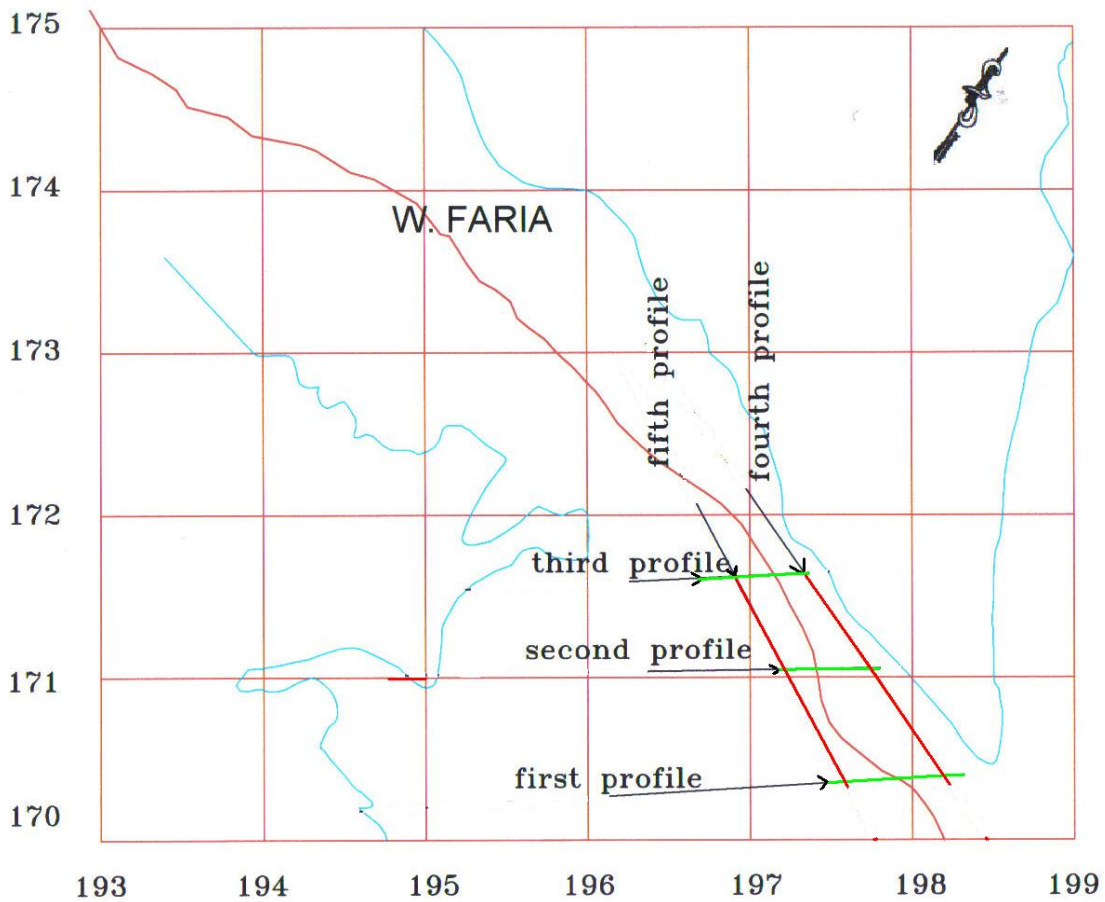


Fig5.2: Location of the profiles

This profile is extended from south to north, five stations was taken in this profile with 50m between each station, in order to satisfy overlapping of the vertical electrical sounding of ERM, the voltage, current and the ratio  $\Delta V/I$  were measured, the results are drawn and modeled as in Fig. (5.3)

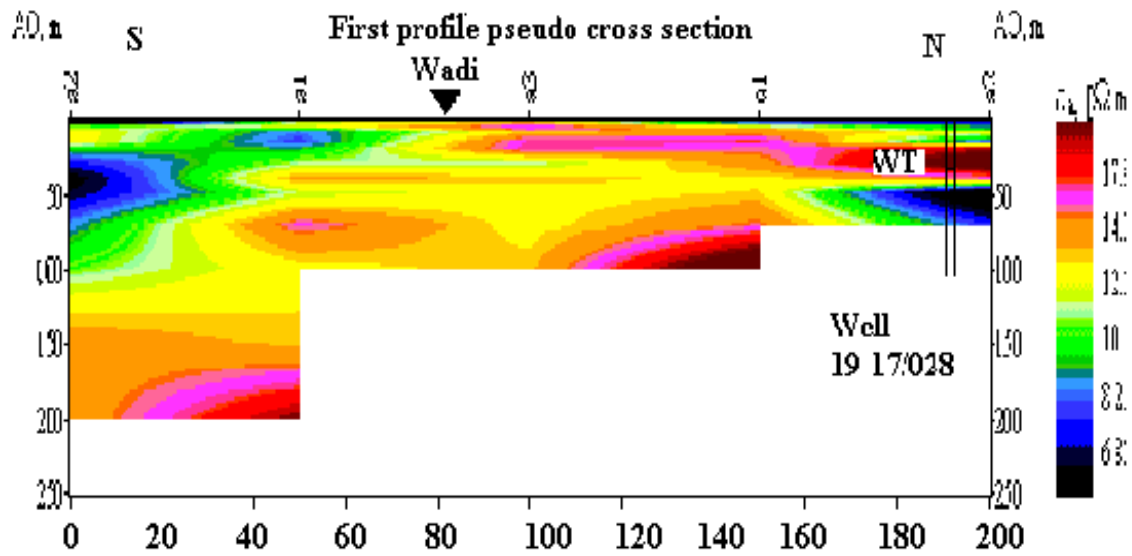


Figure 5.3 Pseudo cross section for the first profile

The pseudo section gives a very approximate picture of the true subsurface resistivity distribution. However it is useful as a means to present the measured apparent resistivity values in a pictorial form, and as an initial guide for further quantitative interpretation. (M.H.Loke, 1996-2001). Evaluation of these data depends on the resistivity of rocks, soils and minerals shown in Fig.(4.2).

The expected lithology corresponding to resistivity could be classified as shown in table (5.3)

Table 5.3: Lithology with the corresponding resistivity according to Loke, 2001

Resistivity $\Omega$	Expected lithology	Shape
1-3	Lisan Formation	—
5-20	Fine Fluvial Material	■
20 -35	Alluvian Aquifer	■
35 – 45	Neogen Formation	■
55 – 70	Carbonate Rock	■

According to the geological map sheet, table 5.1, Fig. 4.2, and from the geoelectrical results and through our field investigations, we developed the next lithological profile shown in Fig.(5.4)

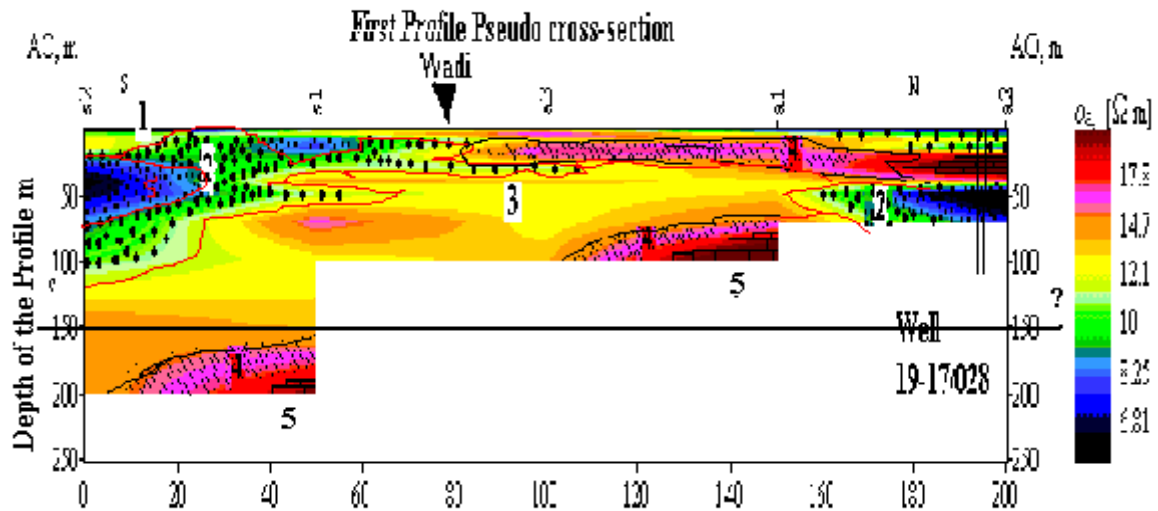


Figure5.4: Expected lithology for the first profile.

As shown in Fig.5.4: five distinguished layers could be seen they are:

### Layer number 1

This layer covers the upper southern surface, it is expected to be divided to two sub layers, dry alluvium layer, with resistivity ranges between (9 - 12  $\Omega$ ), and thickness of about 1- 5 m, and the second sub layer with fine wet fluvial soil material with resistivity (3-8  $\Omega$ ), it locates at 1-20 m below the surface, and nearly horizontal with thickness about 15 m. Lisan formation layer is seen in the southern part with resistivity ranges between (1-3  $\Omega$ ), it locates 3 m below the surface, with thickness about 2m.

### Layer number 2

This layer locates 15-100 m below the surface with average thickness about 50 m. The resistivity of this layer ranges between (9 - 12  $\Omega$ ). It is expected to be alluvium deposit layer inclined from north to south. This layer is located 15 m below the surface of the mid profile, and declined to 100 m below the southern surface of the profile.

Low resistivity zone can be identified inside this layer with resistivity value of (5-9  $\Omega$ ), this zone is located 30- 60 m below the southern part of the section, and has a thickness of 30m

in the south and wedged out in the north with a thickness of less than 10 m. It is expected to be a formation containing saline water, which could be a result of water-rock interaction of Lisan formation.

### **Layer number 3**

This layer is found in the southern part of the section and extends to the north. It has a thickness of 80 m in the south and wedge out in the north with a thickness of less than 10 m. The resistivity of this layer ranges between (12 to 35  $\Omega$ ). This layer is expected to be wet Neogen formation. Dry zone is seen by 50 -70 m below the mid surface of the section, it has a convex lens shape with thickness 15-20 m , the resistivity of this layer ranges between ( 25-35  $\Omega$ ). This layer is expected to be cemented fragment Neogen formation.

### **Layer number 4**

This layer is found in the southern and middle part of the profile. The southern zone locates 150-200m below southern surface of this profile, with resistivity ranges between (15-25  $\Omega$ ). The thickness of this layer is about 30 m. This layer is expected to be alluvial deposit sediment. This layer could be contain water with a high electrical conductivity with chloride contents range 100-1000 mg/L which reduce the resistivity from (45-55  $\Omega$ ) to ( 15 – 12  $\Omega$ ) as in Fig (4.2).

The middle zone, which is found by 10 to 20m below the surface, and between 20 and 40 m below the northern part of the profile. Also same deposit is found about 80 m below the surface of the mid profile. A low resistivity formation is found about 50m below the northern surface with a thickness of about 20 m, the resistivity of this layer ranges between 2-5  $\Omega$ . It is expected to be a formation contains saline water, which could be brine that stored in this layer during and after the formation of Lisan Lake.

### **Layer number 5**

This layer locates at a depth between 180 and 200 m below the southern surface, with resistivity ranges between 55 and 70  $\Omega$ . The thickness of this layer is about 20 m. This layer is expected to be carbonate rock. The same deposit is found at a depth of 80 m below the mid of the surface with thickness of 50 m in the middle and decreases to 10 m in the

south. Also the same formation is found at a depth of about 25 to 30 m below the northern part of the profile.

General view to this profile, we can clearly see that there is a Neogene conglomerate layer that can be used as a possible artificial recharge site to groundwater.

Water table of the nearest well number 19-17/028 is **33m**. The hydrochemistry of this well is shown in appendix A6 page 77.

### 5.1.2: Second Profile

It is 500 m long, and reaches a depth of 200m, it locates within the Palestinian coordinates X = 197332 – 197379 m, Y = 171090 – 171183 m, and elevation of 263 m bsl., as shown in Fig 5.2.

Fig. (5.5) shows the expected lithological layers of the second profile, three stations were taken along this profile with a distance of 50m between each one, in order to satisfy overlapping of the vertical electrical sounding of ERM, the voltage, current and the ratio  $\Delta V/I$  were measured.

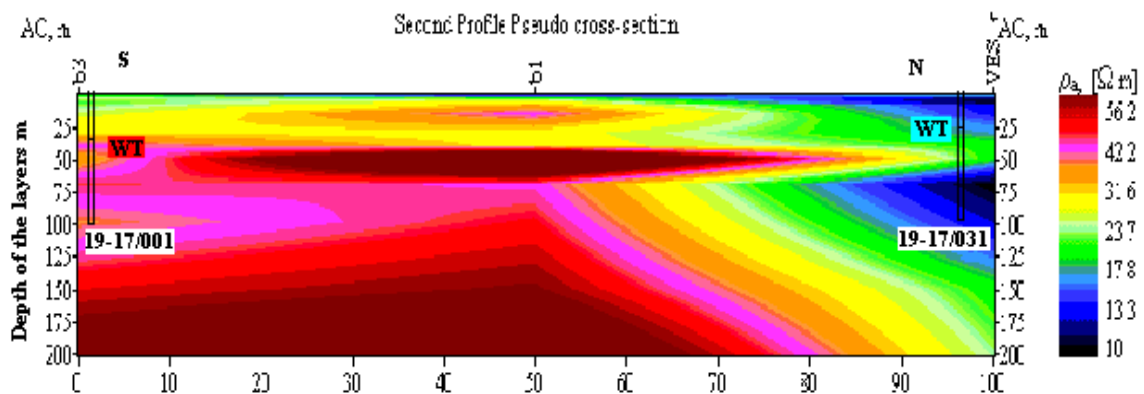


Figure5.5: Pseudo and resistivity cross section for second profile

From the resistivity results and through our field investigations, we developed the lithological profile (Fig.5.6), where five layers are identified.

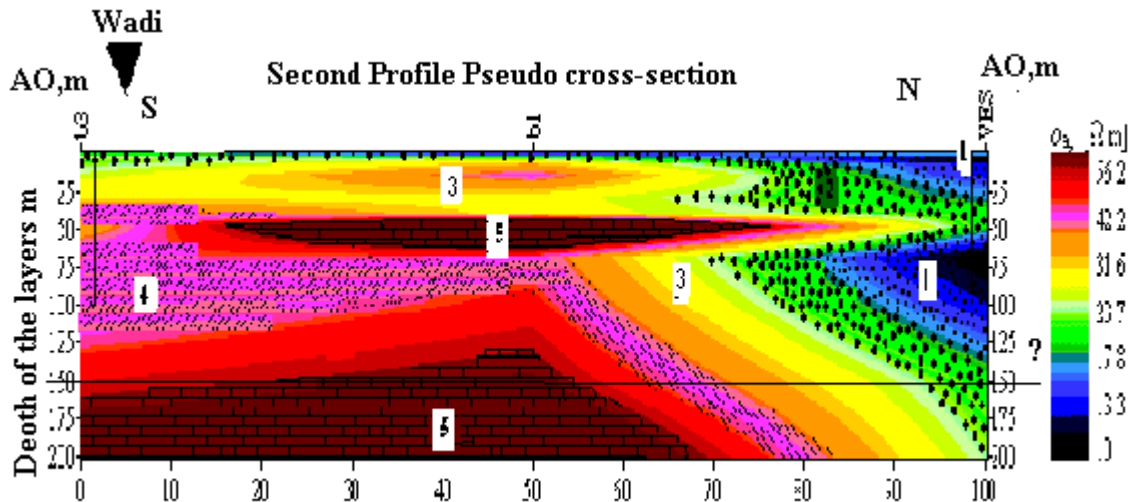


Figure 5.6: Expected lithology of the second profile

### 1. Layer number 1

This layer is the soil horizon located at the surface and is expected to be fine fluvial soil material extended from the north to the south. The fluvial soil material with resistivity ranges from (10 to 15  $\Omega$ ), looks like a triangle, and extend from north with depth about 1 to 20 m below the surface, to the south it become thinner and reach 1 to 2 m below the surface. In the middle, this layer is nearly horizontal with thickness of about 3 to 5 m, and extended to the south of the profile. This layer expected to be formed by soil overlying the Lisan formation layer. The low resistivity of this complex layer is related to the irrigation water as well as the salty evaporate of the Lisan formation.

The same fine fluvial deposit is seen 50-130 m below the northern part, next to the mountain slope, with a triangular shape of 80 m base and wedges out to less than 1m to the south. In this section, low resistivity layer of 2- 5  $\Omega$ , is seen. This layer locates about 60 to 80m below the surface with a thickness of about 20 m. It is expected to be a formation contains water, with high salinity.

### 2. Layer number 2

This layer is expected to be Alluvium deposit; it has a Z shape with a thickness vary between 35 and 75 m, this layer is found mostly in the northern part of the profile. The resistivity ranges between (15 to 25  $\Omega$ ), which could be interpreted as a layer contains

water with a high electrical conductivity. Chloride contents ranges between 100-1000 mg/L and reduce the resistivity of this layer from 45 – 55  $\Omega$ , to 15 -22  $\Omega$  as seen in Fig (4.2). The same deposit layer, with a depth ranging from less than 0.5 m spread at top soil in the southern part of the profile.

Groundwater well number 19-17/031 with a depth of 100 m, and water table of 25m penetrates this layer and abstract water from the alluvium deposit. The electrical conductivity is **3.51 m S/cm** which reflects the lithology of the layer. The hydrochemistry of this well is shown in appendix C1 page 83.

### **3. Layer number 3**

This layer is expected to be Neogene conglomerate deposit. The resistivity ranges between 20 and 45  $\Omega$ . This layer locates in the middle of the profile and has a lens shape extended from south to north in the middle of the profile, and reaches a depth of 10 to 15 m below the surface. Its thickness is about 10 m, and about 100-120 m long. This layer is Neogene conglomerate and act as a good aquifer where the ground water table locate by 25-35 m by wells number 19-17/031 and well number 19-17/001. The wet Neogene conglomerate layer is surrounded by less resistivity layer with resistivity ranges between 20 to 35  $\Omega$ , resulting from the existence of water.

This deposit layer locates by 10 to 30 m below the surface in the southern part of the section, and has a thickness of 20 m and wedge out in the north to two fingers shaped formation with a thickness of less than 10 m each one.

The same deposit can be found at 50m under the middle of this profile and inclined to the northern part at 200m under the surface.

### **4. Layer number 4**

This layer is wet alluvium deposit layer with a thickness of about 100 m in the southern part, and decreases to about 30 m in the middle of the profile, and then it is descended to the northern part of the profile with thickness ranges between 30 to 40 m. The resistivity of this layer ranges between (35-45  $\Omega$ ), which could be interpreted, that this layer contains water that reduce the resistivity from 50  $\Omega$ , to 40  $\Omega$ . Beneath this layer, there is Alluvium deposit with low salinity water, while the thickness is about 25 m, and it locates 125-160 m

below the southern part of the profile, and reaches more than 200 m in the middle. The resistivity of this layer ranges between (45 to 55  $\Omega$ ), this layer act as a good aquifer where the ground water table locate by 25-35 m. Groundwater well number 19-17/001 with a depth of 100 m, and water table of **-32m** penetrates this layer and abstract water from the alluvium deposit, with electrical conductivity of **2.7m S/cm** which reflects the lithology of the layer. The hydrochemistry of this well is shown in appendix A8 page 79.

## **5. Layer number 5**

This layer is carbonate rocks deposit, with resistivity ranges between 55 and 70  $\Omega$ . Two zones of this deposit could be identified, the first one with a lens shape and thickness ranging between 5 and 15 m, located 50 to 65 m below the surface. This layer could be Beida formation of Neogene age, and the second zone is located by 150-200 m below the surface, with a thickness ranging between 40 – 50 m.

General view to this profile confirms the existence of the fault in the study area, which could increase the infiltration of flood water to groundwater. Neogene conglomerate layer existing, and can be used as possible artificial recharge site. Water table in the nearest wells is ranging between **25 to 35 m**.

### **5.1.3: Third profile**

This profile covers a distance of a bout 1300 m long and reaches a depth of 250 m in the southern part and 200 m in the northern part, it locates within the Palestinian coordinates  $X = 196800 - 196950\text{m}$ ,  $Y = 171595 - 171985\text{m}$ , and with an elevation of 251m bsl., as shown in Fig 5.2. This profile streaked south to north, five measuring stations were taken in it with 50m between each station, in order to satisfy overlapping of the vertical electrical sounding of ERM, the voltage, current and the ratio  $\Delta V/I$  were measured, the results are drown and modeled as in Fig. (5.7)

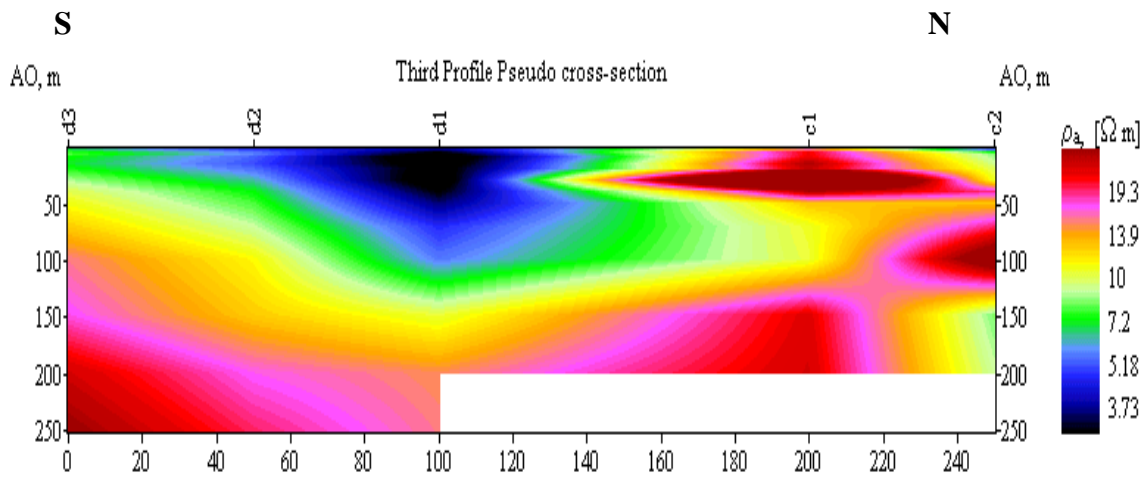


Figure 5.7: Pseudo cross-section of third profile

From the resistivity results and through our field investigations, we developed the next lithological profile Fig. 5.8 through which five layers could be seen.

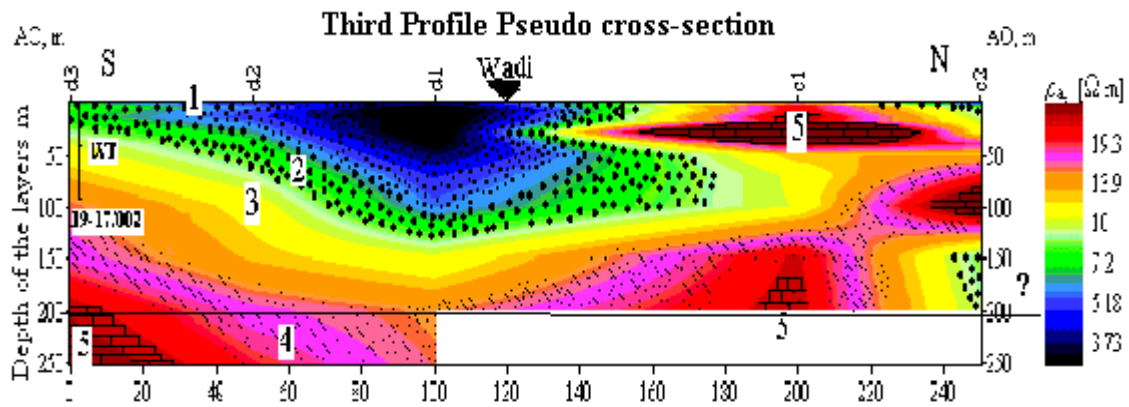


Figure 5.8: Expected lithology to the third profile

### 1. Layer number 1

This layer is expected to be wet fine fluvial material layer, with resistivity ranging between (2 - 5 Ω), the low resistivity of this complex layer related to the irrigation water as well as the salty evaporate deposit. It forms the upper layer and lies in the southern part of the Wadi, it has a convex lens shape with finger extended to the south, the lenses diameter is about 100 m, its thickness is about 70 m, the extended finger is about 60 m long and thickness about 15 m. Low resistivity triangular deposit zone can be identified inside and in the middle of this layer with thickness of about 50 m, the resistivity of this zone is of (2-5 Ω), the low resistivity is due to the existence of high conductivity water.

Lisan formation layer is seen in the southern part with resistivity ranges between (1-3  $\Omega$ ), it locates 3 m below the surface, with an average thickness of 2m.

## **2. Layer number 2**

This layer is expected to be alluvial deposit, which is the local aquifer. The resistivity is ranging between 7 and 10  $\Omega$ , This layer surrounds the fluvial soil layer and its thickness is about 25m and looks like an envelope to the above layer. In the northern part another alluvium deposit with a triangle shape, its base is 10 m to the north, and it is about 60m long. The low resistivity of this layer is due to the existence of water and this water has a high electrical conductivity with chloride contents of 100-1000 mg/L which reduce the resistivity of this layer from (45 – 55  $\Omega$ ) to (7 -10  $\Omega$ ) as seen in in Fig (4.2).

## **3. 3. Layer number 3**

This layer could be the Neogene conglomerate deposit; it is located under the alluvial layer with thickness ranging between 50-90 m. This layer surrounds the alluvial deposit from south to north. It locates by 20-120 m below the southern surface, 130-150 m below the middle surface and 50-100 m below the northern surface. The resistivity of this layer ranges from (9-13  $\Omega$ ), the low resistivity is due to its water content of high electrical conductivity which reduce the resistivity from (20-35  $\Omega$ ), to (9-13  $\Omega$ ). Beneath this layer, Neogene conglomerate formation with water of less electrical conductivity is expected to be inclined from north to south surrounds the wet Neogene layer, the resistivity of this layer is ranging between (20-35  $\Omega$ ), the thickness of this layer ranges between 60-100 m. It is locate 75-110 m, and 160-200m below the southern part, 150-170 m below the middle part and 1-50 m below the northern part. The Neogene layer is a good possible artificial recharge site to groundwater.

Groundwater well number 19-17/002 with a depth of 90 m, and water table of **-37m** penetrates this layer and abstract water from the Neogen conglomerate deposit, with electrical conductivity of **2.4 m S/cm** which reflects the lithology of the layer. The hydrochemistry of this well is shown in appendix A2 page 73.

#### **4. Layer number 4**

This layer is expected to be the alluvium deposit, with a concave shape inclined from north to south surrounds the dry Neogene layer. The resistivity of this layer is ranging between (20-35  $\Omega$ ), and the thickness ranges between 60-100 m. It is located 75-110 m, and 160-200m below the southern surface, 150-170 m below the middle surface and 1-50 m below the southern surface of the profile. Below this layer, a dry alluvium deposit exist with resistivity ranges between (15 to 25  $\Omega$ ), it is locate by 110-160m below southern surface of this profile, 170 – 250 m below the middle surface of the profile, and 50-220 m below the northern surface.

#### **5. Layer number 5**

This layer locate 20-50 m below the northern part , with resistivity ranging between (50-70  $\Omega$ ), this layer is expected to be carbonate rocks of Neogene age, and it has a lens shape, with 30 m thick, and 100 m long, and locate 20-50 m below the southern surface.

Two carbonate rock deposits seem to be located below the northern surface. The first is found by 80-110 m, and has a triangular shape with base of 30 m in the north, and 30 m long. The second deposit is found by 170-200 m.

The same deposit layer locate by 200-250 m below the southern surface of the profile, it has a triangular shape with thickness ranges 150m in the southern part and wedges out to less than 5 m in the north.

#### **5.1.4: Fourth Profile, West -East parallel to the Wadi flow**

This profile covers a distance of a bout 1500 m long and reaches a depth of 200 m in the western part and 125 m in the eastern part of the profile, it locates within the Palestinian coordinates X = 197241 – 198356 m, Y = 171550 – 171137 m, and with an average elevation of 251m bsl.

This profile is drawn from west to east, (Fig.5.2). Three measuring stations were taken in this profile with 500m between each one, in order to satisfy overlapping of the vertical electrical sounding of ERM, the voltage, current and the ratio  $\Delta V/I$  were measured, the

results are drawn and modeled as in Fig. (5.9)

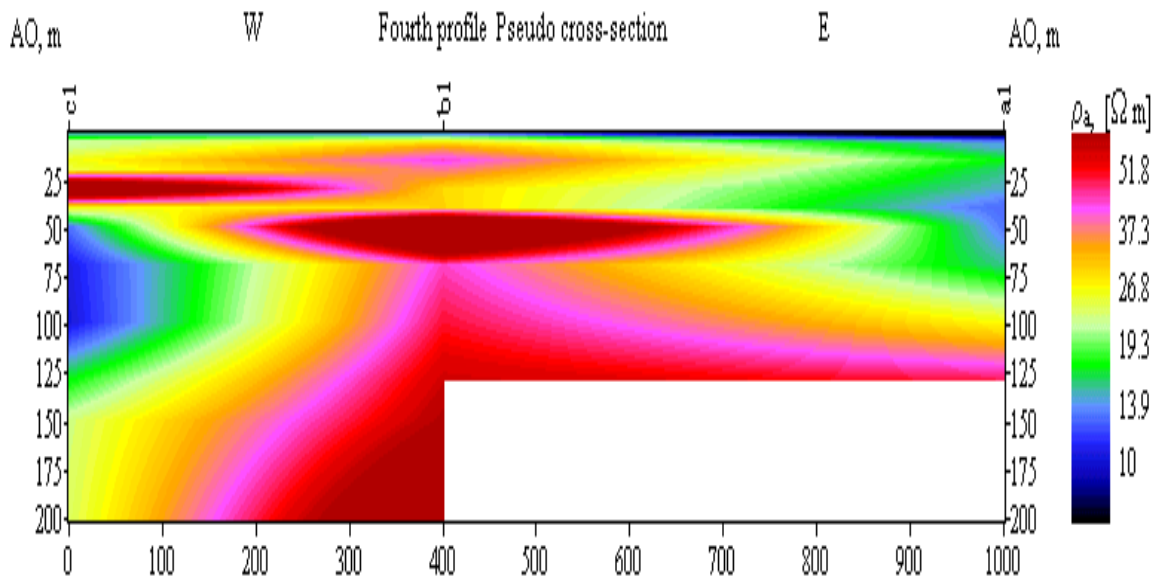


Figure5.9: Pseudo cross-sections for the fourth profile

The lithological results which conducted from the geoelectrical investigation with field investigations, we developed the following lithological profile shown in Fig.(5.10)

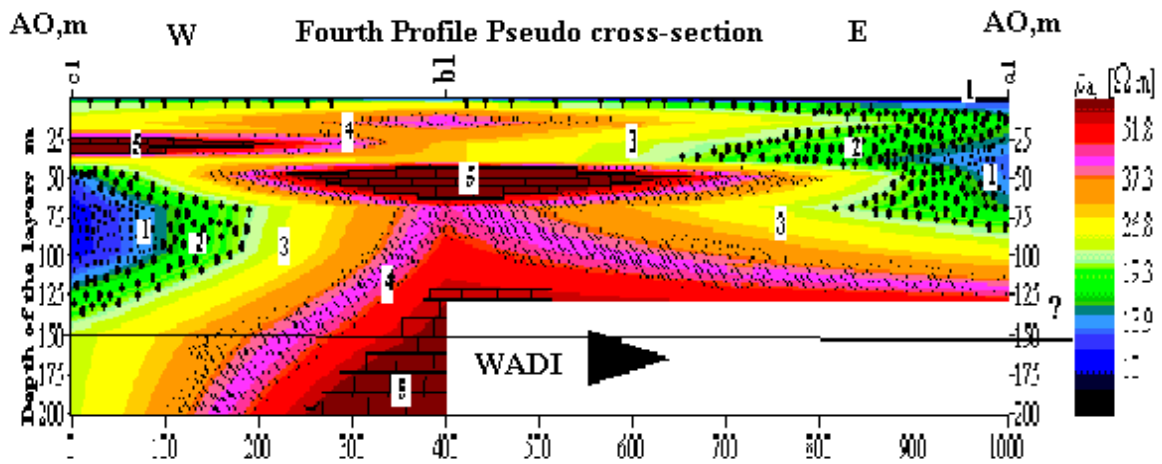


Figure5.10: Expected lithology of the fourth profile

As shown in Fig.(5.10) fluvial fine material, alluvial deposit, Neogen formation, carbonate rocks layers are expected to build up the profile of 150 m thick

## **1. Layer number 1**

This layer locates at the surface and covers the eastern part of the profile. It is expected to be fine fluvial deposit soil, with thicknesses ranging between 2-10 m. The resistivity of this layer is ranging between (5-12  $\Omega$ ). Lisan layer, with low resistivity ranging between (2-5  $\Omega$ ), is expected to be in the eastern part of this profile. The thickness of this layer is about 2-5 m. This layer is located about 3 m below the surface, whereas in the western part is not exist.

The same layer is located at about 25-60 m below the surface in the western part. It has a triangular shape with base of thickness 35 m in the eastern part, and extends to 200m long. The resistivity of this layer ranges between (2-5  $\Omega$ ). It is expected to be a formation contains saline water. The presence of this water type reduces the resistivity of this layer from (5-12  $\Omega$ ) to (2-5  $\Omega$ ).

The same deposit is locating about 40-110 m below the surface in the western part of the profile. It has also a triangular shape with base of thickness 70 m in the western part, 150m long.

## **2. Layer number 2**

This layer is expected to be Alluvium deposit layer. It has a number "3" shape with thickness of about 25 m in the eastern part, and decrease to less than 1 m in the middle part of the profile. The resistivity of this layer ranges between (15 to 20  $\Omega$ ), which could be interpreted as a layer contains water with a high electrical conductivity which reduce the resistivity of this layer from 45 – 55  $\Omega$ , to 15 -20  $\Omega$ . This layer locate 10-80 m below the surface of the eastern part, 25-50 m below the middle part, and 2-5 m below the surface of the western part of this profile.

The same deposit locates 40-140m below the western part of the profile; it has two finger shaped fragments extended from the middle to the west, with thickness of about 15-25m of each.

### **3. Layer number 3**

This layer is Neogene conglomerate. It locates all over the profile because of the existence of a minor fault. It is found by 10-25 m and by 50-200m below the surface of the western part, 5-50 m by the middle part, and 70-100m by the eastern part of the profile.

The resistivity of this layer ranges between (20-35  $\Omega$ ). Since this profile locates to the northern of the Wadi, and the topography of the soil is inclined towards the south drainage, this layer is a dry layer which explains the high resistivity.

The western zone of this layer has a - Z - shape with thickness 10 m in the upper tail, and 30-40 m below the surface of the western part, and 60 m in the lower fragment, this fragment located by 140-200 m below the surface.

The middle zone of this layer has a convex lens shape located 5-50 m below the surface, with thickness of 40 m, and wedges out to less than 2 m in the east, and wedges out to two fingers shaped with thickness less than 5 m in the west.

The eastern zone has a -Z - shape with thickness 5 m in the upper tail, 40-50 m below the surface of the eastern part, by 30 m in the lower fragment, and by 80-110 m below the surface.

### **4. Layer number 4**

This layer locates by 40-60 m, and by 150-200m below the surface of the western part of the profile, and by 60-80 m below the surface of the mid part, and by 50-75 m, 100-130 m below the surface of the eastern profile. The resistivity ranges between (35-45  $\Omega$ ). This zone is expected to be wet alluvium deposit.

Beneath this wet layer, there is an alluvium zone contains water of less salinity. The resistivity ranges between (50-60  $\Omega$ ). The thickness of this zone is 40-50 m by 175-200 m below the surface in the western part, and wedges out in the middle to less than 30 m thick by 80-110 m below the surface, and decrease to less than 5 m by 120-125 m below the surface of the eastern part of the profile.

## 5. Layer number 5

Two different zones are found below the mid of the profile, the upper zone is found by 50 - 70 m. It has a convex lens shape, with thickness of about 20 m, and wedges out in the west and east to less than 2 m. The resistivity of this layer ranges between (55-70  $\Omega$ ), it is expected to be Beida formation of Neogene age.

The lower deposit is found by 120-200 m, with a triangular shape of 60 m base in the middle of the profile, 150 m towards the west.

The same deposit is found by 20-30 m below the western surface of the profile, with a triangular shape of 10 m base in the western of the profile, 200 m towards the east.

General view to this profile, we can clearly see from Fig.(5.8) the west east fault along the Wadi, especially in the location of the layers, up, middle and down the profile.

A wide Neogene conglomerate formation layer exists parallel to the Wadi axis, and can be used as artificial recharge site for groundwater.

### 5.1.5: Profile Five –West- East parallel to the Wadi flow

This profile covers a distance of a bout 1500 m long and reaches a depth of 200 m, it locates within the Palestinian coordinates  $X = 196854 - 197765\text{m}$ ,  $Y = 171050 - 170301\text{m}$ , and with an elevation of 251m bsl.

This profile streaked west to east, parallel to the Wadi axis. Two stations were taken in this profile with total length of 1000m. In order to satisfy overlapping of the vertical electrical sounding of ERM, the voltage, current and the ratio  $\Delta V/I$  were measured, the results are drown and modeled as in Fig.(5.11)

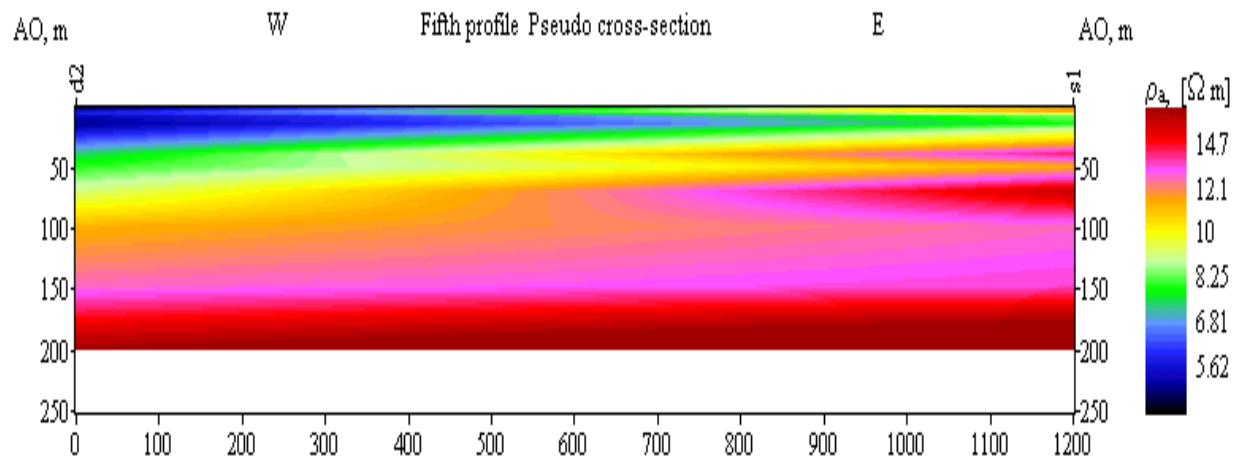


Figure5.11: Pseudo cross-sections for the fifth profile

The lithological results which conducted from the geoelectrical investigation with comparison with field investigations, we developed the following lithological profile Fig.(5.12), through which five distinguished layers are found

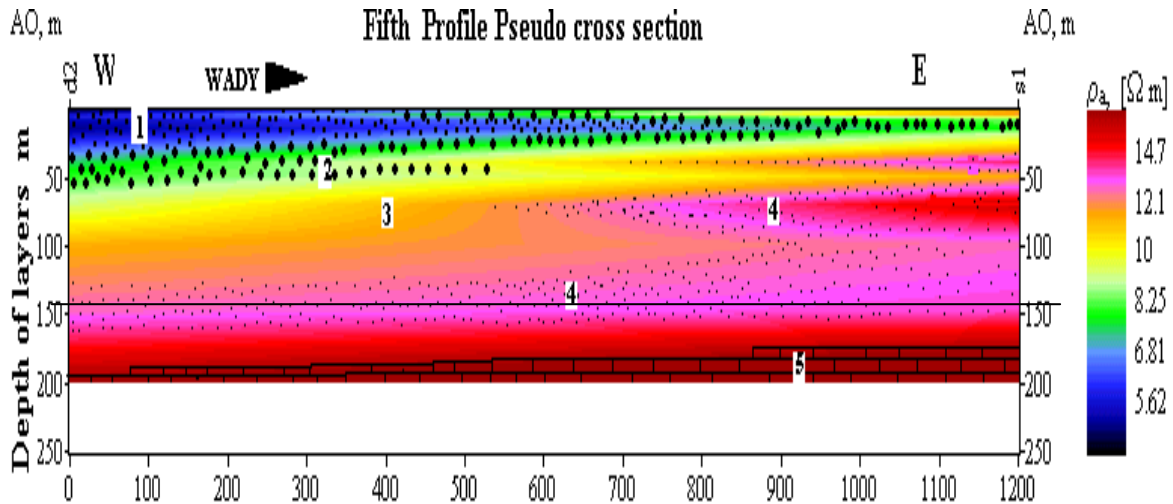


Figure5.12: Expected lithology of the fifth profile

### Layer number 1

This layer is located by 20- 30 m below the western surface. It has a triangular shape with 30 m base in the west and wedges out to less than 5 m in the east. The resistivity of this layer ranges between (3-6  $\Omega$ ), it is expected to be fluvial fine soil. The low resistivity is due to agricultural return flow of irrigated water.

### 2. Layer number 2

This deposit is found by 20 and 60 m below the surface, with a thickness of about 20-30 m in the western part, and wedges out to less than 10 m in the eastern part. It is expected to be alluvium deposit, with resistivity ranges between 7 and 9  $\Omega$ . The low resistivity could be interpreted that this layer contains water with high electrical conductivity which reduces the resistivity of this deposit from (45-55  $\Omega$ ) to (7-9  $\Omega$ ).

### **3. Layer number 3**

This layer has an –S- shape with thickness about 50 m. It is found by 50 and 150 m below the western surface of the profile, and 10 m by 15-25 m below the surface of the eastern part of the profile. The resistivity of this deposit ranges between (9-12  $\Omega$ ), it is expected to be Neogene conglomerate formation. This deposit contains water which decrease the resistivity of this layer from (35-45  $\Omega$ ) to (9-12  $\Omega$ ).

### **4. Layer number 4**

This layer is found by 40-150 m below the surface of the eastern part, and by 130-160 m below the surface of the western part, and by 60-80 m below the surface of the mid part of the profile. The resistivity of this deposit ranges between (12-35  $\Omega$ ), it is expected to be alluvium deposit layer. The upper zone of this deposit contains saline water of high electrical conductivity which reduces the resistivity of this layer to (12-14  $\Omega$ ).

The lower zone is alluvium deposit, with less saline water. This zone has a horizontal shape and is located by 160-200 m below the western surface of the section, and by 150-175 m below the eastern surface of the section. The thickness of this layer is 40 m in the west and wedges out to less than 25 m in the east. The resistivity of this layer ranges between (25-35  $\Omega$ ).

### **5. Layer number 5**

This layer has a triangular shape and is found 175 - 200 m below the surface of the eastern part, and by 190 – 200 m below the surface of the western part of the profile.

Its thickness is about 25 m in the east, and wedges out in the west to less than 10 m. The resistivity of this deposit ranges between (55 – 70  $\Omega$ ), this deposit is expected to be a carbonate rocks.

The porosity of gravel is in the range 24%-36% (McWorter et al. 1997). Depending on the porosity and the existing map in appendix C2, C3 the possible volume at Al-Jiftlik area for artificial recharge can be calculated as

Volume = (1500 x 3000 x 20 x 30%)  $\pm$  15% = 25- 30 mcm. at the whole area, and

Volume = (1000 x 1500 x 20 x 30%)  $\pm$  15% = 8 – 10 mcm at the study area

## 5.2: Sieve Analysis

Porosity, hydraulic conductivity and permeability are hydrogeological parameters that all greatly depend on the size of sediment grains and the percentage of various sediment fractions. The ratio of sand, silt, and clay in soil determines its ability to hold moisture and nutrients. Soil samples should be representative the area. Making a composite by collecting small samples at evenly spaced intervals across the area from where the roots actually grow. Figuring out the percentages of sand, silt, and clay in the sample, and measure the height of the total amount of sediment settled. This number represents 100 percent of the soil sample. To derive the percentages of sand, silt, and clay in the sample, measure the amount of each layer and divide by the amount of total sample. Transfer the results to the soil texture triangle to determine the soil type (Cahilly, 2005).

Seven sediment samples of known weight (500 g) were collected from Wadi Al- Faria (Al-Jiftlik) area, as seen in Fig.(5.13). Sieve analyses was done to all of them, in order to determine grain size distribution, draw the grain size distribution curve, determine the uniformity coefficient, the effective grain size and to calculate the hydraulic conductivity of the aquifer material.

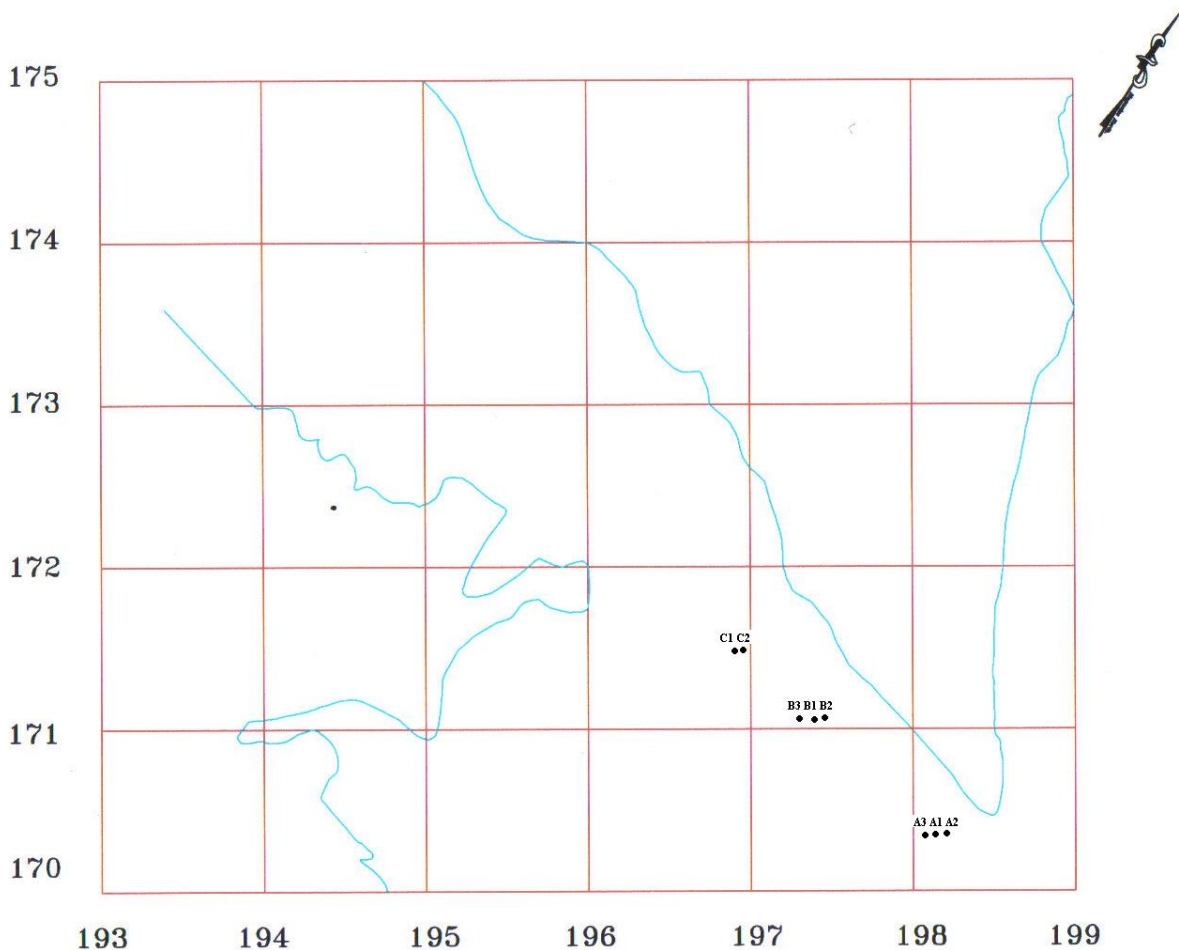


Fig.(5.13): Soil sampling sites

The results of sieve analyses for each sediment is described in the following tables

Table 5-4: Results of laboratory sieve tests for sample A1

Sieve Diameter Mm	Sieve weight g	Final Weight G	Fraction Weight G	Fraction percent	% coarser than sieve dim.
2	513	539.9	26.9	5.38	5.38
1.6	508.4	526.9	18.5	3.7	9.08
1	451.6	499.2	47.6	9.52	18.6
0.71	397	442.5	45.5	9.1	27.7
0.5	434.9	482	47.1	9.42	37.12
0.25	415.1	510.7	95.6	19.12	56.24
0.2	415.3	447.9	32.6	6.52	62.76
0.16	326	353.8	27.8	5.56	68.32
0.09	389.8	453.9	64.1	12.82	81.14
0.075	367.5	394.7	27.2	5.44	86.58
0.063	362.2	379.9	17.7	3.54	90.12
Bottom Pan	306.3	355.7	49.4	9.88	100
		Sum	500	100	
100					
RESULT					
Sand, % =	27.7				
Silt, % =	28.54				
Clay, % =	43.76				

Table 5-5: Results of laboratory sieve tests for sample A2

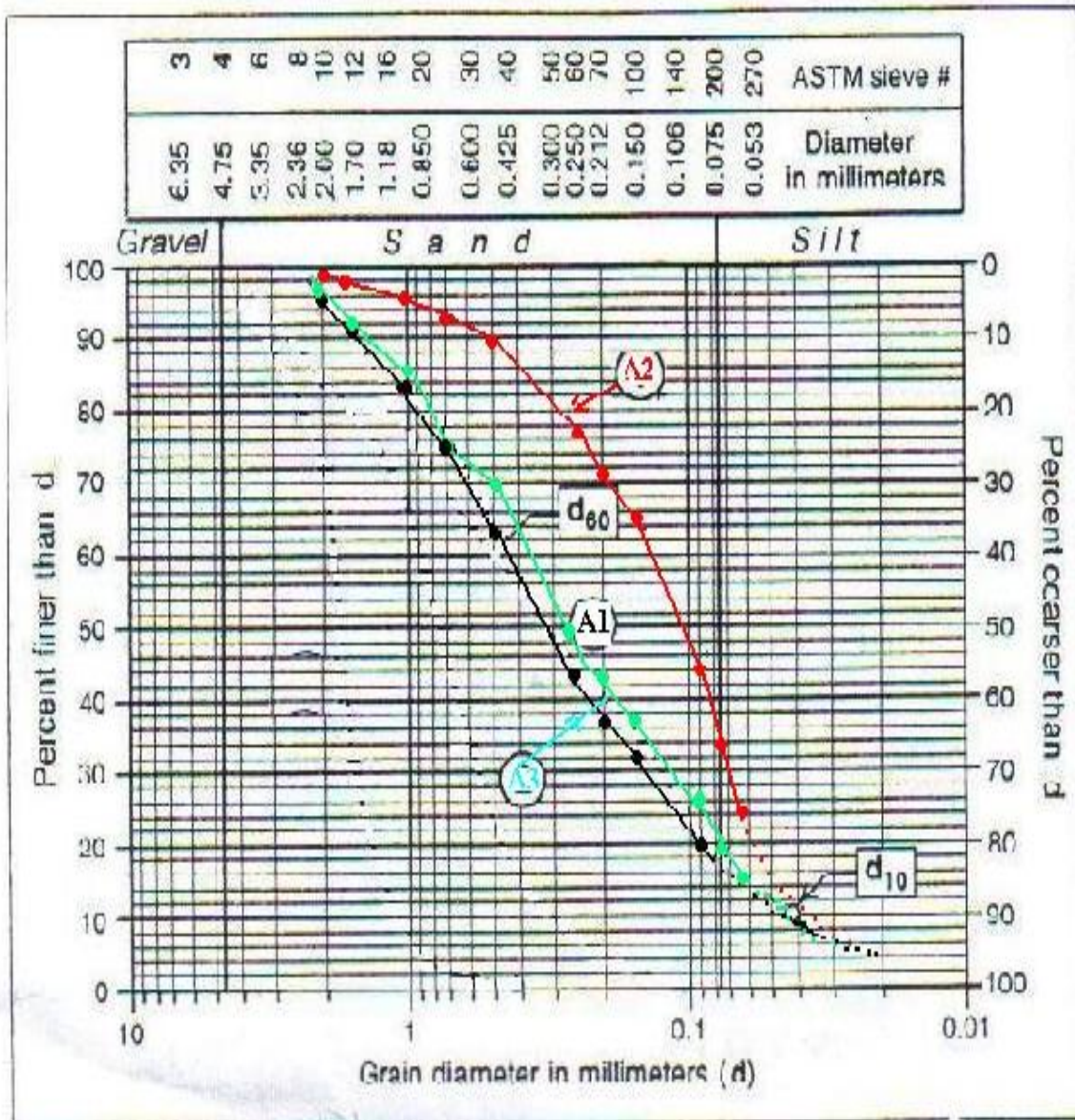
Sieve Diameter, Mm	Sieve weight G	Final Weight, g	Fraction Weight, G	Fraction percent	% coarser than sieve dim.
2	513	518.2	5.2	1.04	1.04
1.6	508.4	512.7	4.3	0.86	1.9
1	451.6	463.9	12.3	2.46	4.36
0.71	397	411	14	2.8	7.16
0.5	434.9	453.1	18.2	3.64	10.8
0.25	415.1	473.9	58.8	11.76	22.56
0.2	415.3	446.6	31.3	6.26	28.82

<b>0.16</b>	<b>326</b>	<b>360.5</b>	<b>34.5</b>	<b>6.9</b>	<b>35.72</b>
<b>0.09</b>	<b>389.8</b>	<b>490.7</b>	<b>100.9</b>	<b>20.18</b>	<b>55.9</b>
<b>0.075</b>	<b>367.5</b>	<b>421.6</b>	<b>54.1</b>	<b>10.82</b>	<b>66.72</b>
<b>0.063</b>	<b>362.2</b>	<b>409.2</b>	<b>47</b>	<b>9.4</b>	<b>76.12</b>
<b>Bottom Pan</b>	<b>306.3</b>	<b>427.2</b>	<b>120.9</b>	<b>24.18</b>	<b>100.3</b>
		<b>Sum</b>	<b>501.5</b>	<b>100.3</b>	
<b>RESULT</b>					
<b>Sand, % =</b>	<b>7.16</b>				
<b>Silt, % =</b>	<b>15.4</b>				
<b>Clay, % =</b>	<b>77.74</b>				

Table 5-6: Results of laboratory sieve tests for sample A3

<b>Sieve Diameter, Mm</b>	<b>Sieve weight g</b>	<b>Final Weight g</b>	<b>Fraction Weight, G</b>	<b>Fraction percent</b>	<b>% coarser than sieve dim.</b>
<b>2</b>	<b>513</b>	<b>533.9</b>	<b>20.9</b>	<b>4.18</b>	<b>4.18</b>
<b>1.6</b>	<b>508.4</b>	<b>527.6</b>	<b>19.2</b>	<b>3.84</b>	<b>8.02</b>
<b>1</b>	<b>451.6</b>	<b>496.1</b>	<b>44.5</b>	<b>8.9</b>	<b>16.92</b>
<b>0.71</b>	<b>397</b>	<b>437.5</b>	<b>40.5</b>	<b>8.1</b>	<b>25.02</b>
<b>0.5</b>	<b>434.9</b>	<b>474.7</b>	<b>39.8</b>	<b>7.96</b>	<b>32.98</b>
<b>0.25</b>	<b>415.1</b>	<b>504.9</b>	<b>89.8</b>	<b>17.96</b>	<b>50.94</b>
<b>0.2</b>	<b>415.3</b>	<b>444.1</b>	<b>28.8</b>	<b>5.76</b>	<b>56.7</b>
<b>0.16</b>	<b>326</b>	<b>355.2</b>	<b>29.2</b>	<b>5.84</b>	<b>62.54</b>
<b>0.09</b>	<b>389.8</b>	<b>458.5</b>	<b>68.7</b>	<b>13.74</b>	<b>76.28</b>
<b>0.075</b>	<b>367.5</b>	<b>391.4</b>	<b>23.9</b>	<b>4.78</b>	<b>81.06</b>
<b>0.063</b>	<b>362.2</b>	<b>383.9</b>	<b>21.7</b>	<b>4.34</b>	<b>85.4</b>
<b>Bottom Pan</b>	<b>306.3</b>	<b>381.8</b>	<b>75.5</b>	<b>15.1</b>	<b>100.5</b>
		<b>Sum</b>	<b>502.5</b>	<b>100.5</b>	
<b>RESULT</b>					
<b>Sand, % =</b>	<b>25.02</b>				
<b>Silt, % =</b>	<b>25.92</b>				
<b>Clay, % =</b>	<b>49.56</b>				

Since porosity, hydraulic conductivity and permeability depend on the size of sediment grains, the grain size distribution curves for the three samples are drawn in (Fig.5.14) below



Curve	$d_{60}$	Effective Grain Size $d_e = d_{10}$	Coefficient of Uniformity $U = d_{60}/d_{10}$
A1	0.48	0.05	9.6
A2	0.15	0.04	3.75
A3	0.34	.045	7.56

Fig.5.14: Grain size distribution curves for three samples A1, A2, and A3

The uniformity coefficient explains the range of grain size present in the sample; this can be done using the equation

$$U = d_{60} / d_{10} \quad (\text{eq.5.1})$$

Where:

$d_{60}$  is the sieve diameter size which allows 60% of the sample by weight to pass,  $d_{10}$  is the sieve diameter size which allows 10% of the sample by weight to pass. As  $U < 5$ , the more uniform the material ("well graded", "well stored"). (K.Neven, 1997)

For the three samples shown in Fig.5.12, only curve A2 indicate well-stored (uniform) sample since its coefficient of uniformity is less than 5, while the two curves A1 and A3 represent a poorly-graded material since their coefficient of uniformity is more than 5.

Experimentally, it is now commonly practiced to use  $d_{10}$  as the effective grain size. The effective grain size expresses the equivalent permeability of a porous material: the smallest 10% of grains, which also fill the pore spaces between large grains, is what actually determines the material's permeability. (K.Neven, 1997)

The hydraulic conductivity can be calculated by Hazen, Kozeny or Breyer equations:

The Hazen equation is:

$$K = (g/v) * C_h f_{(n)} d_{10}^2 \quad (\text{eq.5.2})$$

Where  $C_h = 6 \times 10^{-4} \quad (\text{eq.5.2a})$

$$f_{(n)} = [1 + 10(n - 0.26)] \quad (\text{eq.5.2b})$$

$K$  is the hydraulic conductivity m/s,  $g$  is the gravitational acceleration  $9.807 \text{ m/s}^2$ ,  $v$  is the kinetic viscosity of the fluid which is  $1.14 \times 10^{-6} \text{ m}^2/\text{s}$ .

Hazen equation is applicable for  $U < 5$ , and  $(0.1 \text{ mm} < d_{10} < 3 \text{ mm})$

The Kozeny equation is:

$$K = (g/v) * C_k f_{(n)} d_{10}^2 \quad (\text{eq.5.3})$$

Where  $C_k = 6 \times 10^{-3} \quad (\text{eq.5.3a})$

$$f_{(n)} = n^3 / (1 - n)^2 \quad (\text{eq.5.3b})$$

Kozeny equation is applicable for coarse sand. (K.Neven, 1997)

The Breyer equation is:

$$K = (g/v) * C_b d_{10}^2 \quad (\text{eq.5.4})$$

Where  $C_b = 6 \times 10^{-4} \log(500/U)$  (eq.5.4b)

Breyer equation is applicable for ( $1 < U < 20$ ), and ( $0.06 \text{ mm} < d_{10} < 0.6 \text{ mm}$ ), (K.Neven,1997)

Since our data satisfies the condition of Breyer equation, we use it in calculating the hydraulic conductivity thus:

$$\begin{aligned} KA1 &= (g/v) * C_b d_{10}^2 \\ &= (9.807 / 1.14 \times 10^{-6}) \times 6 \times 10^{-4} \times \log(500/9.6) \times (0.05 \times 10^{-3})^2 = \underline{\underline{22.15 \times 10^{-6} \text{ m/s}}} \end{aligned}$$

$$\begin{aligned} KA2 &= (g/v) * C_b d_{10}^2 \\ &= (9.807 / 1.14 \times 10^{-6}) \times 6 \times 10^{-4} \times \log(500/3.75) \times (0.04 \times 10^{-3})^2 = \underline{\underline{17.55 \times 10^{-6} \text{ m/s}}} \end{aligned}$$

$$\begin{aligned} KA3 &= (g/v) * C_b d_{10}^2 \\ &= (9.807 / 1.14 \times 10^{-6}) \times 6 \times 10^{-4} \times \log(500/7.56) \times (0.045 \times 10^{-3})^2 = \underline{\underline{19.03 \times 10^{-6} \text{ m/s}}} \end{aligned}$$

Table 5-7: Results of laboratory sieve tests for sample B1

Sieve Diameter Mm	Sieve weight g	Final Weight, G	Fraction Weight g	Fraction percent	% coarser than sieve dim.
2	513	550.1	37.1	7.42	7.42
1.6	508.4	529	20.6	4.12	11.54
1	451.6	497.1	45.5	9.1	20.64
0.71	397	433.6	36.6	7.32	27.96
0.5	434.9	472.5	37.6	7.52	35.48
0.25	415.1	501.4	86.3	17.26	52.74
0.2	415.3	446.8	31.5	6.3	59.04
0.16	326	355.6	29.6	5.92	64.96
0.09	389.8	462.4	72.6	14.52	79.48
0.075	367.5	397.4	29.9	5.98	85.46
0.063	362.2	382	19.8	3.96	89.42

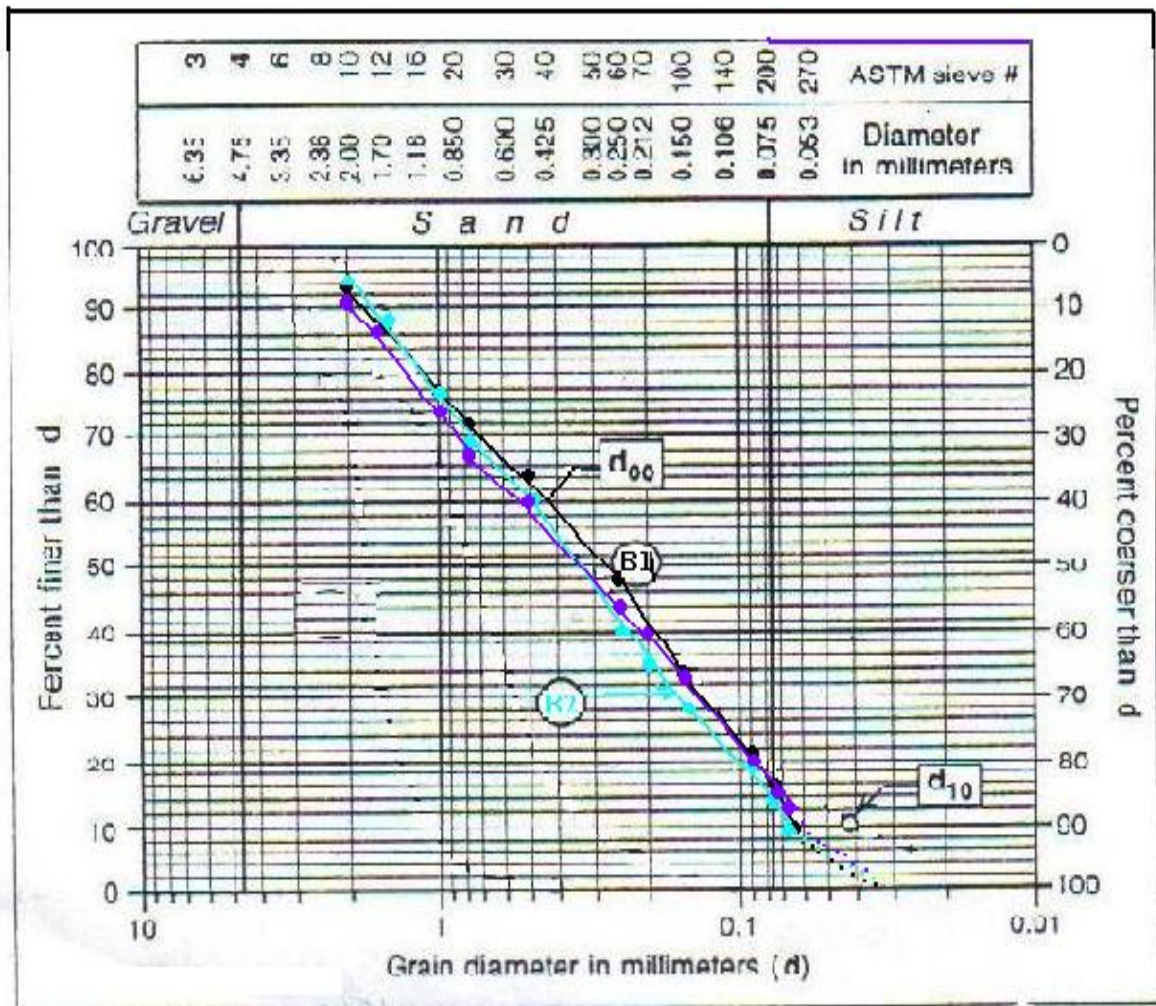
<b>Bottom Pan</b>	<b>306.3</b>	<b>359.7</b>	<b>53.4</b>	<b>10.68</b>	<b>100.1</b>
		<b>Sum</b>	<b>500.5</b>	<b>100.1</b>	
<b>100.1</b>					
<b>RESULT</b>					
<b>Sand, % =</b>	<b>27.96</b>				
<b>Silt, % =</b>	<b>24.78</b>				
<b>Clay, % =</b>	<b>47.36</b>				

Table 5-8: Results of laboratory sieve tests for sample B2

<b>Sieve Diameter, Mm</b>	<b>Sieve weight g</b>	<b>Final Weight G</b>	<b>Fraction Weight g</b>	<b>Fraction percent</b>	<b>% coarser than sieve dim.</b>
<b>2</b>	<b>513</b>	<b>554.3</b>	<b>41.3</b>	<b>8.26</b>	<b>8.26</b>
<b>1.6</b>	<b>508.4</b>	<b>530.8</b>	<b>22.4</b>	<b>4.48</b>	<b>12.74</b>
<b>1</b>	<b>451.6</b>	<b>503.5</b>	<b>51.9</b>	<b>10.38</b>	<b>23.12</b>
<b>0.71</b>	<b>397</b>	<b>439.8</b>	<b>42.8</b>	<b>8.56</b>	<b>31.68</b>
<b>0.5</b>	<b>434.9</b>	<b>478.7</b>	<b>43.8</b>	<b>8.76</b>	<b>40.44</b>
<b>0.25</b>	<b>415.1</b>	<b>510.2</b>	<b>95.1</b>	<b>19.02</b>	<b>59.46</b>
<b>0.2</b>	<b>415.3</b>	<b>444.9</b>	<b>29.6</b>	<b>5.92</b>	<b>65.38</b>
<b>0.16</b>	<b>326</b>	<b>350.9</b>	<b>24.9</b>	<b>4.98</b>	<b>70.36</b>
<b>0.09</b>	<b>389.8</b>	<b>444.8</b>	<b>55</b>	<b>11</b>	<b>81.36</b>
<b>0.075</b>	<b>367.5</b>	<b>397.3</b>	<b>29.8</b>	<b>5.96</b>	<b>87.32</b>
<b>0.063</b>	<b>362.2</b>	<b>377.8</b>	<b>15.6</b>	<b>3.12</b>	<b>90.44</b>
<b>Bottom Pan</b>	<b>306.3</b>	<b>356.7</b>	<b>50.4</b>	<b>10.08</b>	<b>100.52</b>
		<b>Sum</b>	<b>502.6</b>	<b>100.52</b>	
<b>100.52</b>					
<b>RESULT</b>					
<b>Sand, % =</b>	<b>31.68</b>				
<b>Silt, % =</b>	<b>27.78</b>				
<b>Clay, % =</b>	<b>41.06</b>				

Table 5-9: Results of laboratory sieve tests for sample B3

<b>Sieve Diameter Mm</b>	<b>Sieve weight g</b>	<b>Final Weight G</b>	<b>Fraction Weight g</b>	<b>Fraction percent</b>	<b>% coarser than sieve dim.</b>
<b>2</b>	<b>513</b>	<b>558.6</b>	<b>45.6</b>	<b>9.12</b>	<b>9.12</b>
<b>1.6</b>	<b>508.4</b>	<b>529.2</b>	<b>20.8</b>	<b>4.16</b>	<b>13.28</b>
<b>1</b>	<b>451.6</b>	<b>498.6</b>	<b>47</b>	<b>9.4</b>	<b>22.68</b>
<b>0.71</b>	<b>397</b>	<b>432.7</b>	<b>35.7</b>	<b>7.14</b>	<b>29.82</b>
<b>0.5</b>	<b>434.9</b>	<b>470.6</b>	<b>35.7</b>	<b>7.14</b>	<b>36.96</b>
<b>0.25</b>	<b>415.1</b>	<b>498.1</b>	<b>83</b>	<b>16.6</b>	<b>53.56</b>
<b>0.2</b>	<b>415.3</b>	<b>448.2</b>	<b>32.9</b>	<b>6.58</b>	<b>60.14</b>
<b>0.16</b>	<b>326</b>	<b>353.1</b>	<b>27.1</b>	<b>5.42</b>	<b>65.56</b>
<b>0.09</b>	<b>389.8</b>	<b>461</b>	<b>71.2</b>	<b>14.24</b>	<b>79.8</b>
<b>0.075</b>	<b>367.5</b>	<b>404.4</b>	<b>36.9</b>	<b>7.38</b>	<b>87.18</b>
<b>0.063</b>	<b>362.2</b>	<b>378.1</b>	<b>15.9</b>	<b>3.18</b>	<b>90.36</b>
<b>Bottom Pan</b>	<b>306.3</b>	<b>357.9</b>	<b>51.6</b>	<b>10.32</b>	<b>100.68</b>
		<b>Sum</b>	<b>503.4</b>	<b>100.68</b>	
<b>100.68</b>					
<b>RESULT</b>					
<b>Sand, % =</b>	<b>29.82</b>				
<b>Silt, % =</b>	<b>23.74</b>				
<b>Clay, % =</b>	<b>47.12</b>				



Curve	$D_{60}$	Effective Grain Size $d_e = d_{10}$	Coefficient of Uniformity $U = d_{60}/d_{10}$
B1	0.42	0.062	6.77
B2	0.48	0.068	7.06
B3	0.50	0.060	8.33

Fig.5.15: Grain size distribution curves for three samples B1, B2, and B3

Depending on equation 5.1, the three curves shown in (Fig.5.15) B1, B2 and B3 represent a poorly-graded material since their coefficient of uniformity is more than 5.

The effective grain size ( $d_e = d_{10}$ ) for the three samples are obtained from the extrapolated parts of the curves shown in (Fig.5.15)

The hydraulic conductivity can be calculated by Breyer equation (eq.5.4) as follows:

$$KB1 = (g/v) * C_b d_{10}^2$$

$$= (9.807 / 1.14 \times 10^{-6}) \times 6 \times 10^{-4} \times \log(500/6.77) \times (0.063 \times 10^{-3})^2 = \underline{\underline{38.28 \times 10^{-6} \text{ m/s}}}$$

$$KB2 = (g/v) * C_b d_{10}^2$$

$$= (9.807 / 1.14 \times 10^{-6}) \times 6 \times 10^{-4} \times \log(500/7.06) \times (0.068 \times 10^{-3})^2 = \underline{\underline{44.12 \times 10^{-6} \text{ m/s}}}$$

$$KB3 = (g/v) * C_b d_{10}^2$$

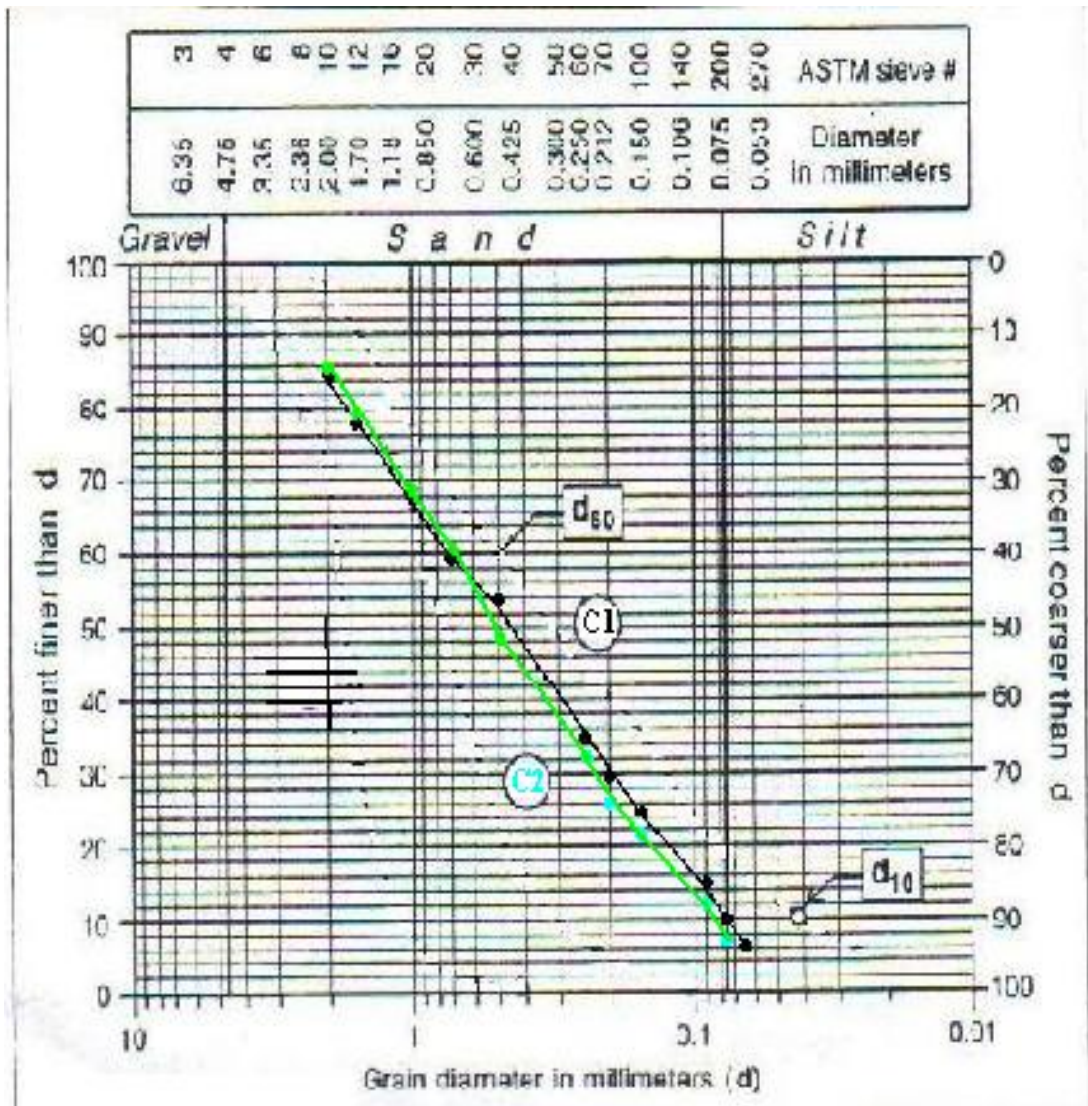
$$= (9.807 / 1.14 \times 10^{-6}) \times 6 \times 10^{-4} \times \log(500/8.33) \times (0.06 \times 10^{-3})^2 = \underline{\underline{33.04 \times 10^{-6} \text{ m/s}}}$$

Table 5-10: Results of laboratory sieve tests for sample C1

Sieve Diameter Mm	Sieve weight G	Final Weight G	Fraction Weight g	Fraction percent	% coarser than sieve dim.
2	513	550.1	37.1	7.42	7.42
1.6	508.4	529	20.6	4.12	11.54
1	451.6	497.1	45.5	9.1	20.64
0.71	397	433.6	36.6	7.32	27.96
0.5	434.9	472.5	37.6	7.52	35.48
0.25	415.1	501.4	86.3	17.26	52.74
0.2	415.3	446.8	31.5	6.3	59.04
0.16	326	355.6	29.6	5.92	64.96
0.09	389.8	462.4	72.6	14.52	79.48
0.075	367.5	397.4	29.9	5.98	85.46
0.063	362.2	382	19.8	3.96	89.42
Bottom Pan	306.3	359.7	53.4	10.68	100.1
		Sum	500.5	100.1	
<b>RESULT</b>					
Sand, % =	27.96				
Silt, % =	24.78				
Clay, % =	47.36				

Table 5-11: Results of laboratory sieve tests for sample C2

<b>Sieve Diameter Mm</b>	<b>Sieve weight G</b>	<b>Final Weight G</b>	<b>Fraction Weight g</b>	<b>Fraction percent</b>	<b>% coarser than sieve dim.</b>
2	513	587.2	74.2	14.84	14.84
1.6	508.4	537.7	29.3	5.86	20.7
1	451.6	515.9	64.3	12.86	33.56
0.71	397	444.5	47.5	9.5	43.06
0.5	434.9	479.2	44.3	8.86	51.92
0.25	415.1	498.4	83.3	16.66	68.58
0.2	415.3	446.4	31.1	6.22	74.8
0.16	326	349.5	23.5	4.7	79.5
0.09	389.8	434.4	44.6	8.92	88.42
0.075	367.5	391.1	23.6	4.72	93.14
0.063	362.2	370.7	8.5	1.7	94.84
Bottom Pan	306.3	336.8	30.5	6.1	100.94
		<b>Sum</b>	<b>504.7</b>	<b>100.94</b>	
<b>100.94</b>					
<b>RESULT</b>					
<b>Sand, % =</b>	<b>43.06</b>				
<b>Silt, % =</b>	<b>25.52</b>				
<b>Clay, % =</b>	<b>32.36</b>				



Curve	$d_{60}$	Effective Grain Size $d_e = d_{10}$	Coefficient of Uniformity $U = d_{60}/d_{10}$
C1	0.7	0.075	9.33
C2	0.65	0.095	6.84

Fig.5.16: Grain size distribution curves for the two samples C1, C2.

Depending on equation 5.1, the two curves shown in (Fig.5.14) C1 and C2 represent a poorly-graded material since their coefficient of uniformity is more than 5.

The effective grain size ( $d_e = d_{10}$ ) for the two samples are obtained from the curves shown in (Fig. 5.16)

The hydraulic conductivity can be calculated by Breyer equation (eq.5.4) as follows:

$$KC1 = (g/v) * C_b d_{10}^2$$

$$= (9.807 / 1.14 \times 10^{-6}) \times 6 \times 10^{-4} \times \log(500/9.33) \times (0.075 \times 10^{-3})^2 = \underline{\underline{50.02 \times 10^{-6} \text{ m/s}}}$$

$$KC2 = (g/v) * C_b d_{10}^2$$

$$= (9.807 / 1.14 \times 10^{-6}) \times 6 \times 10^{-4} \times \log(500/6.84) \times (0.095 \times 10^{-3})^2 = \underline{\underline{86.83 \times 10^{-6} \text{ m/s}}}$$

The textural triangle for the above samples is shown in figure 5.15 bellow

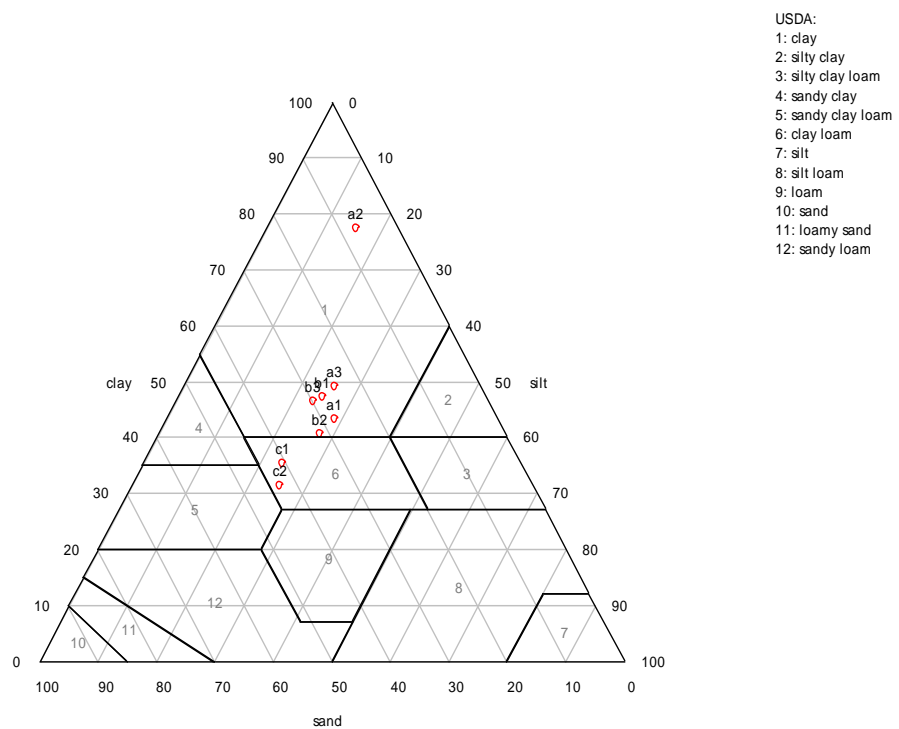


Fig.5.17: Texture triangle for Faria soil

Fig.5.17 shows that the soil is clay in the eastern part of the study area and clay loam in the western part. This kind of soil has low infiltration potential rate and high runoff potential rate.

Because the hydraulic conductivity ranges between  $1.755 \times 10^{-5} \text{ m/s}$  and  $8.683 \times 10^{-5} \text{ m/s}$ , so using surface flooding is not practical to use for artificial recharge. Statistically, and

depending on the average amount of hydraulic conductivity which is  $38.9 \times 10^{-6} \text{m/s}$ , the maximum amount that could be infiltrated is

$$38.9 \times 10^{-6} \text{m/s} \times 60 \times 60 \text{ s/h} \times 1000 \text{m}^2/\text{donum} = 140.04 \text{m}^3/\text{h.donum}.$$

Since the evapotranspiration is 60%, the total infiltration rate will be decreased to less than  $57 \text{ m}^3/\text{h.donum}$ . ( $60\% \times 140.04 \approx 57$ )

Table 5-12: Class name for the above samples, depending on the textural triangle

No.	Sand, %	Silt, %	Clay, %	Soil Class
A1	27.7	28.94	43.78	Clay
A2	7.16	15.4	77.74	Clay
A3	25.02	25.92	49.56	Clay
B1	27.96	24.78	47.36	Clay
B2	31.68	27.78	41.06	Clay
B3	29.82	23.74	47.12	Clay
C1	40.64	23.98	36.26	Clay Loam
C2	43.06	25.52	32.36	Clay Loam

As I mentioned before the soil is clay which has low infiltration potential rate and high runoff potential rate.

### 5.3 Hydrochemistry of the Groundwater

A hydrochemical study is conducted to define groundwater types and to determine hydrochemical parameters of the aquifer system. Eight groundwater wells in Al-Jiftlik area were samples during the period between March 3<sup>rd</sup> and March 6<sup>th</sup>. The depth of these wells range between 90m and 100 m, and tapping water from the alluvial deposits of Neogene age to plio-plistocene age. The salinity of water in them in term of chloride ranges between 700-1000 mg/L. The physical and chemical properties were determined. The major cations  $\text{Ca}^{2+}$ ,  $\text{Mg}^{2+}$ ,  $\text{Na}^+$  and  $\text{K}^+$  and the major anions  $\text{Cl}^-$ ,  $\text{HCO}_3^-$ ,  $\text{SO}_4^{2-}$ ,  $\text{NO}_3^-$ , and  $\text{PO}_4^{3-}$  were analyzed. The ratio of ((cations – anions) / (cations + anions)) were determined. The results are explained in appendix C1

Electrical conductivity: The EC of the tested wells ranges between 2200  $\mu\text{S}$  and 2700  $\mu\text{S}/\text{cm}$  in the western parts and rise to 3220 and 4620  $\mu\text{S}/\text{cm}$  in the eastern parts.

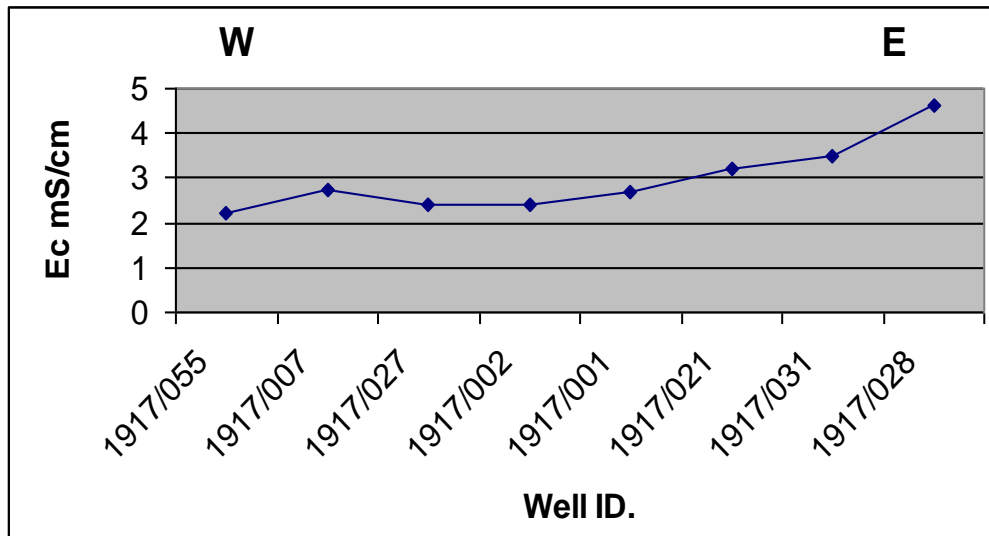


Fig.5.18: The **electrical conductivity** of the wells in the study area

Fig.5.16 shows that the area can be subdivided into two main EC regions: Western phreatic aquifers with low EC, and the eastern phreatic aquifer with high EC. According to this, the eastern phreatic aquifers are unusable for both drinking and agricultural purposes. The rise in Ec eastwards is related to the dissolution of Lisan formation, that interfinger with the alluvial deposits of the Wadi deposits.

pH value: Most of the groundwater in the study area has pH values ranging from 6.78 to 7.3. This indicates the neutralization of water.

Temperature: The average water temperature of the whole aquifer system is 24.2°C.

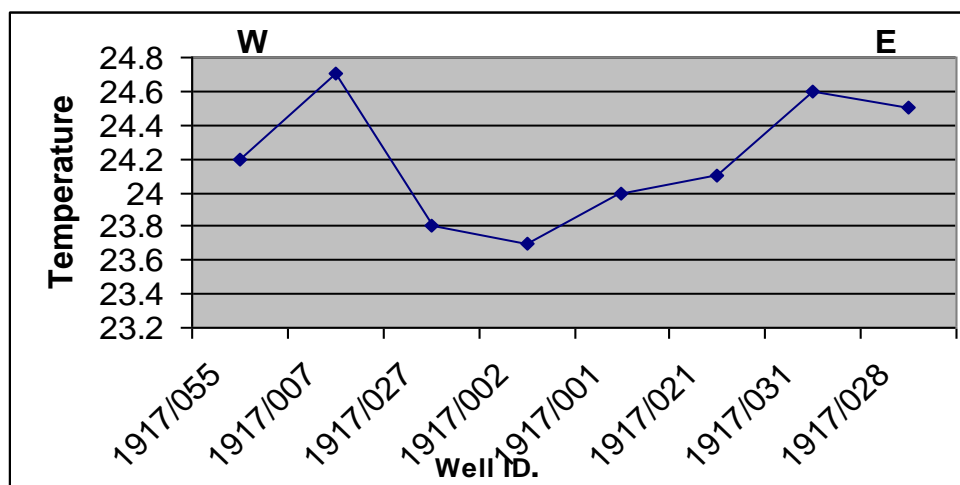


Fig.5.19: The temperature of the wells in the study area

The observed temperatures are close to temperatures expected from the local geothermal gradient.

Dissolved oxygen: The average dissolved oxygen is measured at the field to be 7.13 mg/L. A trend of increasing DO in the western part (6.38 to 8.66 mg/L) and decreasing DO is shown towards the east (5.35 to 6.37 mg/L). This indicates the recharge mechanism in the western part and the stored possibility in the eastern part.

Redox potential (Eh): The average Eh is measured at the field to be (-11.375 m.volts). A trend of increasing Eh in the western part (-11 to -7 m. volts) and decreasing Eh is shown towards the east (-5 to -17 m.volts).

Total dissolved solids (TDS); TDS of the groundwater increases rapidly towards the east. The lowest value of TDS was (2445 mg/L) and rises to (5015 mg/L) in the middle part and reaches (1602 mg/L) in its eastern parts, the results are shown in Fig.5.18.

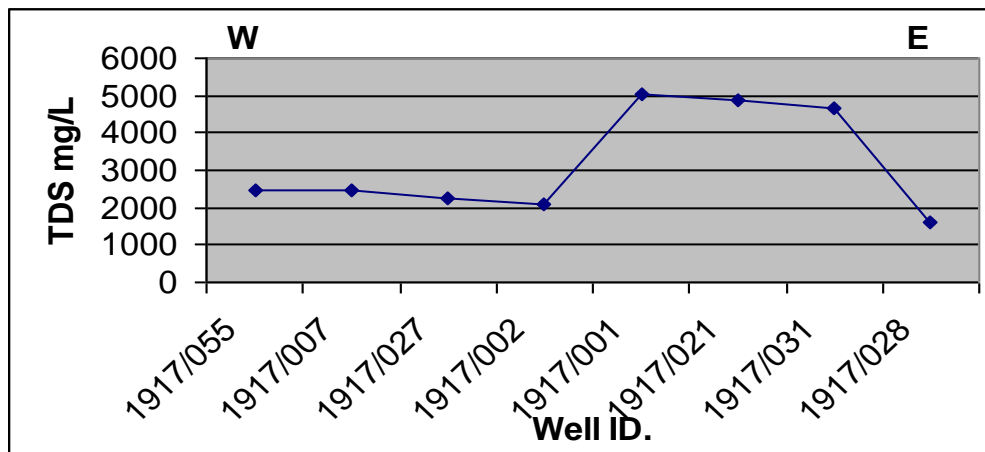


Fig.5.20: Concentration of TDS

Fig. 5.18 shows that in the study area groundwater can be divided into two categories: fresh water with low TDS, and brackish water with high TDS. Both types of water lie within the same aquifer which consists of alluvial deposit and conglomerate. As water moves down the total dissolved solids increase due to the contact with high soluble minerals consisting the aquifer system.

### 5.3.1 MAJOR IONS

Calcium and Magnesium ( $\text{Ca}^{2+}$  and  $\text{Mg}^{2+}$ ): Calcium is derived from calcite dissolution and therefore balanced by  $\text{HCO}_3^-$ .  $\text{Ca}^{2+}$  has a mean value of 259.38 mg/L in the study area.

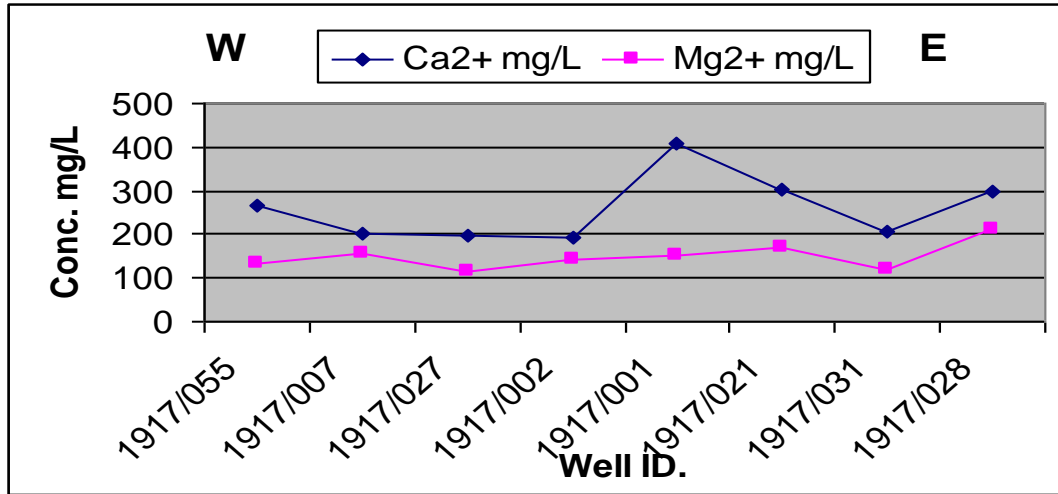


Fig.5.21: Concentration of  $\text{Ca}^{2+}$ ,  $\text{Mg}^{2+}$

Fig. 5.19 shows that the highest  $\text{Ca}^{2+}$  value is recorded in the eastern part of the study area (4871 mg/L), compared with (202.3 mg/L) in the western part. This quick increase of  $\text{Ca}^{2+}$  in short distance of water flow indicates a good source for this ion.

Magnesium shows a mean value of 149.6 mg/L for the whole system, but towards the east,  $\text{Mg}^{2+}$  increase slightly, which reflect the water-rock.

Sodium and potassium ( $\text{Na}^+$  and  $\text{K}^+$ ): the mean value of  $\text{Na}^+$  to the whole system is 1325.9 mg/L. An increase take place in the middy of the section and reach 2600 mg/L, which indicate dissolution of evaporates.

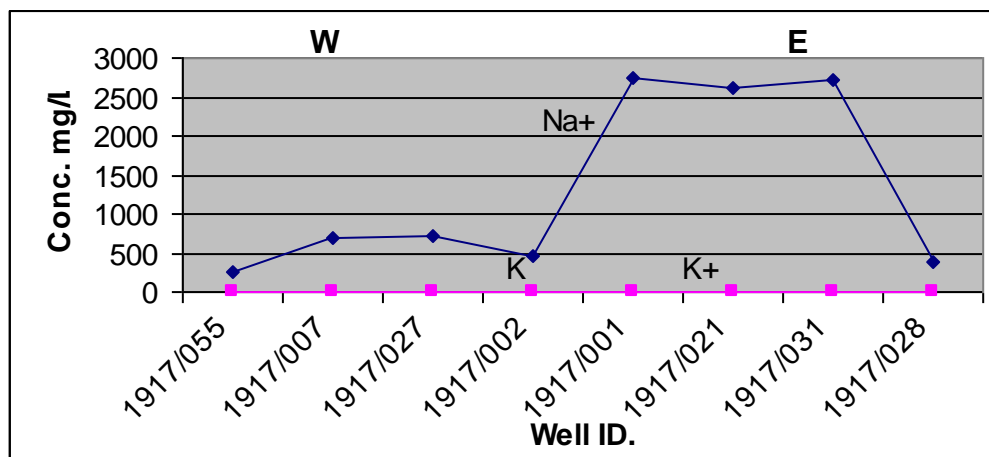


Fig.5.22: Concentration of  $\text{Na}^+$ ,  $\text{K}^+$

Potassium shows a mean value of 10.6 mg/L for the whole system, a small trend of  $K^+$  increasing is shown towards eastern part of the section.

Bicarbonate ( $HCO_3^-$ ) m- and p-Value ( $HCO_3^-$  and  $CO_3^{2-}$ , respectively): the amount of  $HCO_3^-$  concentration range between (301 and 316 mg/L), this reflects the dissolution of carbonate rocks that form the aquifer.

Sulfate ( $SO_4^{2-}$ ): the average value of  $SO_4^{2-}$  is 68.3 mg/L, an increasing trend of  $SO_4^{2-}$  content is recorded towards the east.

Sulfate content was found to be (68.2 mg/L) in the western well number 19-17/055 and reaches its maximum value (80 mg/L) by well number 19-17/028 in the eastern part. The high amount of  $SO_4^{2-}$  is due to the dissolution of gypsum from Lisan Formation that present in the eastern part of the section. Also it is a good indicator about the old path of Wadi Al-Farea.

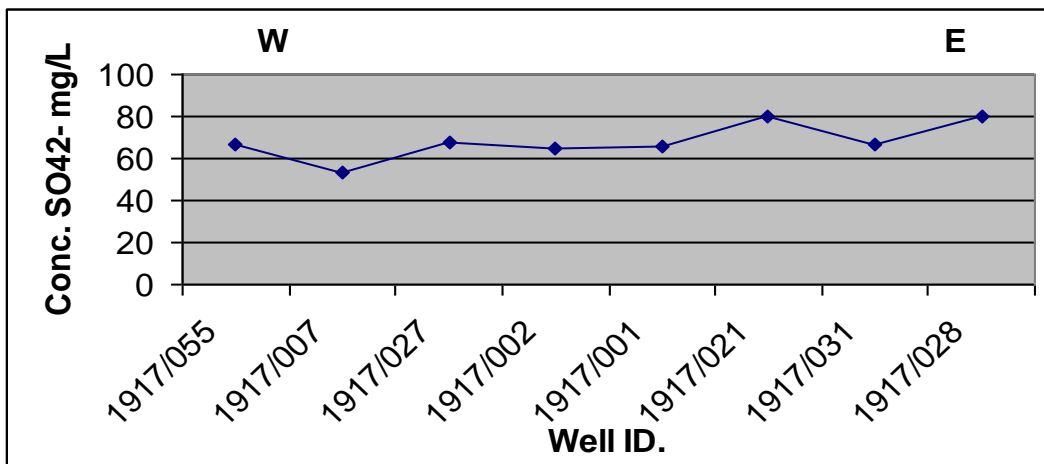


Fig.5.23: Concentration of sulfate

The contour map for the distribution of  $SO_4^{2-}$  is seen in Fig. 5.24

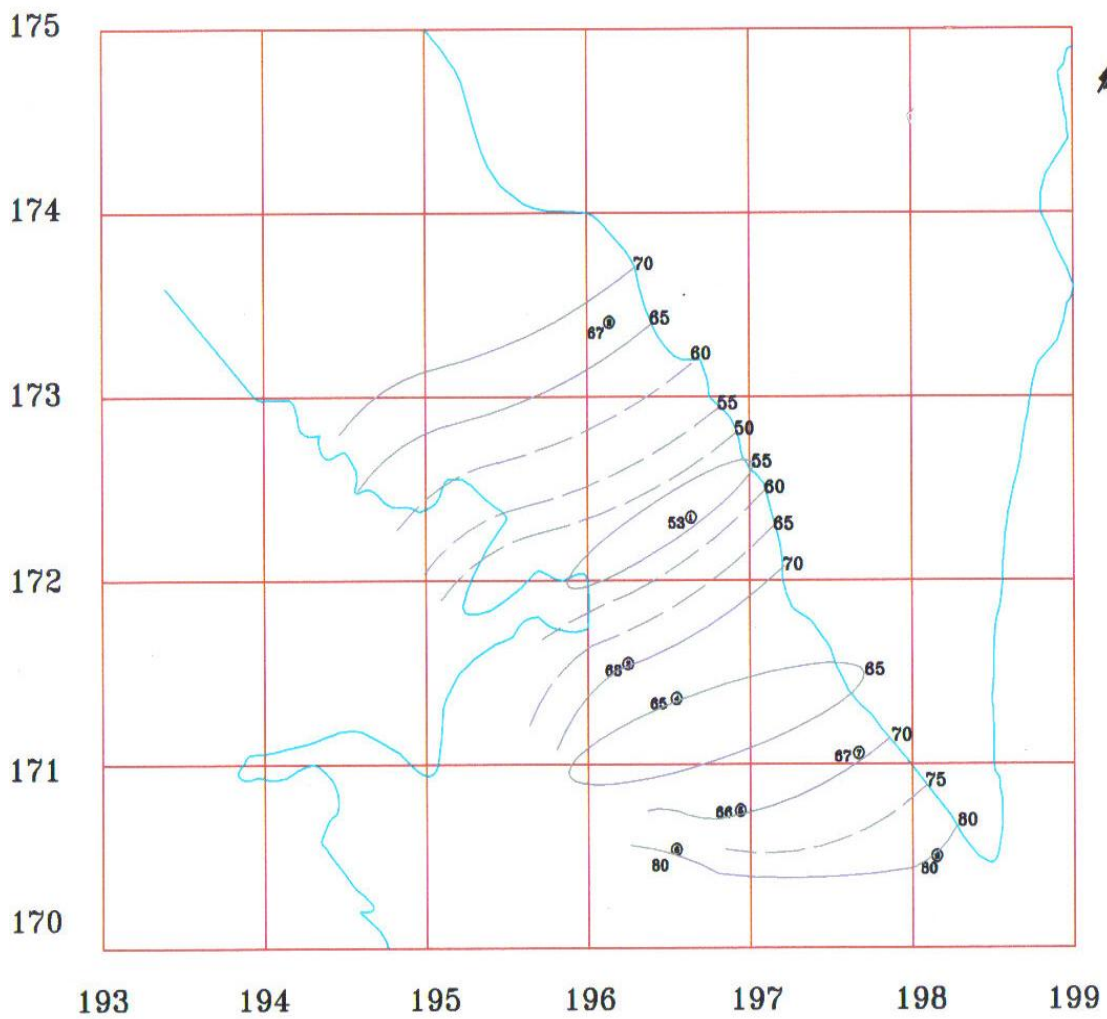


Fig 5.24: Contour map of  $\text{SO}_4^{2-}$

Chloride (Cl<sup>-</sup>): the mean value of chloride in the studied wells is 768.4 mg/L.

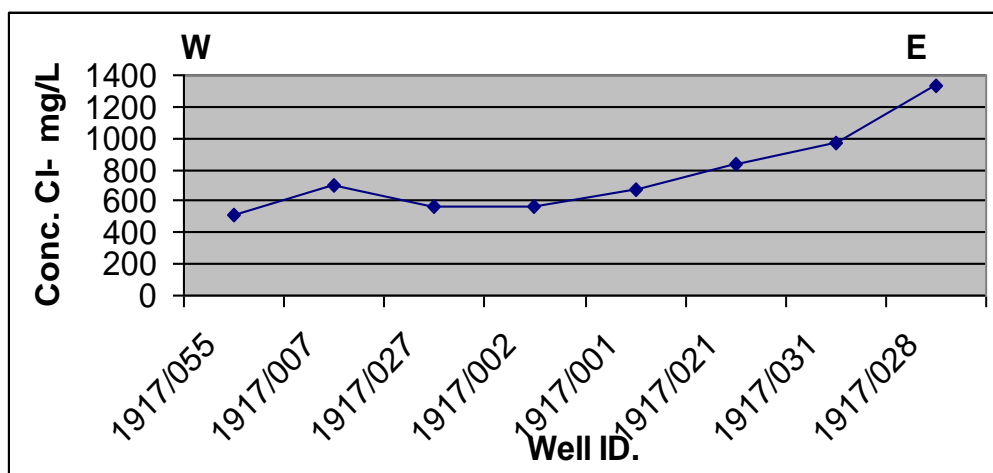


Fig5.25: Concentration of Cl<sup>-</sup> in the wells of the study area

Fig.5.25 shows that chloride content increase eastwards from (517 mg/L in well number 19-17/055, and reaches its maximum value 1333 mg/L by the well number 19-17/028. The high Cl<sup>-</sup> concentration in the eastern part of the study area is due to chlorine-bearing rocks of the Lisan formation, which contains a high amount of NaCl, as shown in Fig.(5.26 ).

Wells number 19-17/031 and 19-17/028 locate by elevation (-265, -268 m.bsl) respectively, and the ground water- table located by 35 and 32 m under the ground respectively. The Na/Cl ratios in well number 19-17/031 is 1.8 and 2.4 in well number 19-17/028 which indicate the dissolution of Halite from the Lisan formation. The water of the eastern phreatic sub-aquifers is not potable for drinking and is used for agriculture. The contour map for the distribution of Cl<sup>-</sup> is seen in Fig. (5.26)

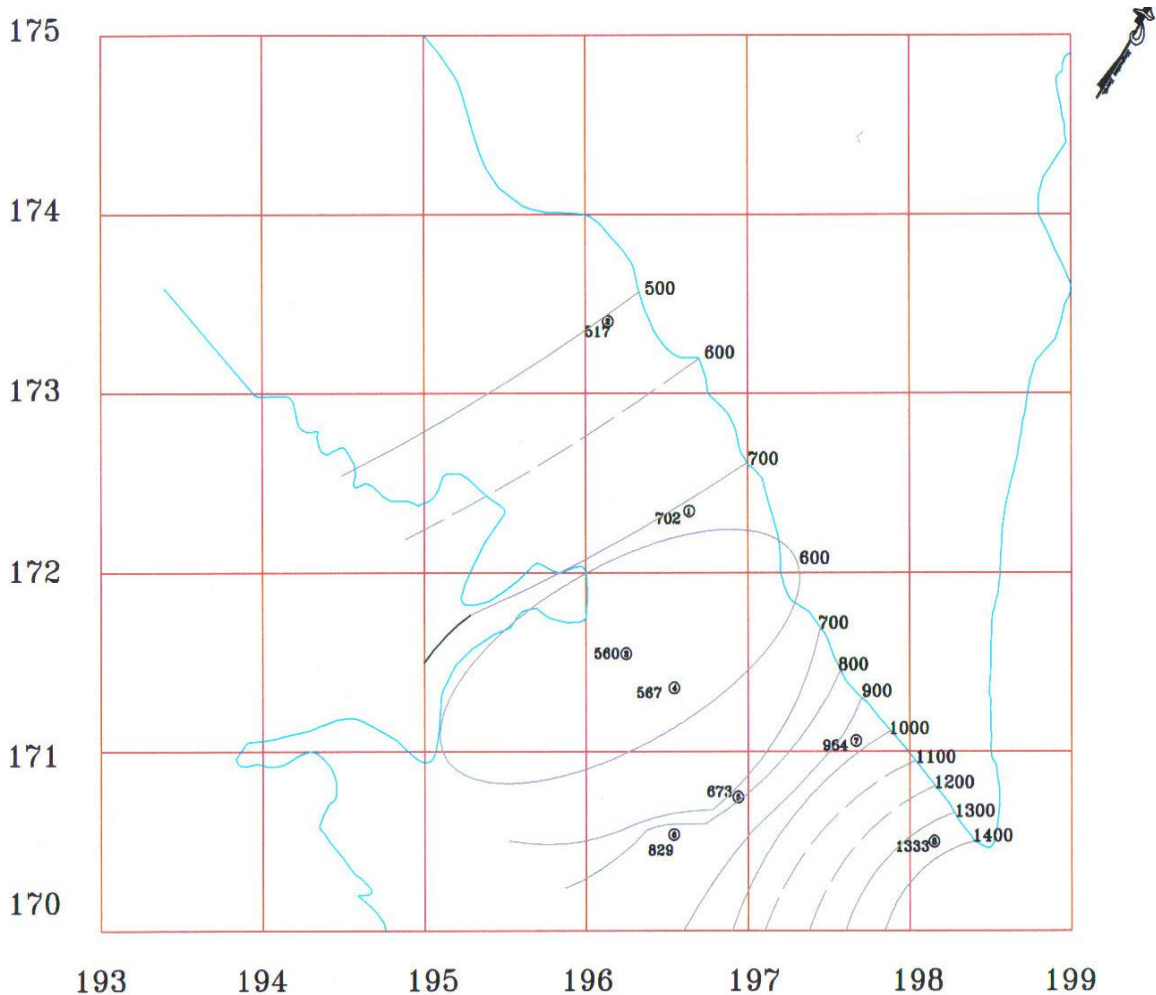


Fig5.26: Contour map of Cl<sup>-</sup>

Nitrate  $\text{NO}_3^-$ : it has a mean value of 21.7 mg/L for the whole system, in the eastern part it ranges between (20.2 to 21.7 mg/L), in the western zone the concentration of nitrate ranges between 14-30.6 mg/L, this trend is apposite to the normal trend of other ions. The low concentration of  $\text{NO}_3^-$  is due to the long stay time of water and due to denitration. The pollution of the Neogene sub-aquifer is due to the wastewater from the Nablus municipality. Agricultural fertilizers are also cause an increase in the amounts of  $\text{NO}_3^-$  in the groundwater in both the Eocene and Neogene sub-aquifers.

Phosphate ( $\text{PO}_4^{3-}$ ): Phosphate mean reaches up to 0.09 mg/L for the whole aquifer system. Its maximum value is seen in the eastern well "number 19-17/031" with 0.28 mg/L.

### 5.3.2: Saturation levels of some minerals in groundwater (Dolomite, Calcite, Aragonite and Gypsum).

Chemical analysis of groundwater samples was interred to the Hydrochem Software, in order to calculate the saturation indices of some minerals. Results are summarized in table 5.11.

Table (5.13) concentration of Dolomite, Calcite, Aragonite and Gypsum of the wells

Well ID	Dolomite-SI	Calcite-SI	Aragonite-SI	Gypsum-SI
19-17/001	2.46	1.26	1.11	-1.88
19-17/002	1.94	0.85	0.71	-1.81
19-17/007	2	0.88	0.73	-1.93
19-17/021	3.36	1.62	1.47	-1.89
19-17/027	1.8	0.84	0.69	-1.81
19-17/028	1.62	0.7	0.56	-1.59
19-17/031	3	1.43	1.29	-2.1
19-17/055	2.03	0.99	0.85	-1.64

Well locations are explained before in Fig.(5.2)

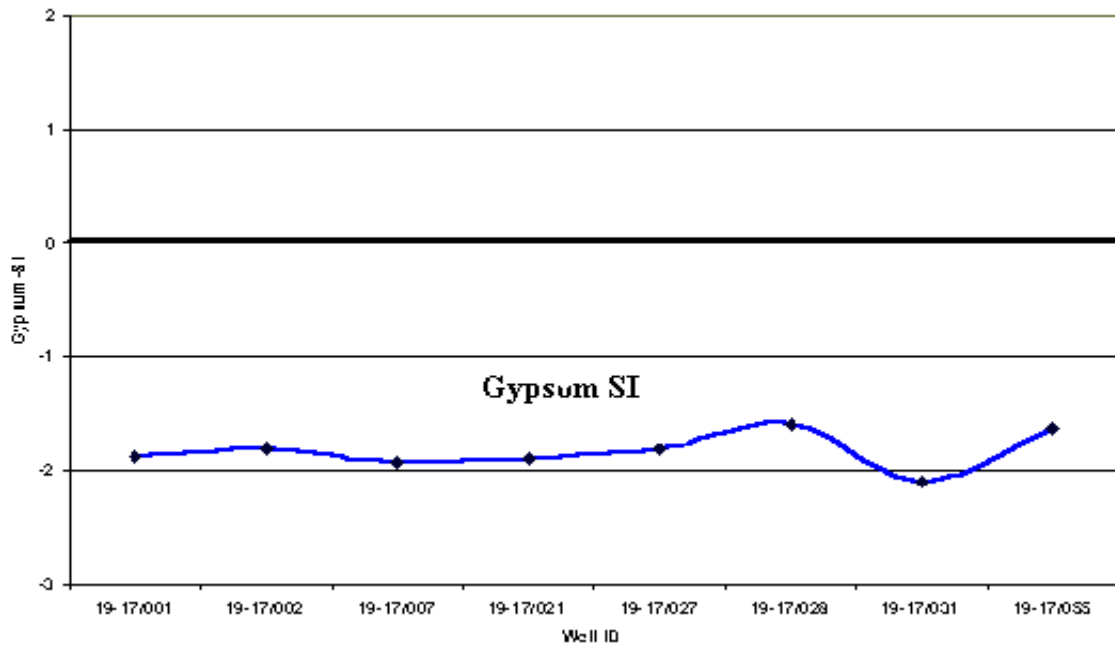


Fig.( 5.27) Gypsum saturated index of the studied wells

Gypsum is under saturated, this means no Lisan formation exist around the groundwater

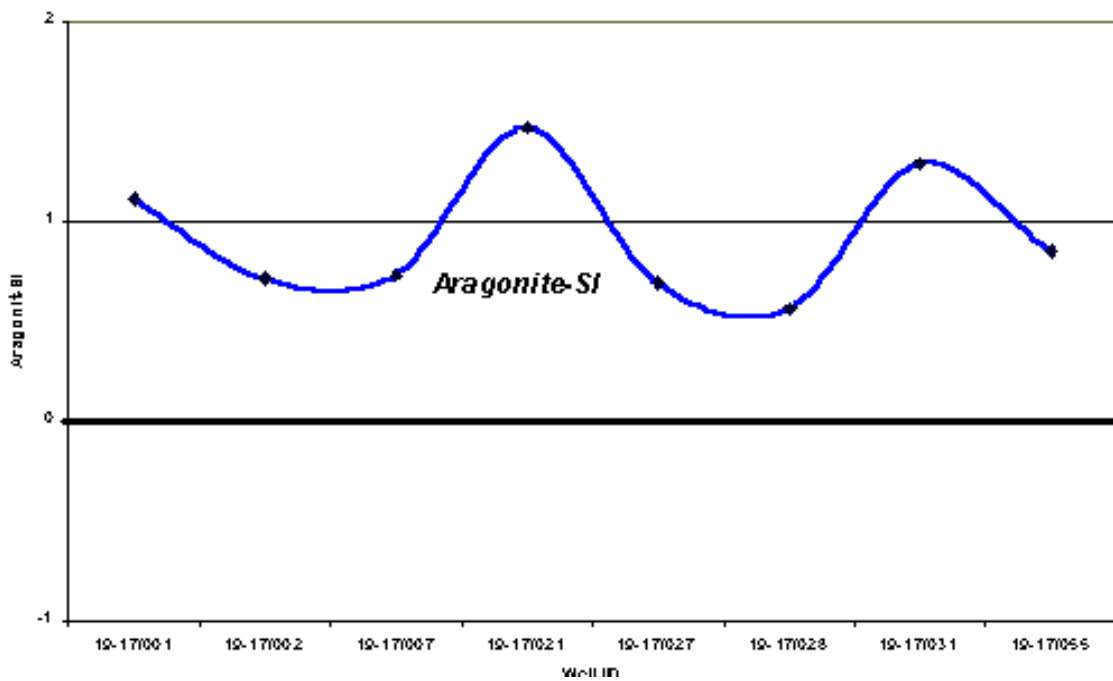


Fig.(5.28): Aragonite saturated index of the wells

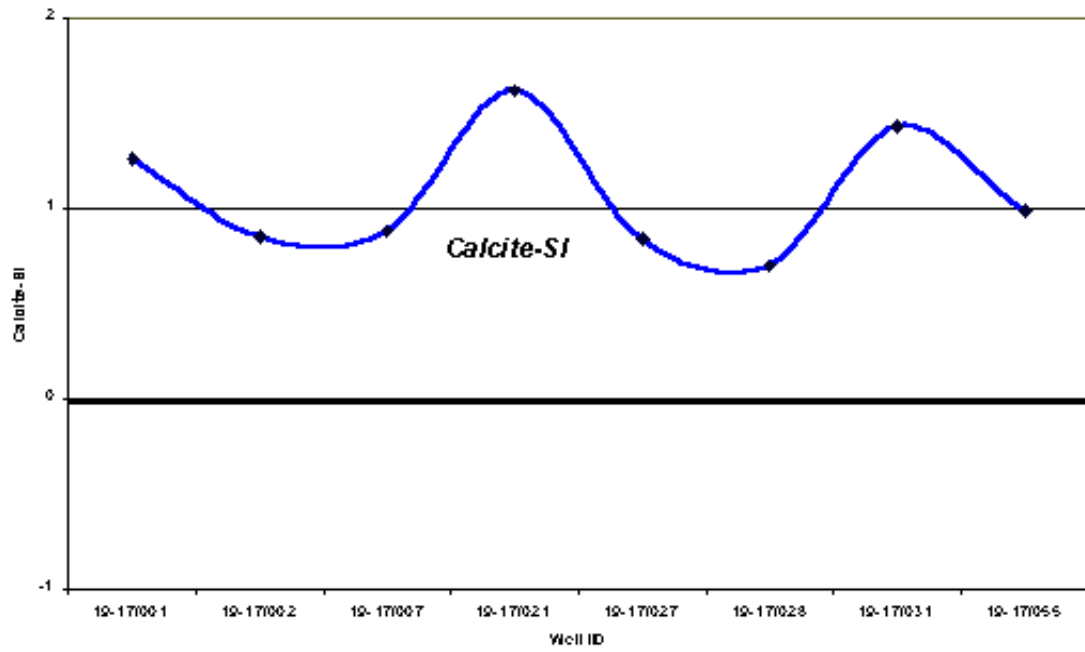


Fig.(5.29): Calcite saturated index of the studied wells

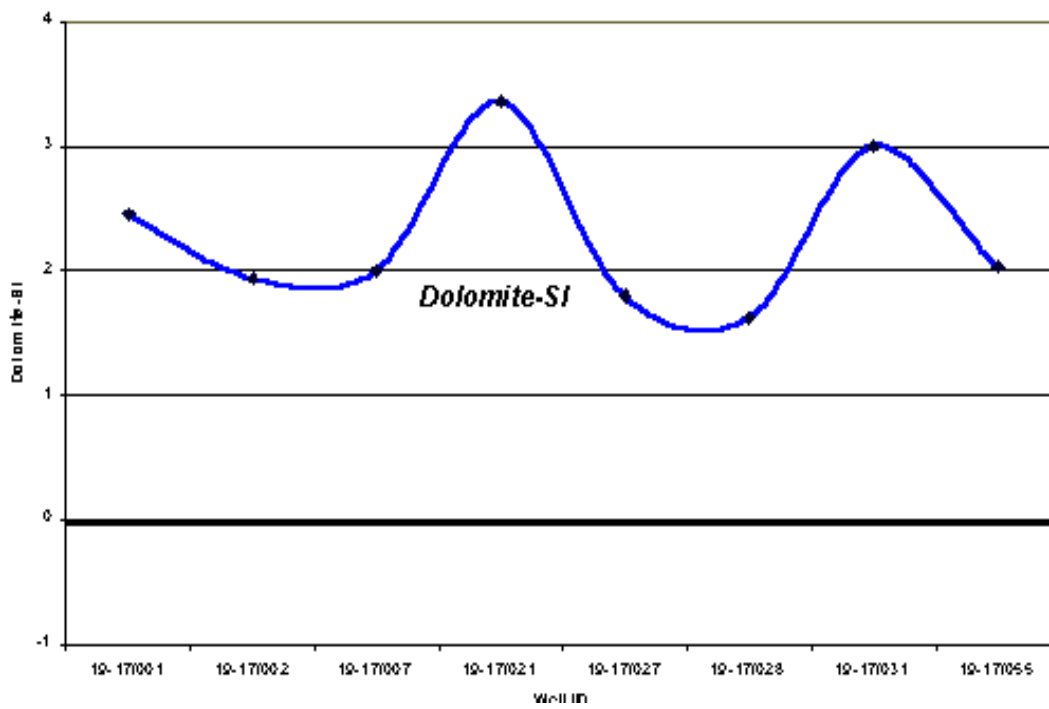


Fig.(5.30): Dolomite saturated index of the studied wells

## CHAPTER 6

### Results, Conclusion, and Recommendations

#### 6.1 Results

Ground water resources in Al-Jiftlik area is very limited. The high salinity of the ground water (1.1-2.4) and the high Ec (2200 – 200  $\mu$ S) makes it unusable for both drinking and agricultural purposes. The quality of the water degraded in the last few years, because of the over pumping, the less rain fall which yields a decrease in recharge water. Rapid population growth (4617 inhabitants According to the PCBS statistics in 2007) associated with rapid development in the Faria basin has put more pressure on the existing limited resources.

#### **The following are the main results of this study**

1- Surface flood water is not suitable as artificial recharge for groundwater due to the clay soil that covers the Wadi which has low infiltration potential rate and high runoff potential rate. This confirms with our fourth hypothesis.

2- The suitable method to be used for artificial recharge is to inject the flood water to the nearest wells or ponds.

3- The thickness of the unsaturated gravel aquifer in the lower part of Al-Jiftlik( about 20 m) could be used to store flood water, about 8-10 mcm of flood water could be injected in the lower part of Al-Jiftlik, this will improve the quality and quantity of the groundwater that is used for agriculture. This result confirms our first and second hypothesis.

4- Litho logical cross section to Faria basin at Al-Jiftlik is determined depending on the resistivity, and geoelectrical profiles for the aquifer system shows that five sub - aquifers are located within the unconfined aquifer systems. These sub - aquifers are Pleistocene, Neogene, Eocene, Upper and Lower Cinomanian aquifers.

5- Hydrochemistry study to eight wells show that the phreatic western sub-aquifers and the confined aquifer show an increasing trend of  $Ca^{2+} > Mg^{2+} > Na^{+} + K^{+}$ . An increasing trend of  $Ca^{2+} > Na^{+} + K^{+} > Mg^{2+}$  is shown for the eastern phreatic sub-aquifers. Three anions increasing trend orders are observed:  $HCO_3^{-} > Cl^{-} > NO_3^{-} > SO_4^{2-}$  in the phreatic western sub-aquifers,  $HCO_3^{-} > Cl^{-} > SO_4^{2-} > NO_3^{-}$  in the confined aquifer and  $Cl^{-} > HCO_3^{-} > SO_4^{2-} > NO_3^{-}$  in the phreatic eastern sub-aquifers. The increasing trend of  $NO_3^{-}$  in reference to  $SO_4^{2-}$  in the phreatic western sub-aquifers is due to pollution caused by cesspools and septic tanks, as

well as the wastewater, that are draining into the Wadi Faria from Nablus municipality( 6000m<sup>3</sup>/d)

The phreatic western sub-aquifers and the confined aquifer are composed of carbonate rocks (limestone and in some places dolomitic limestone) with low salinity (< 800 mg/L). Otherwise, the phreatic eastern sub-aquifers consist of alluvium and Lisan formations (gypsum-marl-Lisan) with high salinity (> 1000 mg/L). Thus, the composition of rocks and soils has a direct influence on water quality. The ratio Mg/Ca is between 0.5 and 0.8, within the same ratio of rainfall, which indicates aquifers of limestone and dolomite nature.

The salinity of the groundwater shows an increase trend towards the east, but the Na/Cl ratio which ranges from 0.2 to 2.3 decreases. This decreased value is due to the absorption of sodium by the clay minerals. An increasing trend of sulfate SO<sub>4</sub><sup>2-</sup> content is recorded towards the eastern groundwater wells. The high amount of SO<sub>4</sub><sup>2-</sup> is due to the dissolution of gypsum from Lisan Formation

6- Sieve analysis to the soil of Al-Farea area was done, the soil is clay to clay loam. It has a low infiltration potential rate and high runoff potential rate. The hydraulic conductivity is very small it is in the range  $2-9 \times 10^{-5}$  m/s.

7- The lower eastern zone of the study area is facing huge salinization problems of aquifer water while nitrate pollution is less notable there. Values of Ec higher than 4,000  $\mu\text{S/cm}$ , are frequent in the lower zone. It is well known that only tolerant crops are able to tolerate salinity levels higher than 2,200  $\mu\text{S/cm}$ . Farmers are to mix brackish well water with Wadi water of lower salinity to obtain irrigation water with tolerable salinity content.

8-Salinity of groundwater increased towards the east where Lisan Formation is dominate, and it dissolute through long duration time reaction between fresh water marl and clay and minerals of Lisan formation especially in the lower part of the study area, and the over pumping by the farmers.

## 6.2: Conclusion

The overall objective of this study is to improve water resources in Al-Jiftlik area by using artificial recharge. Through the geoelectrical investigation, this study prove that there is a gravel layer of 20 m thick which can be used to store 8-10 mcm groundwater. One of the techniques involves the filling of excavations close to wadi beds with a clay liner at the bottom, coarse rocks in the middle and a cover at the top, but the most suitable way is to inject the flood water to the nearest wells.

Within the area, both surface runoff and wastewater are available as sources, while significant amount of wastewater is produced (6000cm/d from Nablus municipality); it is as far as possible used for irrigation following treatment. The alluvial fan aquifers at the inlets of the Wadis to the Jordan valley offer a good potential for aquifer recharge due to their low hydraulic conductivity, the gentle gradients and the long retention time. Planning for aquifer recharge must take the local circumstances into account, such as the strong seasonality of rainfall, and high intensity peak rain events which require large reservoirs to provide temporal storage for runoff during flash floods. This study show that a considerable potential in the lower Faria basin for managed aquifer recharge exists.

### **6.3: Recommendations**

From the results of this study, the following recommendations can be drawn:

- Geoelectrical investigation is recommended to be done to the whole Wadi from Nablus in the west to the River Jordan in the east, in order to have a complete view about the lithology of the Wadi.
- Isotopic composition is recommended to be studied to determine if there is mixing between the wells
- Scientific study is recommended to be done to the existing dam to repair and enlarge it in order to be used to collect rain water, and flood water during rainy months, to be used in later un rainy months.
- At the eastern part especially at Al-Jiftlik it is recommended to study the possibility of establishing an artificial pond to collect flooding water, or to pump the water to the nearest wells. This will increase the groundwater content and decrease it's salinity.

## 7. References

- Al-Nubani, N.i. (2000) .Rainfall-Runoff Process and Rainfall Analysis for Nablus Basin .M.Sc.theses, Faculty of Graduate Studies , Al-Najah National University , Nablus , Palestine. 6- Arora C. L (1986 ) Geoelectric Study of Some Indian Geothermal Areas : Geothrowth american Srmal 15:(677-688 ).
- Awadallah W. ,and Owaiwi M ,( 2005) ,Springs and Dug Wells of Hebron District , p19.
- Barakat, M.H ( 2000) , Rainfall Runoff Process and Modeling for Soreq Stream sub-basin near Jerusalem Msc. thesis , Faculty of Graduate Studies , Al-Najah National University , Nablus , Palestine.
- Bashir, B. 2003. Rainfall Runoff Analysis using the synthetic unit hydrograph for wadi Faria Catchmnet, Msc. thesis, Bir Zeit University
- Ben-Avraham Zvi (1996), The Dead Sea: The Lake and its Setting
- Birzeit University and Calvin College ,(2003) .Wadi Al-Faria Project Report :An Environmental Assessment of the Wadi Al-Faria Watershed ,USAID, Palestine ..
- Burger H.R. ( 1992) ,Exploration Geophysics of the Shallow Surface. Printice Hall,NJ,485pp.
- California Irrigation Management System, CIMS 2005.
- Dahlin T 1996,2D Resistivity Survey for Environmental and Engineering Application. First Break, 14,p 275-284.
- De Breuk E, De Moor G 1985 ,The Water Table Aquifer in the Eastern Coastal Area of Belgium.Bull .Assoc .Sci. Hydro . 14 :p 137-155
- De Laat, P.J.M.,1999, Workshop on Hydrology, Lecture Notes, Delft University, The Netherlands
- Environment Quality Authority. The Faria and Jerash Integrated Watershed Management Project FJIWMP ,2006 )
- Forward, (1998) .The Potential for Stormwater Harvesting in the Eastern Surface Catchment of the West Bank. Prepared for the United States Agency for International Development.
- Fouad F, Parasnis 86 ,Shaaban 2001 , Vertical Electric Sounding for Groundwater investigation in Egypt :A case Study In A coastal Area , African Earth Sciences 33 : (2001) , p 673-686.

- Ghanem, M. 1999. Hydrogeology and Hydrochemistry of Faria drainage basin, West Bank ,ph.d. diss ,Wissenschaftliche Mitteilungen , institut Fur Geologie .Technische Universital Berbakademie Freiburger ,Germany .
- Ghayoumian, J ,Ghermezcheshme B , Feiznia S ,Noroozi A 2005 , Integration GIS and DSS for Identification of suitable Areas for Artificial Recharge , Case Study Meimeh Basin ,Isfahan , Iran ,Environmental Geology ,47: 493-500.
- Griffiths D.H. and Barker R.D.,1993. Two-dimensional resistivity imaging and modeling in areas of complex geology. Journal of Applied Geophysics, 29, 211-129.
- Hasan R. Shabana, 1996. Irrigation Scheduling of Palm Trees in the United Arab Emirates.
- Koefoed O 1979, Geosounding Principles 1: Resistivity Sounding Measurements. Elsevier Science Publishing, Company, Amsterdam.
- Loke M.H 2002 ,Tutorial 2D Electrical Imaging Surveys.
- Marei A,Ghanem , Artificial Recharge Investigation in a semi arid region, case Study: Wadi Al Faria, 2007.
- Marei A .( 2003 ),The origin and mechanisms of stalinization of lower Jordan River .
- McWorter, D.B., and D.K. Sunada, 1977. Groundwater Hydrology and Hydroloulics, Water resources Publications, Ft. Collins,Co.
- Meteorological service, 1997. Meteorological data: Rainfall, Temperature, Wind, Humidity and Evapotranspiration: Unpublished data, Rahovet - Tel Avi
- Ministry of Transport 1998, Palestine Climate Data Handbook.(MoT,1998)
- Nebel B.J.,Wright R.T., 1998,Environmental Science, Sixth Edition ,p 263-292 .
- Paarkhurst, D. L., Thorsternson, D.C. and Plummer, L. N. 1980.PhreEQA– a computer program for geochemical calculations. U.S: geological Survey, Water Resources Invest., 80-96, NTIS Tech. Report. PB81-167801, Springfield, 210pp
- Palestinian Water Authority (PWA) 2002, Hydrological Data Base, West Bank – Palestine.
- Rofe and Raffety Consulting Eng. ( 1965 ) . West Bank Hydrology ( 1963-1965) Analysis .
- Schwartz, J., 1980. Water Resources in Judea, Samaria and Gaza Strip.  
UNESCO, 1979. Aridity definition (UN documents): New York GWW. 1994. Groundwater for Windows (manual and software): United Nation, New York.
- Neven K., 1997, Quantitative Solutions in Hydrology and Groundwater

### Modeling.

- Telford W. M. Geldart L .P. ,Sheriff R.E. 1990 , Applied Geophysical ,Second Edition , Cambridge University Press.
- Verma R.K,Reo M.K.,Rro C.V. ,1980 ,Resistivity Investigations for Groundwater in Metamorphic Areas Near Dhanbad ,India .Groundwater 18 (1):p 46-55.
- Zohdy A.A.R. 1969 , The Use of Schlumberger and Equatorial Sounding on Groundwater Investigation Near El Paso ,TX .Geophysics 34 :713-728.
- UNDP ,Palestinian Ministry of Agriculture,AOFAD ,

## 8. Appendices

### A1: Aquachim to well number 19-17/055

SampleID : 19-17/055  
Location : Jawad Al Masri  
Site : Al Jiftlik  
Sampling Date : 08/03/2008  
Geology : Eocene  
Watertype : Ca-Na-Mg-HCO3-Cl

Sum of Anions (meq/l) : 35.5599  
Sum of Cations (meq/l) : 35.5465  
Balance: : -0.02%

Calculated TDS(mg/l) : 2444.4

Hardness : meq/l °f °g mg/l CaCO3  
Total hardness : 24.09 120.45 67.45 1204.5  
Permanent hardness : 4.82 24.08 13.48 240.8  
Temporary hardness : 19.28 96.38 53.97 963.8  
Alkalinity : 19.28 96.38 53.97 963.8  
(f = 10 mg/l CaCO3/1 °g = 10 mg/l CaO° 1)

#### Major ion composition

%mg/l	mmol/l	meq/l	meq
Na+	257.0	11.179	11.179 15.721
K+	10.72	0.274	0.274 0.385
Ca++	266.8	6.657	13.313 18.723
Mg++	131.0	5.389	10.777 15.156
Cl-	517.0	14.583	14.583 20.509
SO4--	67.0	0.698	1.395 1.962
HCO3-	1175.979	19.276	19.276 27.109

#### Ratios Comparison to Seawater

mg/l	mmol/l	mg/l	mmol/l
Ca/Mg	2.037	1.235	0.319 0.194
Ca/SO4	3.982	9.544	0.152 0.364
Na/Cl	0.497	0.767	0.556 0.858

#### Dissolved Minerals: mg/l mmol/l

Halite (NaCl)	: 653.958	11.1788
Sylvite (KCl)	: 20.44	0.2758
Carbonate (CaCo3)	: 57.102	0.571
Dolomite (CaMg(CO3)2):	992.065	5.389
Anhydrite (CaSO4)	: 95.001	0.698

**A2: Aquachim to well number 19-17/002**

SampleID : 19-17/002  
 Location : Amed Al Masri  
 Site : Al Jiftlik  
 Sampling Date : 08/03/2008  
 Geology : Eocene  
 Watertype : Na-Mg-Ca-HCO3-Cl

Sum of Anions (meq/l) : 42.3801  
 Sum of Cations (meq/l) : 42.2923  
 Balance: : -0.10%

Calculated TDS(mg/l) : 2076.1

Hardness : meq/l °f °g mg/l CaCO3  
 Total hardness : 21.4 107.01 59.93 1070.1  
 Permanent hardness : 0.0 0.00 0.00 0.0  
 Temporary hardness : 21.4 107.01 59.93 1070.1  
 Alkalinity : 24.67 123.34 69.07 1233.4  
 (f = 10 mg/l CaCO3/ 1 °g = 10 mg/l CaO° 1)

**Major ion composition**

	%mg/l	mmol/l	meq/l	meq
Na+	474.0	20.618	20.618	24.35
K+	10.54	0.27	0.27	0.319
Ca++	191.5	4.778	9.556	11.286
Mg++	144.0	5.923	11.847	13.992
Cl-	567.2	15.999	15.999	18.895
SO4--	65.0	0.677	1.353	1.598
HCO3-	1504.976	24.669	24.669	29.135

Ratios	Comparison to Seawater			
	mg/l	mmol/l	mg/l	mmol/l

Ca/Mg	1.33	0.807	0.319	0.194
Ca/SO4	2.946	7.061	0.152	0.364
Na/Cl	0.836	1.289	0.556	0.858

Dissolved Minerals:	mg/l	mmol/l
---------------------	------	--------

Halite (NaCl)	: 920.151	15.7291
Sylvite (KCl)	: 20.096	0.2712
Dolomite (CaMg(CO3)2):	755.041	4.101
Anhydrite (CaSO4)	: 92.165	0.677

**A3: Aquachim to well number 19-17/007**

SampleID : 19-17/007  
 Location : Fathalla Al Masri  
 Site : Al Jiftlik  
 Sampling Date : 08/03/2008  
 Geology : Eocene  
 Watertype : Na-Mg-HCO3-Cl

Sum of Anions (meq/l) : 52.9786  
 Sum of Cations (meq/l) : 52.9403  
 Balance: : -0.04%

Calculated TDS(mg/l) : 2473.7

Hardness : meq/l °f °g mg/l CaCO3  
 Total hardness : 22.81 114.07 63.88 1140.7  
 Permanent hardness : 0.0 0.00 0.00 0.0  
 Temporary hardness : 22.81 114.07 63.88 1140.7  
 Alkalinity : 31.84 159.19 89.15 1591.9  
 (f = 10 mg/l CaCO3/ 1 °g = 10 mg/l CaO° 1)

**Major ion composition**

	%mg/l	mmol/l	meq/l	meq
Na+	688.0	29.926	29.926	28.254
K+	7.75	0.198	0.198	0.187
Ca++	202.3	5.047	10.095	9.531
Mg++	154.6	6.36	12.719	12.008
Cl-	701.91	19.798	19.798	18.692
SO4--	53.0	0.552	1.104	1.042
HCO3-	1942.377	31.838	31.838	30.059

Ratios	Comparison to Seawater			
	mg/l	mmol/l	mg/l	mmol/l

Ca/Mg	1.309	0.794	0.319	0.194
Ca/SO4	3.817	9.148	0.152	0.364
Na/Cl	0.98	1.512	0.556	0.858

Dissolved Minerals:	mg/l	mmol/l
---------------------	------	--------

Halite (NaCl)	: 1146.607	19.6001
Sylvite (KCl)	: 14.777	0.1994
Dolomite (CaMg(CO3)2):	827.648	4.496
Anhydrite (CaSO4)	: 75.15	0.552

**A4: Aquachim to well number 19-17/021**

SampleID : 19-17/021  
 Location : Haza'a Majed  
 Site : Al Jiftlik  
 Sampling Date : 08/03/2008  
 : Geology  
 Watertype : Na-HCO<sub>3</sub>

Sum of Anions (meq/l) : 143.6273  
 Sum of Cations (meq/l) : 143.4144  
 Balance: : -0.07%

Calculated TDS(mg/l) : 4870.9

Hardness : meq/l °f °g mg/l CaCO<sub>3</sub>  
 Total hardness : 29.17 145.86 81.68 1458.6  
 Permanent hardness : 0.0 0.00 0.00 0.0  
 Temporary hardness : 29.17 145.86 81.68 1458.6  
 Alkalinity : 118.07 590.35 330.60 5903.5  
 (f = 10 mg/l CaCO<sub>3</sub>/ 1 °g = 10 mg/l CaO° 1)

## Major ion composition

	%mg/l	mmol/l	meq/l	meq
Na+	2620.0	113.963	113.963	39.703
K+	10.82	0.277	0.277	0.097
Ca++	305.3	7.617	15.235	5.308
Mg++	169.4	6.968	13.937	4.855
Cl-	829.53	23.398	23.398	8.151
SO <sub>4</sub> --	80.0	0.833	1.666	0.58
HCO <sub>3</sub> -	7203.219	118.07	118.07	41.133

Ratios	Comparison to Seawater			
	mg/l	mmol/l	mg/l	mmol/l

Ca/Mg	1.802	1.093	0.319	0.194
Ca/SO <sub>4</sub>	3.816	9.146	0.152	0.364
Na/Cl	3.158	4.871	0.556	0.858

Dissolved Minerals: mg/l mmol/l

Halite (NaCl)	: 1352.596	23.1213
Sylvite (KCl)	: 20.63	0.2784
Dolomite (CaMg(CO <sub>3</sub> ) <sub>2</sub> ):	1249.011	6.784
Anhydrite (CaSO <sub>4</sub> )	: 113.434	0.833

**A5: Aquachim to well number 19-17/027**

SampleID : 19-17/027  
 Location : Ali Smadi  
 Site : Al Jiftlik  
 Sampling Date : 08/03/2008  
 Geology : Alluvium  
 Watertype : Na-HCO3-Cl

Sum of Anions (meq/l) : 51.3098  
 Sum of Cations (meq/l) : 51.1981  
 Balance: : -0.11%

Calculated TDS(mg/l) : 2237.3

Hardness	: meq/l	°f	°g	mg/l CaCO3
Total hardness	: 19.26	96.30	53.93	963.0
Permanent hardness	: 0.0	0.00	0.00	0.0
Temporary hardness	: 19.26	96.30	53.93	963.0
Alkalinity	: 33.71	168.56	94.39	1685.6

(f = 10 mg/l CaCO3/ 1 °g = 10 mg/l CaO° 1)

**Major ion composition**

%mg/l	mmol/l	meq/l	meq
Na+	728.0	31.666	30.891
K+	10.53	0.269	0.262
Ca++	196.7	4.908	9.575
Mg++	114.8	4.722	9.214
Cl-	560.11	15.799	15.412
SO4--	68.0	0.708	1.381
HCO3-	2056.67	33.711	32.886

Ratios	Comparison to Seawater		
mg/l	mmol/l	mg/l	mmol/l

Ca/Mg	1.713	1.039	0.319	0.194
Ca/SO4	2.893	6.933	0.152	0.364
Na/Cl	1.3	2.004	0.556	0.858

Dissolved Minerals: mg/l mmol/l

Halite (NaCl)	: 908.467	15.5294
Sylvite (KCl)	: 20.077	0.2709
Dolomite (CaMg(CO3)2):	773.177	4.2
Anhydrite (CaSO4)	: 96.419	0.708

**A6: Aquachim to well number 19-17/028**

SampleID : 19-17/028  
 Location : Ali Al Dahdour  
 Site : Al Jiftlik  
 Sampling Date : 08/03/2008  
 : Geology  
 Watertype : Mg-Na-Ca-Cl

Sum of Anions (meq/l) : 49.3512  
 Sum of Cations (meq/l) : 49.3436  
 Balance: : -0.01%

Calculated TDS(mg/l) : 2934.4

Hardness : meq/l °f °g mg/l CaCO<sub>3</sub>  
 Total hardness : 32.49 162.44 90.97 1624.4  
 Permanent hardness : 22.73 113.67 63.65 1136.7  
 Temporary hardness : 9.76 48.78 27.32 487.8  
 Alkalinity : 9.76 48.78 27.32 487.8  
 (f = 10 mg/l CaCO<sub>3</sub>/1 °g = 10 mg/l CaO° 1)

## Major ion composition

	%mg/l	mmol/l	meq/l	meq
Na+	380.0	16.529	16.529	16.748
K+	12.56	0.321	0.321	0.325
Ca <sup>++</sup>	300.4	7.495	14.99	15.188
Mg <sup>++</sup>	212.7	8.749	17.499	17.73
Cl <sup>-</sup>	1332.9	37.596	37.596	38.093
SO <sub>4</sub> <sup>--</sup>	80.0	0.833	1.666	1.688
HCO <sub>3</sub> <sup>-</sup>	595.157	9.755	9.755	9.884

Ratios	Comparison to Seawater			
	mg/l	mmol/l	mg/l	mmol/l

Ca/Mg	1.412	0.857	0.319	0.194
Ca/SO <sub>4</sub>	3.755	8.999	0.152	0.364
Na/Cl	0.285	0.44	0.556	0.858

Dissolved Minerals: mg/l mmol/l

Halite (NaCl)	: 966.942	16.5289
Sylvite (KCl)	: 23.948	0.3232
Dolomite (CaMg(CO <sub>3</sub> ) <sub>2</sub> ):	1226.504	6.662
Anhydrite (CaSO <sub>4</sub> )	: 113.434	0.833

**A7: Aquachim to well number 19-17/031**

SampleID : 19-17/031  
 Location : Suliman Abu Eweg  
 Site : Al Jiftlik  
 Sampling Date : 08/03/2008  
 Geology : Alluvium  
 Watertype : Na-HCO<sub>3</sub>

Sum of Anions (meq/l) : 138.5755  
 Sum of Cations (meq/l) : 138.5361  
 Balance: : -0.01%

Calculated TDS(mg/l) : 4661.8

Hardness	: meq/l	°f	°g	mg/l CaCO <sub>3</sub>
Total hardness	: 19.94	99.69	55.82	996.9
Permanent hardness	: 0.0	0.00	0.00	0.0
Temporary hardness	: 19.94	99.69	55.82	996.9
Alkalinity	: 109.66	548.29	307.04	5482.9

(f = 10 mg/l CaCO<sub>3</sub>/ 1 °g = 10 mg/l CaO° 1)

## Major ion composition

%mg/l	mmol/l	meq/l	meq
Na+	2720.0	118.312	118.312 42.695
K+	11.0	0.281	0.281 0.101
Ca++	205.0	5.115	10.23 3.692
Mg++	118.0	4.854	9.708 3.503
Cl-	964.24	27.198	27.198 9.815
SO <sub>4</sub> --	67.0	0.698	1.395 0.503
HCO <sub>3</sub> -	6689.959	109.657	109.657 39.571

Ratios	Comparison to Seawater		
mg/l	mmol/l	mg/l	mmol/l

Ca/Mg	1.737	1.054	0.319	0.194
Ca/SO <sub>4</sub>	3.06	7.333	0.152	0.364
Na/Cl	2.821	4.35	0.556	0.858

Dissolved Minerals: mg/l mmol/l

Halite (NaCl)	: 1574.608	26.9164
Sylvite (KCl)	: 20.973	0.283
Dolomite (CaMg(CO <sub>3</sub> ) <sub>2</sub> ):	813.218	4.417
Anhydrite (CaSO <sub>4</sub> )	: 95.001	0.698

**A8: Aquachim to well number 19-17/001**

SampleID : 19-17/001  
 Location : 'Inad Al Masri  
 Site : Al Jiftlik  
 Sampling Date : 08/03/2008  
 Geology : Alluvium  
 Watertype : Na-HCO3

Sum of Anions (meq/l) : 152.3583  
 Sum of Cations (meq/l) : 152.2771  
 Balance: : -0.03%

Calculated TDS(mg/l) : 5014.8

Hardness : meq/l °f °g mg/l CaCO3  
 Total hardness : 32.82 164.11 91.90 1641.1  
 Permanent hardness : 0.0 0.00 0.00 0.0  
 Temporary hardness : 32.82 164.11 91.90 1641.1  
 Alkalinity : 131.63 658.15 368.57 6581.5  
 (f = 10 mg/l CaCO3/ 1 °g = 10 mg/l CaO° 1)

**Major ion composition**

	%mg/l	mmol/l	meq/l	meq
Na+	2740.0	119.182	119.182	39.123
K+	10.59	0.271	0.271	0.089
Ca++	407.3	10.162	20.324	6.672
Mg++	151.9	6.248	12.497	4.102
Cl-	673.55	18.998	18.998	6.236
SO4--	66.0	0.687	1.374	0.451
HCO3-	8030.54	131.631	131.631	43.209

Ratios	Comparison to Seawater			
	mg/l	mmol/l	mg/l	mmol/l

Ca/Mg	2.681	1.626	0.319	0.194
Ca/SO4	6.171	14.79	0.152	0.364
Na/Cl	4.068	6.273	0.556	0.858

Dissolved Minerals:	mg/l	mmol/l
---------------------	------	--------

Halite (NaCl)	: 1095.562	18.7275
Sylvite (KCl)	: 20.192	0.2725
Carbonate (CaCo3)	: 322.984	3.2298
Dolomite (CaMg(CO3)2):	1150.341	6.248
Anhydrite (CaSO4)	: 93.583	0.687

B1: Durove diagram for the collected samples

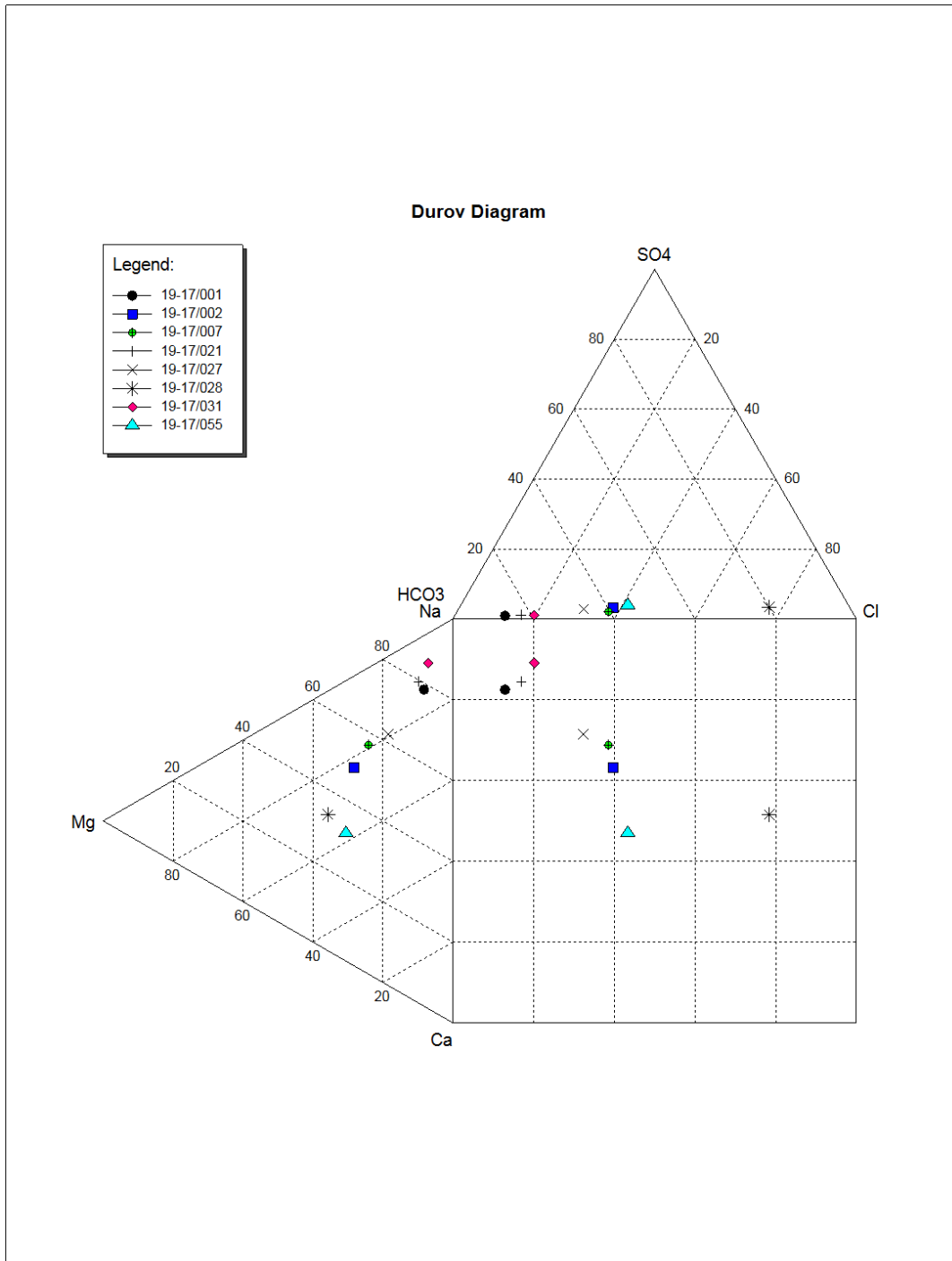


Fig.(B1): Durove diagram for the collected groundwater samples

B2: Piper diagram to the studied groundwater

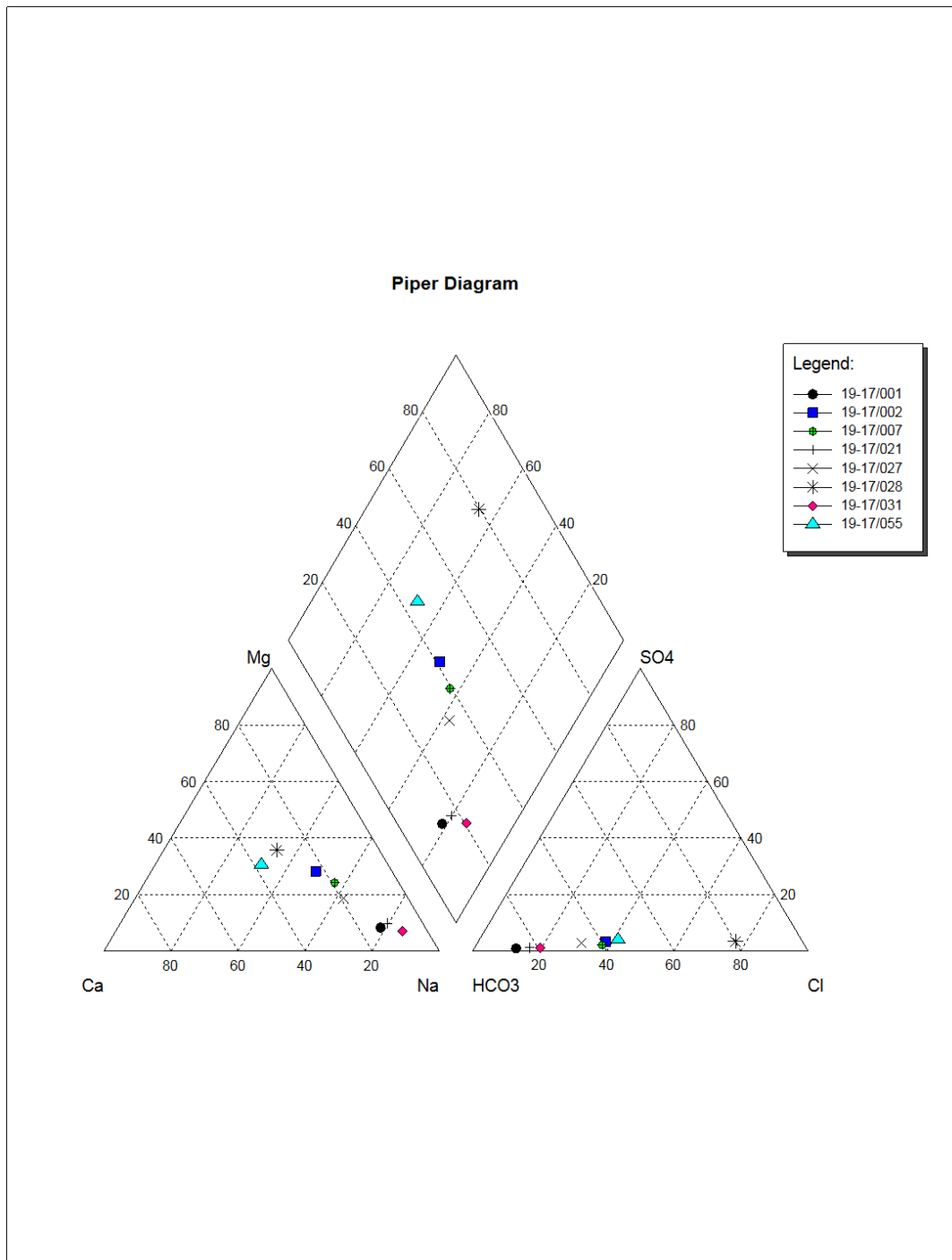


Fig.(B2): Piper diagram to the studied groundwater

### B3: Shoeller Diagram

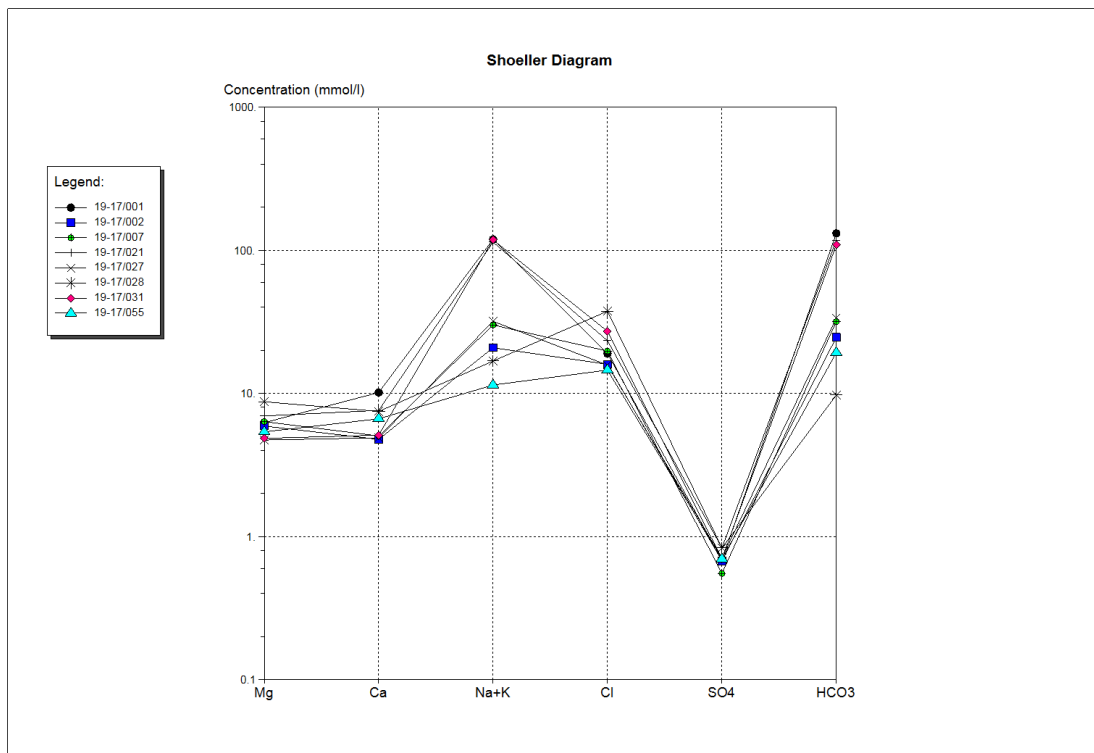


Fig.(B3): Shoeller Diagram



The porosity of gravel is in the range 24%-36% (McWorter et al. 1997). Depending on the porosity and the existing map in appendix C2, the allowed volume for artificial recharge can be calculated as

$$\text{Volume} = 1500 \times 3000 \times 20 \times 30\% = 27 \text{ mcm. } \pm 15\%$$

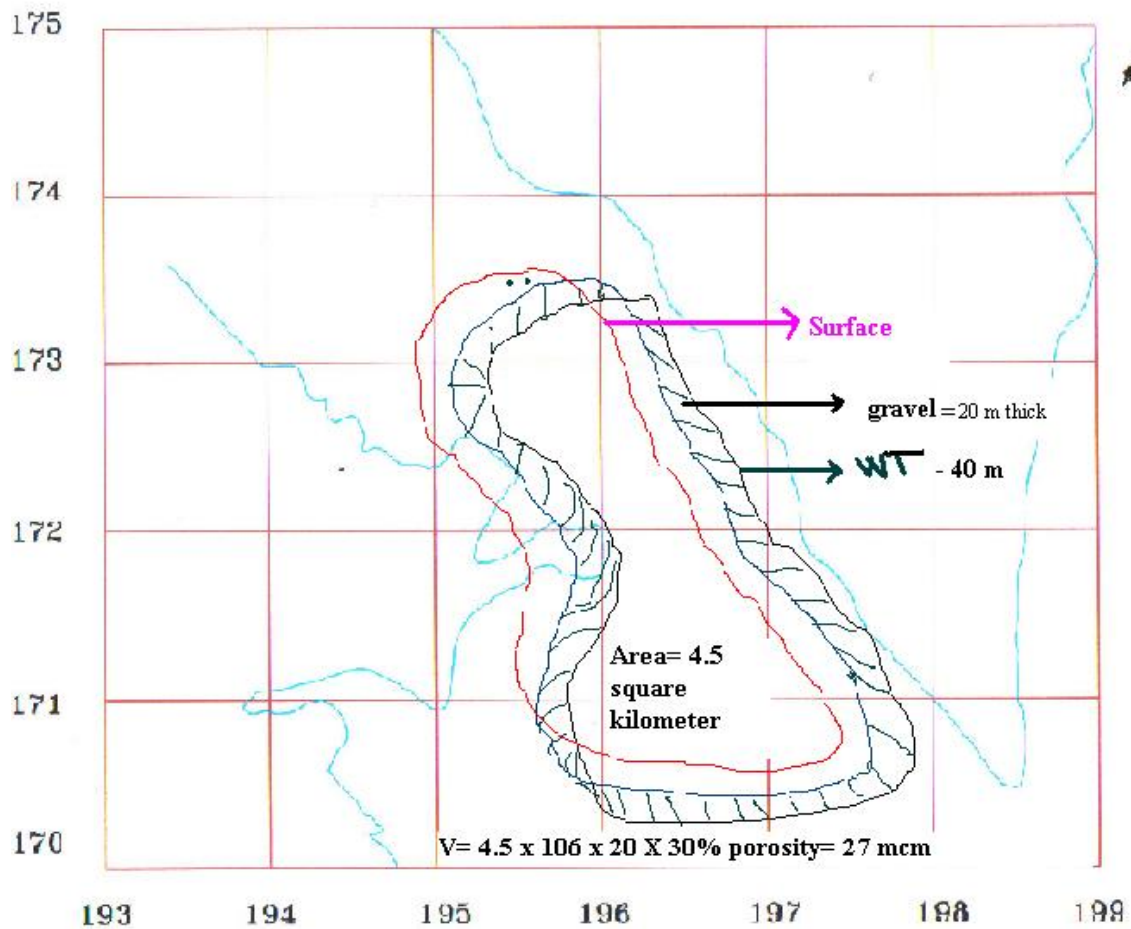
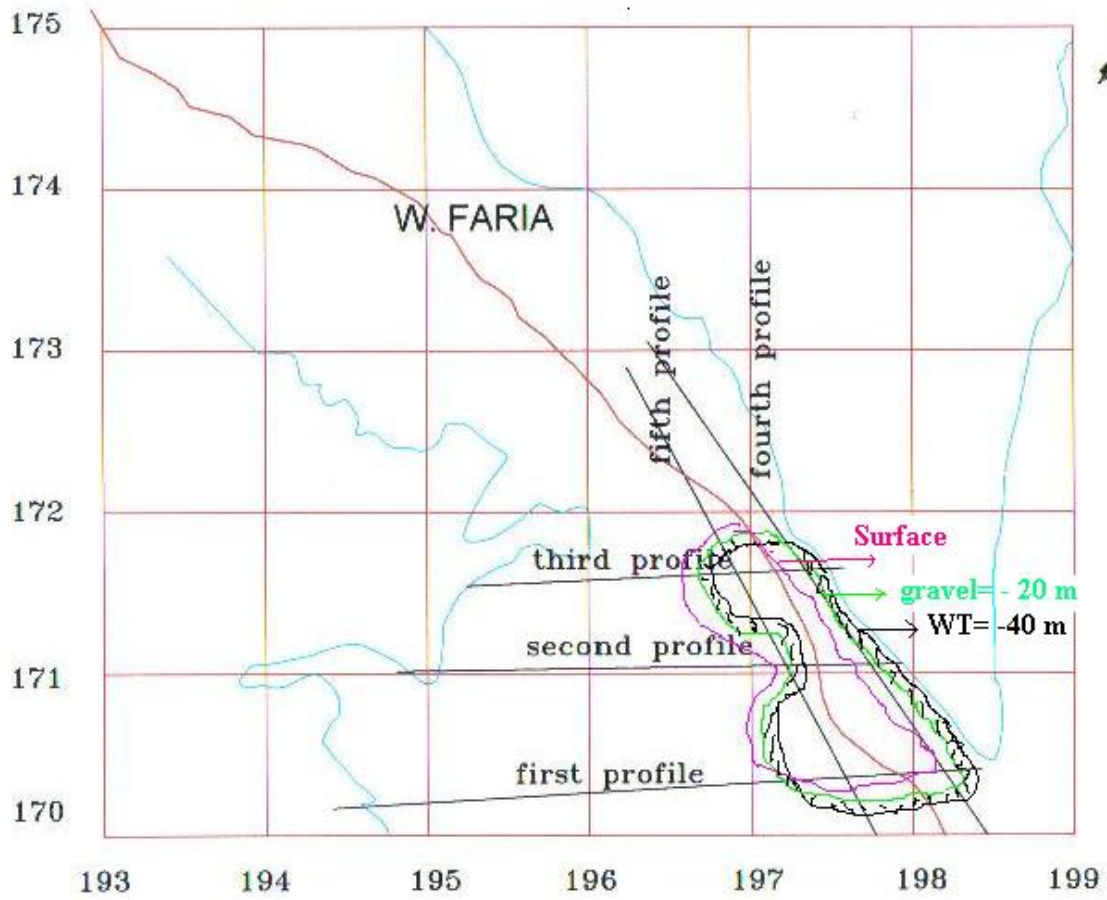


Fig. C2: The allowed volume for artificial recharge in the whole Al-Jiftlik area

The possible volume for artificial recharge to groundwater in the study area / Al-Jiftlik is  
 $v = (1000 \times 1500 \times 20 \times 30\%) \pm 15\% = 8-10 \text{ mcm}$ .



C3: Possible site for artificial recharge at the study area /Al-Jiftlik